



University Library

Author/Filing Title GAVLEVICH, D.....

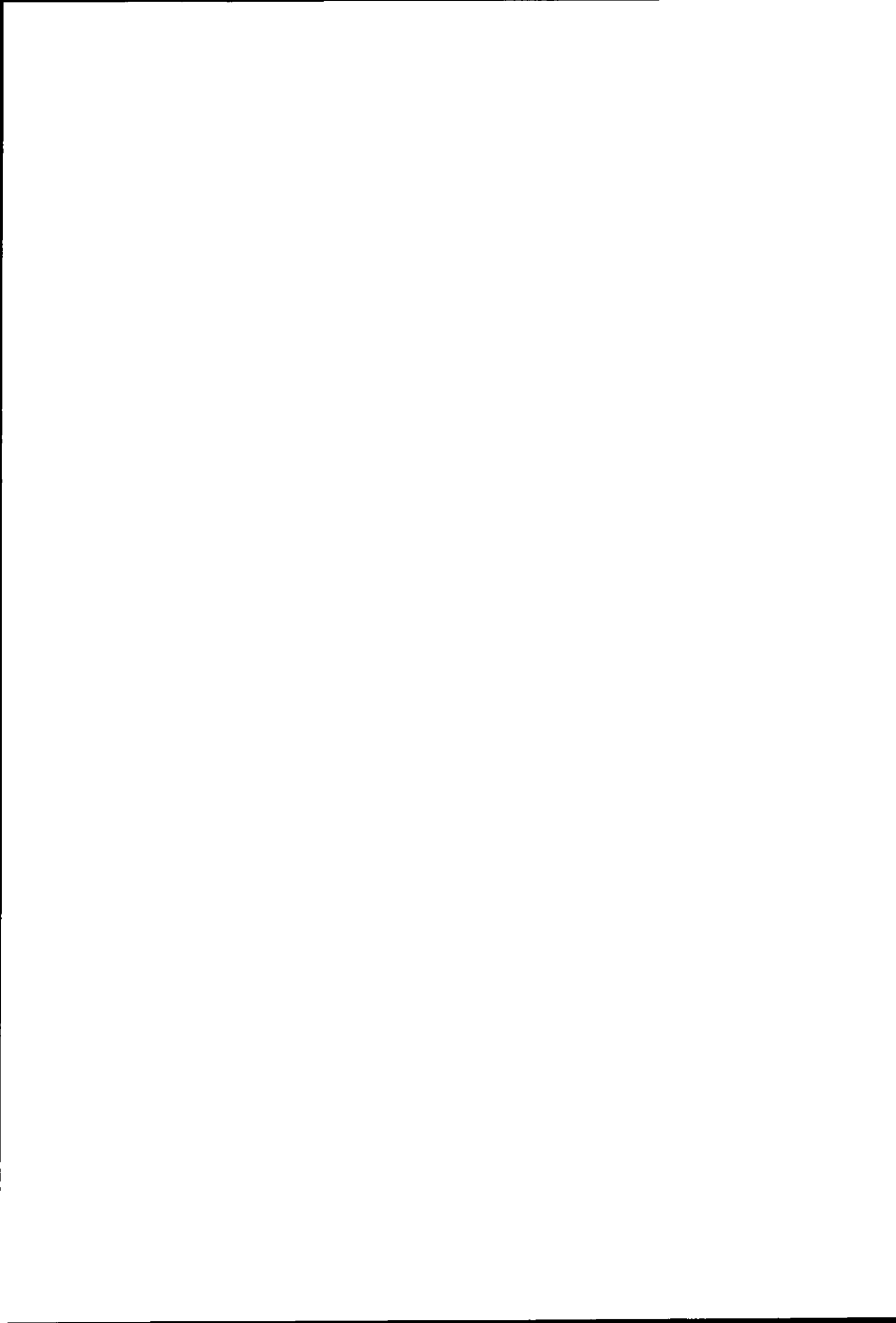
Class Mark T.....

Please note that fines are charged on ALL
overdue items.

FOR REFERENCE ONLY

0403272114





**Tunneling and Switching Phenomena in
Superconducting Quantum Dots and
Josephson Junctions**

by

Dmitry R. Gulevich

Doctoral Thesis

Submitted in partial fulfilment
of the requirements for the award of
Doctor of Philosophy of Loughborough University

October 2006

© D. R. Gulevich 2006



Loughborough
University
Pikington Library

Date JAN 2007

Class T

Acc
No. 0403272114

Abstract

This work is devoted to investigation of tunnelling and switching phenomena arising in Condensed Matter Physics. In the first part I investigate quantum tunnelling of a single Abrikosov vortex in a superconducting quantum dot. The escape of a vortex carrying magnetic flux leads to a switching of a quantum dot to non-magnetic state. Tunneling of a vortex manifests itself as a spontaneous relaxation of magnetization. I showed that it is possible to use an instanton technique based on path integral formalism even in presence of forces breaking time-reversal symmetry. For instance, I adapted this method for such systems as a charged particle tunnelling in a magnetic field or a quantum vortex subjected to a Magnus force. The comparison with the standard WKB method revealed complete coincidence of the results. The second part of the thesis is dedicated to investigation of superconducting Josephson contacts, in particular, I devoted the main attention to the annular realization. I have developed a model of switching to resistive state due to both quantum tunneling and thermal activation. The developed theory appears in a good agreement with available experimental data. I have proposed a model of a qubit for quantum computation that is based on two states of a vortex in an annular Josephson junction with microshort. Finally, I summarized the switching characteristics of annular Josephson junctions on a single phase diagram. The symmetry of the obtained graph perfectly manifests the fundamental analogy between quantum mechanics of n -dimensional systems and classical statistical mechanics in $(n+1)$ -dimensions.

Keywords: Josephson junctions, superconductors, quantum tunneling, quantum computation, vortices, fluxons

Acknowledgements

I would like to thank my research supervisor Feo Kusmartsev for encouragement and guidance during my PhD studies and his flexibility as a research supervisor. I am also grateful to John Samson for proof of many research drafts, Andreas Wallraff for instructive conversations and group of Prof. A. Ustinov, especially Astria Price, Alexander Kemp and Alexei himself for collaboration and providing invaluable experimental data. I would like to thank organizers of SET for Britain for giving me opportunity to present my research results to members of British parliament at the Britain's Younger Scientists Poster Competition held at the House of Commons. This work would not have been possible without financial support of the European Mobility Scheme for Physics Students (EMSPS) granted by European Physical Society, Overseas Research Studentship (ORS) award and Loughborough University Research Studentship. Also, this research has been supported by European Science Foundation providing visit grants and support for the conferences, and the network programme Arrays of Quantum Dots and Josephson Junctions (AQDJJ) which has allowed exchange of knowledge with other scientists and presentation of the results at international workshops.

Contents

Introduction	2
I TUNNELING OF ABRIKOSOV VORTEX	5
1 Abrikosov vortex in superconducting quantum dot	6
1 1 Quantum tunneling of vortices	6
1 2 Surface barriers	8
1 3 Dissipation	8
1 4 Vortex mass	9
1 5 Physical model	9
2 Instanton method	11
2 1 Euclidean Lagrangian	11
2 2 Analytic continuation in ω_c	12
2 3 Classical trajectories	14
2 4 Jacobi fields	17
2 5 Elimination of zero eigenvalues	22
2 6 Calculation of the Green function	25
2 7 Integrals over the peculiar eigenmodes	27
2 8 Contribution of the trivial trajectory	29

2 9	Instanton gas	30
3	WKB method	32
3.1	Hamiltonian	32
3.2	The use of symmetries	33
3.3	WKB expansion	34
3.4	Correspondence with the previous results	36
4	Summary	38
	Appendix A Useful integrals	41
	Appendix B Faddeev-Popov procedure	41

II SWITCHING PHENOMENA IN LARGE JOSEPHSON JUNCTIONS **43**

5	Annular Josephson Junction of Intermediate Length	44
5.1	Introduction	44
5.2	Formulation	46
5.3	Critical $\delta_c(h)$	49
5.4	Barrier height	49
5.5	Standard deviation	51
5.6	The deviation from $T^{2/3}$ law	52
5.7	Quantum case	53
5.8	Vortex-antivortex pairs dissociation and annihilation	55
5.9	Annular Josephson junction with impurity	56
5.10	Conclusion	59

6	Long Annular Josephson Junction	63
6.1	Long Annular Josephson Junction limit simple considerations	63
6.2	Long - short junction crossover . . .	64
6.3	Another derivation . . .	66
7	Fluxon in an Annular Josephson Junction. Microshort Qubit.	70
7.1	Introduction . . .	70
7.2	Microshort qubit general considerations	72
7.3	Annular Josephson junction with different microshort types	72
7.4	Switching current branches	74
7.5	Quantum properties . . .	75
8	Perturbation Theory of Localized Excitations. Decay of a Breather.	77
8.1	Introduction . . .	77
8.2	Perturbation theory for localized solutions . . .	79
8.3	Pinning by a microresistor . . .	85
8.4	Decay of a breather	85
8.5	Conclusion	86
9	Two-dimensional Josephson Junctions	89
9.1	2D Josephson junctions	89
9.2	Square geometries . . .	91
9.3	Derivation of the microshort models	93
	Summary and Conclusions	99
	Bibliography	102

Introduction

Quantum tunneling attracts much interest because of its importance for such physical systems as helium surface structures, quantum dots, superconductors, that are among the most promising for realization of large scale quantum computers. Being one of the most important manifestation of quantum mechanics, tunneling process occurs in many phenomena in physics, chemistry and biology.

The first part of the thesis is dedicated to the problem of a vortex tunneling in mesoscopic superconductors. In order to describe this process I apply quantum field theory methods, in particular the instanton technique mentioned above. The escape of a vortex trapped in a quantum dot leads to switching of a superconducting dot to non-magnetic state. This results in higher expulsion magnetic fields than expected from pure thermodynamical considerations. Study of tunneling vortex is important not only from fundamental point of view, but from the practical point as it is responsible for low temperature creep in HTSC superconductors [YMS96].

The subsequent chapters have been written during a close collaboration with experimental group of Prof. Ustinov in Erlangen (Germany). I have developed a model describing an annular Josephson junctions that allowed interpretation of experimental data obtained by the experimental group and proposed new experiments. Josephson junction represents a contact of two thin superconducting films separated by insulator. When subjected to a magnetic field or an external current, the junction may switch to

a resistive state where it loses superconducting properties. Normally, this switching is induced by thermal activation or quantum tunnelling.

Potential applications of Josephson junctions can be hardly overestimated. Understanding of their switching characteristics also reveals prospects for the use of superconductors in our everyday lives. Because of fast switching times and extreme sensitivity, Josephson junctions have been always attractive for developing high frequency electronics, magnetic sensors and digital applications. AJJ can be also used to implement particle and radiation detectors [NC97, CEF⁺99, LAB⁺00, FLP⁺01, NCL⁺02, BCL⁺06]. An annular Josephson junction (AJJ) represents a very clean system for study solitons – elementary excitations that propagate in non-linear systems similar to particles. With respect to Josephson junctions such solitons are called Josephson vortices or fluxons. In an AJJ one may accelerate them up to light velocities so that they experience relativistic effects like Lorentz contraction.

I proposed a new type of elementary cell for superconducting quantum computer based on an AJJ – the microshort qubit. The qubit is based on a Josephson vortex (fluxon) trapped in an AJJ and subjected to a magnetic field. A small impurity called a microshort, introduced in the AJJ, induces a double well potential where two quantum states available for quantum computation arise. Independently from our research group, similar system has been designed by experimental group of Prof Ustinov.

The intermediate results of this work include advances in the theory of sine-Gordon solutions. I have developed a perturbation method for periodic solutions of sine-Gordon equation. The most illustrative example of such solutions is a bound state of two solitons called a breather [Raj82]. The developed theory enables one to describe localized sine-Gordon solutions in a more simple and accurate manner compared with the seminal McLaughlin-Scott approach [MS78].

I collaborated with a number of scientists and research groups, both theoretical and

experimental. These are A Ustinov's group, Erlangen, Germany, R Wördenweber, ISG, Juüich, Germany, E Il'ichev, Jena, Germany, A Barone's group, Napoli, Italy, F Nori and S Savel'ev RIKEN, Japan, K Kadowaki's group, Tsukuba, Japan, K Hirata's and H Wang's group, NIMS, Japan, A. Maeda, JSTA, Japan, T Bojadjev, Sofia, Bulgaria, V P Koshelets, IREE, Moscow, Russia, A L Pankratov, Nizhny Novgorod, Russia, K N Alekseev, Oulu, Finland, N Pedersen, Lyngby, Denmark, A. Vagov, Lancaster, UK, V Zolpaev, Liverpool, UK, P Warburton, UCL, UK. There is specific expertise available for the research at the Department of Physics in Loughborough. Staff of the Physics Department comprises top experts in superconductivity and material science. Nobel Prize winner Prof. Alexei Abrikosov, Prof. Sasha Andreev, Prof. Danya Khomskii, Prof. A. Alexandrov, Prof. F. Kusmartsev, Dr. B. Chesca and Dr. S. Savel'ev.

Present work devoted to investigation of Josephson junctions was distinguished by a prize of the Britain's Younger Scientists Poster Competition held at House of Commons in November 2005 [SET06]. My progress was highlighted in British and international journals [AtS05, New06].

Part I

TUNNELING OF ABRIKOSOV
VORTEX

Chapter 1

Abrikosov vortex in superconducting quantum dot

1.1 Quantum tunneling of vortices

The concept of quantum tunneling of vortices in superconductors (see Refs in the review [YMS96] about magnetic relaxation in HTSCs) first appeared when measurements of magnetic relaxation at ultralow temperatures have been made (Refs [5-10] in [KS02]). The experiments have shown that the relaxation rate does not disappear at zero temperature. This phenomenon has been attributed to the quantum tunneling, but many details about it are not well understood until now. Neither vortex mass nor Hall coefficient are known exactly. We suggest that quantum tunneling of a vortex can be also responsible for spontaneous relaxation of their magnetization in mesoscopic superconductors. The escape of a vortex trapped in a quantum dot leads to switching of a superconducting dot to non-magnetic state. This results in higher expulsion magnetic fields than expected from pure thermodynamical considerations.

Similar to vortices in gases and fluids, Abrikosov vortices are subjected to Magnus

force. From mathematical point of view, the system of a moving vortex is analogous to a particle moving in a magnetic field. The problem of a charged particle tunneling in presence of magnetic field has itself both theoretical and practical interest. As the tunneling is strongly affected by magnetic field, applied in transverse direction, this could be efficiently used to control qubits in possible quantum computer realizations of the future. In absence of magnetic field the decay rate is related to the imaginary part of the free energy as $\Gamma = \frac{2}{\hbar} \text{Im}F$ [Lan67]. The escape rate can be found making semiclassical approximations in the Euclidean path integral. The term corresponding to the ground state gives the greatest contribution to the propagator transformed to imaginary times in the limit of large time interval. It makes possible to determine the imaginary part of the ground state energy [KST00]. The same considerations must be valid when the magnetic field is applied. However, because of the broken time-reversal symmetry, a complex action appears under the path integral, when transformed to Euclidean space. Furthermore the imaginary time trajectories which extremize the action become complex and the operator corresponding to the second variation of the action is non-hermitian and possesses complex eigenvalues [SDP02, SDP00]. In this case one could make analytic continuation of the path integral to a complex coordinate space or change the time contour in the complex plane. Nevertheless we show that it is possible to make analytic continuation in cyclotron frequency to transform the action to a real one. This makes the task much more transparent because of a close analogy with classical mechanics. The coincidence with the result obtained by usual WKB (Wentzel-Kramers-Brillouin) technique [LL65, KST00] could also serve as a proof of validity of the method.

Normally the polar coordinates are used to study the systems that possess rotational invariance. However, it becomes hard to work with path integrals in curved coordinates, because of additional terms appearing in the action [EG64, PI69, Kle00]. Usually one always begins with time-sliced path integral in cartesian coordinates be-

fore transformed to the curved ones, since change of variables in path integrals is not a direct procedure. Everywhere in this paper we work with path integrals written in orthogonal coordinates.

Thus, we consider an Abrikosov vortex trapped in a round superconducting quantum dot. Let us investigate the problem of quantum escape of the vortex through a barrier associated with the surface of a superconductor. In the next sections we present the possible factors that may affect the quantum dynamics of a vortex.

1.2 Surface barriers

The barrier near the surface of type-II superconductors was first studied by Bean and Livingstone [BL64]. It arises from competition of two forces: attraction to the image antivortex near the border and interaction with the Meissner current. Usually, the effect of the surface roughness is to suppress the barrier when a vortex enters a superconductor [BL64]. In our case we may completely neglect the influence of the surface irregularities as it is much less pronounced for a vortex leaving a superconductor [TS72].

Another obstacle affecting flux dynamics in HTSCs in transverse magnetic field is the geometrical barrier [SIK⁺94a, ZLG⁺94]. Normally geometrical barrier affects the magnetic behaviour of HTSCs of flat non-elliptic form [SIK⁺94b, BC96, BI93, CDJ⁺99]. As we consider a superconducting dot in a form of a disk, we neglect the contribution of the geometrical barrier.

1.3 Dissipation

There are two main forces affecting vortex dynamics in superconductors: Magnus (Hall) force and dissipation. Feigel'man et al [FGLL93] proposed that the Magnus

force is dominant in clean superconductors, while other authors [vDGM⁺96, vDGL⁺96, vDGK96] argued that the vortex tunneling may occur in an intermediate regime. As long as we consider the HTSCs, the dissipative term must not be crucial because of small coherence lengths (as well as vortex cores). The evidence for a low dissipation regime in cuprate superconductors has been presented by [HYT⁺94].

1.4 Vortex mass

The same authors [HYT⁺94] argued that the Magnus force is also smaller than standard estimates [PSO⁺95]. Thus, the mass of vortex can be relevant to the low-temperature physics of clean HTSCs in superclean limit [CK03] and should be taken into account in our model. In 1965 two contributions to the vortex mass were calculated by Suhl [Suh65] due to the kinetic energy of the vortex core and due to electromagnetic energy. Recently, Chudnovsky and Kuklov [CK03] have shown that transversal displacements of the crystal lattice can give a significant contribution to the vortex mass. This contribution must be crucial in metals with high concentration of superconducting electrons. In our case of small coherence length ξ , the most important contribution to the mass arises from the quantization of the electron states inside the vortex core (the same paper [CK03]). It has been shown to exceed the core mass by the factor $(\epsilon_F/\Delta)^2$ (Refs [7-9] in [CK03]).

1.5 Physical model

Let us summarize the basic points of the physical model of Abrikosov vortex tunneling from superconducting quantum dot. 1. We investigate HTSC quantum dot at low temperature.

- 2 Point Abrikosov vortex is trapped in the quantum dot by its surface barrier
- 3 We neglect surface roughness because irregularities on the edges are less important for leaving than for entry
- 4 No geometrical barrier
- 5 No dissipation – "superclean" limit
- 6 No bulk pinning.
- 7 Vortex mass is relevant
- 8 Magnus force is relevant

The typical parameters of the physical system under investigation could be the follows disk diameter $\sim 10 - 100 \text{ nm}$, thickness $\sim 1 \text{ nm}$, coherence length $\xi \sim 1 \text{ nm}$, bulk penetration depth $\lambda \sim 100 \text{ nm}$

Chapter 2

Instanton method

2.1 Euclidean Lagrangian

The system of a vortex in HTSC quantum dot can be modelled as a charged particle trapped in 2D potential well and subjected to a magnetic field playing a role of a Magnus force. For simplicity we assume $\hbar = 1$ and $m = 1$ and consider the limit of large time T (i.e. small decay rates), that is usual for the instanton technique. We take the potential in the form of rotationally symmetric inverted double well. The case of a particle trapped inside one-dimensional inverted double well is studied in details by [Sch81]. See also [KST00] and [Col77, CC77, Col85] for 1D tunneling problems with potential of another shapes.

The Lagrangian of our 2D model in the Poincare gauge (which coincides with the Coulomb gauge in this case) $\vec{A} = (-\frac{yB}{2}, \frac{xB}{2}, 0)$

$$L = \frac{x^2 + y^2}{2} - \frac{\omega_c}{2}(xy - yx) - U(r) \quad (2.1)$$

$$U(r) = \frac{\omega^2}{2}r^2 - \alpha r^4 = \frac{\omega^2}{2}(x^2 + y^2) - \alpha(x^2 + y^2)^2$$

Here ω denotes the frequency at the bottom of the parabolic potential well, while

$\omega_c = \frac{eB}{mc} = \frac{eB}{c}$ is the cyclotron frequency

The survival amplitude at the bottom of the well expressed in terms of the Feynman path integral

$$G(\vec{0}, T, \vec{0}, -T) = \langle \vec{0} | e^{-i2HT} | \vec{0} \rangle = \int \mathcal{D}\vec{r}(t) e^{i \int_{-T}^T L dt} \quad (2.2)$$

implying the coordinates of the center by $\vec{0}$ Transforming to imaginary times $t \rightarrow -i\tau$,

$$\langle \vec{0} | e^{-2HT} | \vec{0} \rangle = \int \mathcal{D}\vec{r}(\tau) e^{-\int_{-T}^T L d\tau}$$

with Lagrangian

$$L = \frac{x^2 + y^2}{2} + i \frac{\omega_c}{2} (xy - yx) + U(r)$$

where $x = dx/d\tau$ and $y = dy/d\tau$ (for simplicity we keep the same notation x and y)

As it has been mentioned early, the action acquires a complex part after transforming to imaginary time, in contrast with the case of zero magnetic field

2.2 Analytic continuation in ω_c

We have found useful to make analytic continuation in charge (or cyclotron frequency ω_c) In order to validate this procedure, we cite the next theorem from Ref [Fed77]

Theorem Consider the next multiple integral

$$F(\lambda, \alpha) = \int_{\gamma} f(\vec{z}, \alpha) \exp(\lambda S(\vec{z}, \alpha)) d\vec{z}$$

where $\alpha = (\alpha_1, \dots, \alpha_k)$ is a set of parameters, γ is a contour in \mathbf{C}^n , with conditions that the functions $f(\vec{z}, \alpha)$ and $S(\vec{z}, \alpha)$ are analytic, $S(\vec{z}, \alpha)$ has non-degenerate saddle points at $\vec{z}_1, \dots, \vec{z}_s$ and contour γ goes through the saddle points when $\alpha = \alpha_0$, Then the asymptotics of the integral when $\lambda \rightarrow \infty$ is given by the contribution of the saddle points $\vec{z}_1(\alpha), \dots, \vec{z}_s(\alpha)$, such that $\vec{z}_1(\alpha) = \vec{z}_1$, $\dots, \vec{z}_s(\alpha) = \vec{z}_s$, if α is close enough to α_0

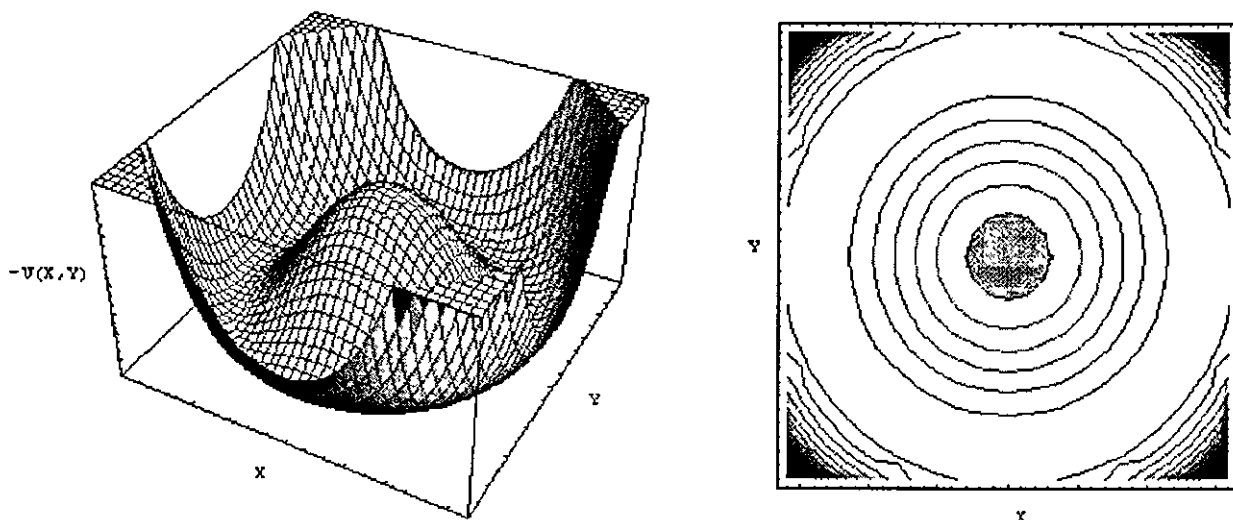


Figure 2.1 *Inverted potential $-U(r)$ that appear when transformation to imaginary times $t \rightarrow -i\tau$ is made inside the Lagrangian. The classical trajectories corresponding to a particle subjected to an inverted potential are called instantons*

It is straightforward to make generalization of the theorem cited above to the case of path integrals, implying "path integral" instead of "n-dimensional integral" and "trajectory" instead of "n-dimensional stationary point". We have only one parameter ω_c instead of the set of parameters $\alpha = (\alpha_1, \dots, \alpha_k)$ and the condition $\alpha = \alpha_0$ corresponds to $\omega_c = 0$. But we have a real solution of the equation of motion at $\omega_c = 0$. It follows from the theorem that the asymptotics of the path integral is given by the same analytic formula inside some circle around $\omega_c = 0$ on the complex plane. Thus if we calculate that one for which the stationary trajectories are real ones, the asymptotics inside all the circle can be found by continuation in ω_c .

In order to have more ground, let us look at the convergence of the path integral

Written in the sliced form the path integral is

$$\begin{aligned}
& \int dx_1 \dots dx_{N-1} \int dy_1 \dots dy_{N-1} \exp \left\{ -\epsilon \sum_{j=0}^{N-1} \left[\frac{1}{2} \left(\frac{x_{j+1} - x_j}{\epsilon} \right)^2 + \frac{1}{2} \left(\frac{y_{j+1} - y_j}{\epsilon} \right)^2 + \right. \right. \\
& \left. \left. + \frac{i\omega_c}{2} \left[\left(\frac{x_{j+1} - x_j}{\epsilon} \right) \left(\frac{y_{j+1} + y_j}{2} \right) - \left(\frac{y_{j+1} - y_j}{\epsilon} \right) \left(\frac{x_{j+1} + x_j}{2} \right) \right] + U(x_j, y_j) \right] \right\} = \\
& = \int dx_1 \dots dx_{N-1} \int dy_1 \dots dy_{N-1} \exp \left\{ -\sum_{j=0}^{N-1} \left[\frac{(x_{j+1}^2 - 2x_{j+1}x_j + x_j^2)}{2\epsilon} + \frac{(y_{j+1}^2 - 2y_{j+1}y_j + y_j^2)}{2\epsilon} + \right. \right. \\
& \left. \left. + \frac{i\omega_c}{4} [(x_{j+1} - x_j)(y_{j+1} + y_j) - (y_{j+1} - y_j)(x_{j+1} + x_j)] + \epsilon U(x_j, y_j) \right] \right\}
\end{aligned}$$

Consider the terms with the index k inside the sum

$$\begin{aligned}
& \frac{1}{2\epsilon} (2x_k^2 - 2x_k x_{k-1} - 2x_{k+1} x_k) + \frac{1}{2\epsilon} (2y_k^2 - 2y_k y_{k-1} - 2y_{k+1} y_k) + \\
& + \frac{i\omega_c}{4} [\tau_{k+1} y_k - x_k y_{k+1} - x_k y_k - y_{k+1} \tau_k + y_k \tau_{k+1} + y_k \tau_k + \\
& + \tau_k y_k + \tau_k y_{k-1} - \tau_{k-1} y_k - y_k \tau_k - y_k \tau_{k-1} + y_{k-1} \tau_k] + \epsilon U(\tau_k, y_k) = \\
& = \frac{1}{\epsilon} \left(x_k^2 - x_k (x_{k-1} + x_{k+1}) - \epsilon \frac{i\omega_c}{2} x_k (y_{k+1} - y_{k-1}) \right) + \\
& + \frac{1}{\epsilon} \left(y_k^2 - y_k (y_{k-1} + y_{k+1}) + \epsilon \frac{i\omega_c}{2} y_k (x_{k+1} - x_{k-1}) \right) + \epsilon U(x_k, y_k)
\end{aligned}$$

It can be seen that the term with ω_c must not affect convergence of the Gauss integrals because of small factor ϵ in front

Thus at least for small ω_c we can reduce the stationary point (steepest-descent) method to that of Laplace, which is more simple. As a result, all the equations become real and the instanton trajectories correspond to those of a classical particle moving in the inverted potential under transverse magnetic field

2.3 Classical trajectories

With these considerations in mind, after transforming to imaginary times $t \rightarrow -i\tau$ as well as $\omega_c \rightarrow i\omega_c$ (in fact the sign in the last procedure must not be the matter) we

get the following Lagrangian

$$L = \frac{\dot{x}^2 + \dot{y}^2}{2} - \frac{\omega_c}{2}(xy - yx) + U(r) \quad (23)$$

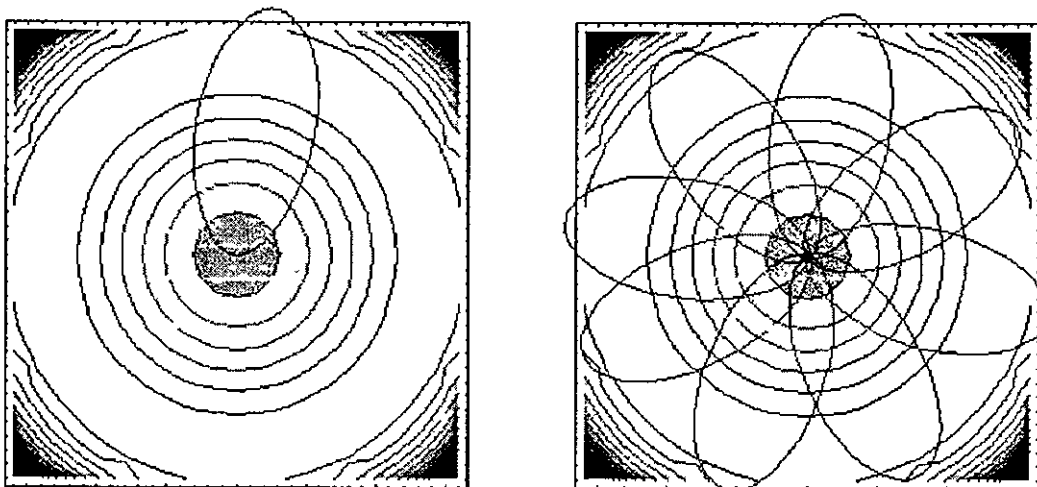


Figure 2.2 *The instanton trajectory slides down from the hill at the center with almost zero velocity, bounces from the wall drawing a hump and returns back to the origin in infinite time. There could be multiple instanton trajectory consisting of many turns, differing both in time and angular position.*

The trajectories extremising the action corresponding to this Lagrangian are that ones, which correspond to a classical particle moving in the inverted potential $-U(r)$ and transverse magnetic field applied in the same direction as before. Now we are going to make a little step back from the promise to work in cartesian coordinates and find the classical trajectories from the equations of motion written in polar coordinates. Thus

$$L = \frac{\dot{r}^2 + r^2\dot{\phi}^2}{2} + \frac{\omega_c}{2}r^2\phi + U(r)$$

equations of motion

$$r^2\left(\phi + \frac{\omega_c}{2}\right) = \text{const}$$

$$r - r\phi^2 - \omega^2 r + 4\alpha r^3 - \omega_c r\phi = 0$$

We consider the limit $T \rightarrow \infty$ as usual for description of ground state decay in the instanton approach. The classical trajectories that give the greatest contribution to the path integral are that ones, that spend almost all their time at the origin, as the action is zero there. This gives $E = 0$. Let us consider the first equation of motion and the energy conservation law

$$r^2\left(\phi + \frac{\omega_c}{2}\right) = \text{const}$$

$$0 = E = \frac{r^2 + r^2\phi^2}{2} - U(r)$$

Because the trajectory comes from the center of the system, $r \rightarrow 0$ gives $\text{const} = 0$ (Suppose the opposite. Then at least $\phi \sim 1/r^2$ when $r \rightarrow 0$. Obviously this contradicts to the energy conservation law as the potential tends to zero under this limit.) Hence $\phi = -\omega_c/2$ and the equations of motion transform to

$$r - \Omega^2 r + 4\alpha r^3 = 0$$

with $\Omega^2 = \omega^2 - \omega_c^2/4$. The solution of this equation is

$$r_{cl}(\tau) = \frac{\Omega}{\sqrt{2\alpha} \cosh \Omega\tau}$$

It corresponds to the instanton with the center at $\tau = 0$. There are many other classical trajectories with different positions of the centers. Obviously, all of them have the same action

$$S_{cl} = \frac{\Omega^3}{3\alpha} \tag{2.4}$$

We will take them into account when taking integral over time zero-mode below. Also, there are trajectories with the same position in time, but differing from each other by

rotation around the origin. Similarly, these ones will be counted by the integral over ϕ -mode below

The instanton trajectory transformed to cartesian coordinates reads

$$\begin{cases} x_{cl}(\tau) = r_{cl}(\tau) \cos\left(-\frac{\omega_c \tau}{2} + \phi_0\right) = \frac{\Omega \cos\left(-\frac{\omega_c \tau}{2} + \phi_0\right)}{\sqrt{2\alpha} \cosh \Omega \tau} \\ y_{cl}(\tau) = r_{cl}(\tau) \sin\left(-\frac{\omega_c \tau}{2} + \phi_0\right) = \frac{\Omega \sin\left(-\frac{\omega_c \tau}{2} + \phi_0\right)}{\sqrt{2\alpha} \cosh \Omega \tau} \end{cases} \quad (2.5)$$

Where $1/\Omega$ plays a role of the "lifetime" of the instanton, $\omega_c/2$ is the frequency of rotation around the center. For instance, when $\omega_c/2 \sim \Omega$ the instanton makes approximately one turn during his "life", while for bigger $\omega_c/2$ the trajectories become spirals spinning around the center.

2.4 Jacobi fields

Let us calculate the contribution of quantum fluctuations near the classical trajectories. Obviously, there is a set of them associated with different ϕ_0 . We can fix the one corresponding to $\phi_0 = 0$. The other classical trajectories, as well as the fluctuations around them, will be taken into account later integrating over the rotation symmetry group.

In the semiclassical approximation the action is decomposed about the classical trajectory (for sake of simplicity we omit the normalization constants in front of path integrals)

$$\int D\vec{r}(\tau) e^{-S[\vec{r}]} = e^{-S_{cl}} \int D\delta\vec{r}(\tau) e^{-\frac{1}{2}\delta^2 S} \quad (2.6)$$

where

$$\vec{r}(\tau) = \vec{r}_{cl}(\tau) + \delta\vec{r}(\tau) \quad \text{and} \quad \delta^2 S = \int_{-T}^T (\delta\vec{r}, \hat{A} \delta\vec{r}) d\tau$$

The operator \hat{A} inside the second variation of the Euclidean action is

$$\hat{A} = \begin{pmatrix} -\partial_\tau^2 + U''_x & \omega_c \partial_\tau + U''_{xy} \\ -\omega_c \partial_\tau + U''_{xy} & -\partial_\tau^2 + U''_y \end{pmatrix}$$

with

$$\begin{aligned}
 U_x'' &= -\frac{2\Omega^2 + 4\Omega^2 \cos^2 \frac{\omega_c \tau}{2}}{\cosh^2 \Omega \tau} + \Omega^2 + \omega_c^2/4 \\
 U_y'' &= -\frac{2\Omega^2 + 4\Omega^2 \sin^2 \frac{\omega_c \tau}{2}}{\cosh^2 \Omega \tau} + \Omega^2 + \omega_c^2/4 \\
 U_{xy}'' &= \frac{4\Omega^2}{\cosh^2 \Omega \tau} \sin \frac{\omega_c \tau}{2} \cos \frac{\omega_c \tau}{2} = \frac{2\Omega^2}{\cosh^2 \Omega \tau} \sin(\omega_c \tau)
 \end{aligned}$$

being the second derivatives of the potential evaluated along the classical trajectory. It has been convenient here to express the frequency ω via Ω and ω_c .

An arbitrary quantum deviation can be decomposed through normalized eigenfunctions $\vec{\chi}_i$ of the operator \hat{A}

$$\delta\vec{r}(\tau) = \sum C_i \vec{\chi}_i \quad (27)$$

Substitution to the path integral leads to the Gaussian integrations over the coefficients C_i

$$\int D\delta\vec{r}(\tau) e^{-\frac{1}{2}\delta^2 S} = (\sqrt{2\pi})^N (\det' \hat{A})^{-1/2} \int \frac{dC_\phi}{\sqrt{2\pi}} \int \frac{dC_\tau}{\sqrt{2\pi}} \int \frac{dC_-}{\sqrt{2\pi}} e^{-\frac{1}{2}C_-^2 \lambda_-}$$

where $\det' \hat{A}$ denotes product of the eigenvalues of \hat{A} omitting the zero eigenvalues λ_ϕ , λ_τ and the negative one λ_- . They require special treatment and we will pay attention to them in the next sections.

It is convenient to express the resulting survival amplitude $G(\vec{0}, T, \vec{0}, -T)$ in terms of that one for pure parabolic well, that coincides with the contribution of the trivial classical trajectory $r_{cl}^\vec{r} \equiv 0$ up to the second order

$$\frac{Z_1}{Z_0} = e^{-S_{cl}} \left[\frac{\det' \hat{A}}{\det \hat{A}_0} \right]^{-1/2} \int \frac{dC_\phi}{\sqrt{2\pi}} \int \frac{dC_\tau}{\sqrt{2\pi}} \int \frac{dC_-}{\sqrt{2\pi}} e^{-\frac{1}{2}C_-^2 \lambda_-} \quad (28)$$

in this formula Z_1 defines single instanton contribution, while Z_0 is reserved for the trivial trajectory.

In the multidimensional case [Pap75, LS77] the ratio of the determinant $\det' \hat{A}$ and $\det \hat{A}_0$ can be expressed through that one of the determinants J and J_0 of Jacobi fields

$$\frac{\det' \hat{A}}{\det \hat{A}_0} = \frac{J}{J_0 \lambda_\phi \lambda_\tau \lambda_-} \quad (2.9)$$

The Jacobi fields satisfy.

$$\frac{d}{dt} \left(\frac{\partial^2 L}{\partial x_i \partial x_l} J_{lk} \right) + \left(\frac{\partial^2 L}{\partial x_i \partial x_l} - \frac{\partial^2 L}{\partial x_l \partial x_i} \right) J_{lk} + \left[\frac{d}{dt} \left(\frac{\partial^2 L}{\partial x_i \partial x_l} \right) - \frac{\partial^2 L}{\partial x_i \partial x_l} \right] J_{lk} = 0 \quad (2.10)$$

with boundary conditions

$$J_{ik} = 0, \quad \frac{\partial J_{ik}}{\partial t} = \frac{1}{m} \delta_{ik} = \delta_{ik}$$

The determinant J_0 as well as the eigenvalues in the formula (2.9) will be calculated later. Now we begin with evaluation of J .

The system of four differential equations of the second order (2.10) written for the Lagrangian (2.3) decouples into two subsystems, each one of the form

$$\begin{cases} -\xi + \omega_c \eta + U_x'' \xi + U_{xy}'' \eta = 0 \\ -\eta - \omega_c \xi + U_y'' \eta + U_{xy}'' \xi = 0 \end{cases} \quad (2.11)$$

or in terms of the operator \hat{A} introduced above

$$\hat{A} \vec{\varphi}(\tau) = 0, \quad \text{with} \quad \vec{\varphi}(\tau) = \begin{pmatrix} \xi \\ \eta \end{pmatrix}$$

The boundary conditions are

$$\xi(-T) = 0, \quad \xi(T) = 1, \quad \eta(-T) = 0, \quad \eta(T) = 0 \quad (2.12)$$

for the first subsystem (for which $\xi \equiv J_{xx}$, $\eta \equiv J_{yx}$), and

$$\xi(-T) = 0, \quad \xi(T) = 0, \quad \eta(-T) = 0, \quad \eta(T) = 1 \quad (2.13)$$

for the second one ($\xi \equiv J_{yx}, \eta \equiv J_{yy}$)

Let us find 4 independent solutions of the system. Two solutions of this problem are the zero eigenmodes, corresponding to the τ - and ϕ -symmetries. They can be easily found by differentiating the classical trajectory (2.5) with respect to τ and ϕ_0 . One can check by straightforward substitution that the following solutions are indeed zero-modes of the system

ϕ -mode

$$\vec{\varphi}_1(\tau) \equiv \begin{pmatrix} \xi_1 \\ \eta_1 \end{pmatrix} = \frac{1}{\cosh \Omega \tau} \begin{pmatrix} \sin \frac{\omega_c \tau}{2} \\ \cos \frac{\omega_c \tau}{2} \end{pmatrix}$$

τ -mode

$$\vec{\varphi}_2(\tau) \equiv \begin{pmatrix} \xi_2 \\ \eta_2 \end{pmatrix} = \frac{\sinh \Omega \tau}{\cosh^2 \Omega \tau} \begin{pmatrix} -\cos \frac{\omega_c \tau}{2} \\ \sin \frac{\omega_c \tau}{2} \end{pmatrix}$$

where we have chosen the time zero mode without the ϕ -shifting term, $\phi_0 = 0$

There are two more solutions left. It could seem sophisticated to find them, however we will use the following trick. Suppose we deal with a 1-dimensional case. If one solution of the second order homogeneous differential equation (written in the Liouville form) is

$$f = \frac{1}{\cosh \Omega \tau}$$

then the second one can be found as (for example [But68] or [Kle00]-2.7.4)

$$g = f \int^t \frac{dt'}{f(t')^2} = \frac{\sinh \Omega \tau}{2\Omega} + \frac{\tau}{2 \cosh \Omega \tau}$$

and if

$$f = \frac{\sinh \Omega \tau}{\cosh^2 \Omega \tau}$$

the second one is

$$g = f \int^t \frac{dt'}{f(t')^2} = \frac{1}{\cosh \Omega \tau} = \frac{\sinh^2 \Omega \tau}{2\Omega \cosh \Omega \tau} + \frac{3}{2} \tau \frac{\sinh \Omega \tau}{\cosh^2 \Omega \tau} - \frac{1}{\Omega \cosh \Omega \tau}$$

The idea to take the anzats in the similar form multiplied by sines or cosines turns out to be successful. Indeed, making a straightforward substitution of functions

$$\vec{\varphi}_3(\tau) \equiv \begin{pmatrix} \xi_3 \\ \eta_3 \end{pmatrix} = \left[\frac{\sinh \Omega \tau}{2\Omega} + \frac{\tau}{2 \cosh \Omega \tau} \right] \begin{pmatrix} \sin \frac{\omega_c \tau}{2} \\ \cos \frac{\omega_c \tau}{2} \end{pmatrix}$$

$$\vec{\varphi}_4(\tau) \equiv \begin{pmatrix} \xi_4 \\ \eta_4 \end{pmatrix} = \left[\frac{\sinh^2 \Omega \tau}{2\Omega \cosh \Omega \tau} + \frac{3}{2} \tau \frac{\sinh \Omega \tau}{\cosh^2 \Omega \tau} - \frac{1}{\Omega \cosh \Omega \tau} \right] \begin{pmatrix} -\cos \frac{\omega_c \tau}{2} \\ \sin \frac{\omega_c \tau}{2} \end{pmatrix}$$

into the system (2 11), we conclude that they are indeed the solutions we were looking for

Let us analyze the properties of this 4 independent solutions. It is easy to note that

$$\eta_1(\tau), \eta_2(\tau), \xi_3(\tau), \xi_4(\tau) \text{ are EVEN functions} \quad (2 14)$$

$$\xi_1(\tau), \xi_2(\tau), \eta_3(\tau), \eta_4(\tau) \text{ are ODD functions}$$

These important properties will be used in future for further calculations

At last we are able to find the solution of the system, satisfying the desired boundary conditions (2 12) and (2 13). Expanding

$$\vec{\varphi}(\tau) = \sum_{i=1}^4 c_i \vec{\varphi}_i(\tau)$$

we get the coefficients

$$c_1 = -\xi_3(-T), \quad c_2 = -\xi_4(-T), \quad c_3 = \xi_1(-T), \quad c_4 = \xi_2(-T)$$

for the vector $\vec{\varphi}(\tau) = \begin{pmatrix} J_{x\tau} \\ J_{y\tau} \end{pmatrix}$, and

$$d_1 = -\eta_3(-T), \quad d_2 = -\eta_4(-T), \quad d_3 = \eta_1(-T) \quad d_4 = \eta_2(-T)$$

for $\vec{\varphi}(\tau) = \begin{pmatrix} J_{xy} \\ J_{yy} \end{pmatrix}$

Now let us look at their behavior in the limit $T \rightarrow \infty$. For simplicity we can choose T in such a way that $\sin \frac{\omega_c T}{2} = 0$ and $\cos \frac{\omega_c T}{2} = 1$. Obviously, the final result must not depend on our specific choice of T , hence choosing T in this way we get significant simplification.

$$\xi_1(T) = 0, \quad \xi_2(T) \simeq -2e^{-\Omega T}, \quad \xi_3(T) = 0, \quad \xi_4(T) \simeq -\frac{1}{4\Omega}e^{\Omega T}, \quad (2.15)$$

$$\eta_1(T) \simeq 2e^{-\Omega T}, \quad \eta_2(T) = 0, \quad \eta_3(T) \simeq \frac{1}{4\Omega}e^{\Omega T}, \quad \eta_4(T) = 0 \quad (2.16)$$

and

$$\xi_1(-T) = 0, \quad \xi_2(-T) \simeq 2e^{-\Omega T}, \quad \xi_3(-T) = 0, \quad \xi_4(-T) \simeq -\frac{1}{4\Omega}e^{\Omega T},$$

$$\eta_1(-T) \simeq 2e^{-\Omega T}, \quad \eta_2(-T) = 0, \quad \eta_3(-T) \simeq -\frac{1}{4\Omega}e^{\Omega T}, \quad \eta_4(-T) = 0$$

Bearing this in mind we rewrite our coefficients in the following asymptotic form

$$c_1 = 0, \quad c_2 \simeq \frac{1}{4\Omega}e^{\Omega T}, \quad c_3 = 0, \quad c_4 \simeq 2e^{-\Omega T}$$

$$d_1 \simeq \frac{1}{4\Omega}e^{\Omega T}, \quad d_2 = 0, \quad d_3 \simeq 2e^{-\Omega T}, \quad d_4 = 0$$

Finally, the determinant J can be found

$$J = \det \begin{pmatrix} J_{xy} & J_{yx} \\ J_{yx} & J_{yy} \end{pmatrix} \simeq -\frac{1}{\Omega^2}$$

2.5 Elimination of zero eigenvalues

Now we need to get rid of the zero eigenvalues in the determinant J . This could be done by several ways. One could introduce eigenvalue λ as a small parameter, perturbing the system of differential equations and take the limit $\lambda \rightarrow 0$ of the determinant divided by λ^2 at the end (as we have two zero eigenvalues). Note, that this limit must be taken *after* the limit $T \rightarrow \infty$, as the zero eigenvalues are not exactly zero but tend to it as an exponential of T . However this requires the precision at

least $o(\lambda^2)$. Thus it seems more convenient to eliminate λ_ϕ and λ_τ separately using the boundary perturbation method, just looking at the behavior of these eigenvalues at large T . As has been mentioned above we must expect exponential dependence of T .

Consider the Green function

$$\hat{A}\hat{G}(\tau, \tau') = -\hat{I}\delta(\tau - \tau') \quad (2.17)$$

The reason to introduce the minus sign into the definition will be clear below: we will receive just the same boundary conditions for the system of differential equations that was solved earlier. The boundary conditions for the Green function are

$$\hat{G}(-T, \tau') = \hat{0}, \quad \frac{\partial \hat{G}}{\partial \tau}(-T, \tau') = \hat{0} \quad \forall \tau' \quad (2.18)$$

Then the general solution of $\hat{A}\vec{\psi} = \lambda_0\vec{\psi}$ is

$$\vec{\psi} = \vec{\psi}_0 - \lambda_0 \int_{-T}^T \hat{G}(\tau, \tau') \vec{\psi}(\tau') d\tau'$$

where $\vec{\psi}_0$ is a solution of the homogeneous equation $\hat{A}\vec{\psi}_0 = 0$. The eigenvalues λ_ϕ and λ_t can be calculated requiring $\vec{\psi}(-T)$ and $\vec{\psi}(T)$ to be strictly zero (note, that the zero modes that we have found early do not satisfy these boundary conditions exactly for finite values of T , but only in the limit $T \rightarrow \infty$). This leads to the following conditions

$$\vec{\psi}_0(-T) = 0 \quad \text{and} \quad \vec{\psi}_0(T) - \lambda_0 \int_{-T}^T \hat{G}(T, \tau') \vec{\psi}_0(\tau') d\tau' = 0$$

where we have made the Born approximation substituting $\vec{\psi}$ by $\vec{\psi}_0$ inside the integral as λ_0 is small.

First let us find $\lambda_0 \equiv \lambda_\phi$. Then the solution of homogeneous system can be expressed via ϕ -zero mode and other solutions as

$$\vec{\psi}_0 = \vec{\varphi}_1 + \alpha \vec{\varphi}_2 + \beta \vec{\varphi}_3 + \gamma \vec{\varphi}_4$$

and the boundary conditions become

$$\begin{cases} \vec{\varphi}_1(-T) + \alpha\vec{\varphi}_2(-T) + \beta\vec{\varphi}_3(-T) + \gamma\vec{\varphi}_4(-T) = 0 \\ \vec{\varphi}_1(T) + \alpha\vec{\varphi}_2(T) + \beta\vec{\varphi}_3(T) + \gamma\vec{\varphi}_4(T) = \lambda_\phi \int_{-T}^T \hat{G}(T, \tau') \vec{\varphi}_1(\tau') d\tau' \end{cases} \quad (2.19)$$

In the last formula the corrections were neglected inside the integral, as they give less contribution than $\vec{\varphi}_1$ (more strictly one can find the values of the coefficients from the equations below, substitute them into this integral and prove that it is indeed the case)

Taking the same T , chosen so that $\sin \frac{\omega_c T}{2} = 0$ and $\cos \frac{\omega_c T}{2} = 1$, we get

$$\begin{cases} \begin{pmatrix} 0 \\ 2e^{-\Omega T} \end{pmatrix} + \alpha \begin{pmatrix} 2e^{-\Omega T} \\ 0 \end{pmatrix} + \beta \begin{pmatrix} 0 \\ -\frac{1}{4\Omega} e^{\Omega T} \end{pmatrix} + \gamma \begin{pmatrix} -\frac{1}{4\Omega} e^{\Omega T} \\ 0 \end{pmatrix} = 0 \\ \begin{pmatrix} 0 \\ 2e^{-\Omega T} \end{pmatrix} + \alpha \begin{pmatrix} -2e^{-\Omega T} \\ 0 \end{pmatrix} + \beta \begin{pmatrix} 0 \\ \frac{1}{4\Omega} e^{\Omega T} \end{pmatrix} + \gamma \begin{pmatrix} -\frac{1}{4\Omega} e^{\Omega T} \\ 0 \end{pmatrix} = \lambda_\phi \int_{-T}^T \hat{G}(T, \tau') \vec{\varphi}_1(\tau') d\tau' \end{cases}$$

Note, that we have the products of two functions of τ' inside the integral, that are either even or odd (2.14). Thus only that terms contribute, that consist of functions, both even or odd at the same time. Using the explicit form the Green function from the next section (2.21) we get the following expression for the integral

$$\int_{-T}^T \hat{G}(T, \tau') \vec{\varphi}_1(\tau') d\tau' = \frac{e^{\Omega T}}{4\Omega} \int_{-T}^T \begin{pmatrix} -\xi_2(\tau')\xi_1(\tau') - \eta_2(\tau')\eta_1(\tau') \\ \xi_1(\tau')^2 + \eta_1(\tau')^2 \end{pmatrix} d\tau'$$

The two equations from which the desired eigenvalue can be determined are

$$\begin{cases} 2e^{-\Omega T} - \beta \frac{1}{4\Omega} e^{\Omega T} = 0 \\ 2e^{-\Omega T} + \beta \frac{1}{4\Omega} e^{\Omega T} = \lambda_\phi \frac{e^{\Omega T}}{4\Omega} \int_{-T}^T (\xi_1(\tau')^2 + \eta_1(\tau')^2) d\tau' \end{cases}$$

In the limit of large T this leads to (see Appendix)

$$\lambda_\phi \simeq 8\Omega^2 e^{-2\Omega T}$$

Using the same procedure we find the second zero-eigenvalue λ_τ . Decomposing the solution of the homogeneous system as

$$\vec{\psi}_0 = \vec{\varphi}_2 + \alpha\vec{\varphi}_1 + \beta\vec{\varphi}_3 + \gamma\vec{\varphi}_4$$

we write the boundary condition

$$\begin{cases} \vec{\varphi}_2(-T) + \alpha\vec{\varphi}_1(-T) + \beta\vec{\varphi}_3(-T) + \gamma\vec{\varphi}_4(-T) = 0 \\ \vec{\varphi}_2(T) + \alpha\vec{\varphi}_1(T) + \beta\vec{\varphi}_3(T) + \gamma\vec{\varphi}_4(T) = \lambda_\tau \int_{-T}^T \hat{G}(T, \tau') \vec{\varphi}_2(\tau') d\tau' \end{cases} \quad (2.20)$$

Eventually, we get

$$\lambda_\tau \simeq 24\Omega^2 e^{-2\Omega T}$$

Note, that λ_τ has the same form as for the 1-dimensional case [Sch81] (there $\epsilon \rightarrow \frac{\Omega^2}{2}$ and the operator, for which the eigenvalue is calculated is defined two times smaller than our \hat{A}), but the frequency Ω is dependent on magnetic field now $\Omega = \sqrt{\omega^2 - \omega_c^2/4}$

2.6 Calculation of the Green function

The Green function, satisfying (2.17) and (2.18) has the next matrix form:

$$\hat{G}(\tau, \tau') = \begin{pmatrix} g_{11} & g_{12} \\ g_{21} & g_{22} \end{pmatrix}$$

where $g_{ij} = g_{ij}(\tau, \tau')$

The equation (2.17) splits into two independent subsystems

$$\hat{A} \begin{pmatrix} g_{11} \\ g_{21} \end{pmatrix} = \begin{pmatrix} -\delta(\tau - \tau') \\ 0 \end{pmatrix}$$

and

$$\hat{A} \begin{pmatrix} g_{12} \\ g_{22} \end{pmatrix} = \begin{pmatrix} 0 \\ -\delta(\tau - \tau') \end{pmatrix}$$

with zero initial conditions following from (2.18) for both of them

Consider the first one. It corresponds to the homogeneous system considered above in the regions $\tau < \tau'$ and $\tau > \tau'$. In that terms $g_{11}(\tau, \tau') \equiv \xi(\tau)$ and $g_{21}(\tau, \tau') \equiv \eta(\tau)$. Both "left" and "right" solutions must be connected in such a way, that the delta function comes out. If we integrate the system over a small interval with the joint inside

$$\begin{cases} -\xi|_{\tau'-\epsilon}^{\tau'+\epsilon} + \omega_c \eta|_{\tau'-\epsilon}^{\tau'+\epsilon} + \int_{\tau'-\epsilon}^{\tau'+\epsilon} (U_x'' \xi + U_{xy}'' \eta) = -1 \\ -\eta|_{\tau'-\epsilon}^{\tau'+\epsilon} - \omega_c \xi|_{\tau'-\epsilon}^{\tau'+\epsilon} + \int_{\tau'-\epsilon}^{\tau'+\epsilon} (U_y'' \eta + U_{xy}'' \xi) = 0 \end{cases}$$

as ξ and η are continuous on the joint, the last terms at the left hand sides of the equations tend to zero. Obviously, the solution in the "left" region ($\tau < \tau'$) is the trivial one $\xi(\tau)|_{\tau < \tau'} = 0$, $\eta(\tau)|_{\tau < \tau'} = 0$. Thus we get the initial conditions for the "right" one

$$\begin{cases} \xi(\tau)|_{\tau=\tau'+\epsilon} = 1 \\ \eta(\tau)|_{\tau=\tau'+\epsilon} = 0 \end{cases}$$

Together with two other conditions coming from the continuity on the border of two regions, we have

$$\xi(\tau') = 0, \quad \xi(\tau') = 1, \quad \eta(\tau') = 0, \quad \eta(\tau') = 0$$

With the replacement $\tau' \rightarrow -T$ this boundary conditions exactly coincide with (2.12) (and (2.13) for the second subsystem). Thus the coefficients (that actually are functions of τ')

$$\begin{aligned} c_1 &= -\xi_3(\tau'), & c_2 &= -\xi_1(\tau'), & c_3 &= \xi_1(\tau'), & c_4 &= \xi_2(\tau') \\ d_1 &= -\eta_3(\tau'), & d_2 &= -\eta_1(\tau'), & d_3 &= \eta_1(\tau'), & d_4 &= \eta_2(\tau') \end{aligned}$$

Hence the Green function becomes

$$\hat{G}(\tau, \tau') = \begin{pmatrix} g_{11} & g_{12} \\ g_{21} & g_{22} \end{pmatrix} = \theta(\tau - \tau') \left(\sum_{i=1}^4 c_i(\tau') \vec{\varphi}_i(\tau), \sum_{i=1}^4 d_i(\tau') \vec{\varphi}_i(\tau) \right)$$

Using the asymptotic forms (2.15) for $\tau = T$ we have

$$\hat{G}(T, \tau') \simeq \theta(T - \tau') \begin{pmatrix} -\frac{1}{4\Omega} e^{\Omega T} \xi_2(\tau') + 2e^{-\Omega T} \xi_4(\tau') & -\frac{1}{4\Omega} e^{\Omega T} \eta_2(\tau') + 2e^{-\Omega T} \eta_4(\tau') \\ \frac{1}{4\Omega} e^{\Omega T} \xi_1(\tau') - 2e^{-\Omega T} \xi_3(\tau') & \frac{1}{4\Omega} e^{\Omega T} \eta_1(\tau') - 2e^{-\Omega T} \eta_3(\tau') \end{pmatrix} \quad (2.21)$$

2.7 Integrals over the peculiar eigenmodes

Having found the determinant J and the zero eigenvalues, the integrals over zero modes left to be evaluated explicitly, as they require special treatment. Recall that the ϕ - and τ - modes were found differentiating the classical trajectory $\vec{r}_{cl}(\tau)$. We can express \vec{r}_{cl} through these modes

$$\vec{r}_{cl} = \frac{\Omega}{\sqrt{2\alpha}} \left[-\frac{\omega_c}{2} \vec{\varphi}_1 + \Omega \vec{\varphi}_2 \right]$$

$$\frac{\partial \vec{r}_{cl}}{\partial \phi_0} \Big|_{\phi_0=0} = \frac{\Omega}{\sqrt{2\alpha}} \vec{\varphi}_1$$

so that

$$\vec{r}_{cl}(\tau + d\tau) \Big|_{\phi_0=d\phi} \simeq \vec{r}_{cl}(\tau) \Big|_{\phi_0=0} + \vec{r}_{cl} d\tau + \frac{\partial \vec{r}_{cl}}{\partial \phi_0} \Big|_{\phi_0=0} d\phi =$$

$$\vec{r}_{cl}(\tau) \Big|_{\phi_0=0} - \frac{\Omega}{\sqrt{2\alpha}} \frac{\omega_c}{2} \vec{\varphi}_1 d\tau + \frac{\Omega}{\sqrt{2\alpha}} \Omega \vec{\varphi}_2 d\tau + \frac{\Omega}{\sqrt{2\alpha}} \vec{\varphi}_1 d\phi$$

This Taylor series needs to be compared with our expansion (2.7) over the normalized eigenfunction of the operator \hat{A}

$$\vec{r} = \vec{r}_{cl} + C_\phi \vec{\chi}_\phi + C_\tau \vec{\chi}_\tau + \dots = \vec{r}_{cl} + C_\phi \frac{\vec{\varphi}_1}{\|\vec{\varphi}_1\|} + C_\tau \frac{\vec{\varphi}_2}{\|\vec{\varphi}_2\|} + \dots$$

where the zero eigenmodes were extracted from the sum explicitly. In order to complete the integration over the zero modes, the integrals over the coefficients C_ϕ , C_τ must be transformed to the integrals over angular and time positions. The expressions above

make clear the procedure of changing variables from C_ϕ, C_τ to ϕ, τ

$$\begin{cases} \frac{dC_\phi}{\|\vec{\varphi}_1\|} = -\frac{\Omega}{\sqrt{2\alpha}} \frac{\omega_c}{2} d\tau + \frac{\Omega}{\sqrt{2\alpha}} d\phi \\ \frac{dC_\tau}{\|\vec{\varphi}_2\|} = \frac{\Omega^2}{\sqrt{2\alpha}} d\tau \end{cases}$$

The Jacobian of this transformation is

$$J_{\phi\tau} = \det \begin{pmatrix} \frac{\partial C_\phi}{\partial \phi} & \frac{\partial C_\phi}{\partial \tau} \\ \frac{\partial C_\tau}{\partial \phi} & \frac{\partial C_\tau}{\partial \tau} \end{pmatrix} = \det \begin{pmatrix} \frac{\Omega}{\sqrt{2\alpha}} \|\vec{\varphi}_1\| & -\frac{\Omega}{\sqrt{2\alpha}} \frac{\omega_c}{2} \|\vec{\varphi}_1\| \\ 0 & \frac{\Omega^2}{\sqrt{2\alpha}} \|\vec{\varphi}_2\| \end{pmatrix} = \frac{\Omega^3}{2\alpha} \|\vec{\varphi}_1\| \|\vec{\varphi}_2\| = \frac{\Omega^2}{\sqrt{3\alpha}}$$

where we have substituted $\|\vec{\varphi}_1\|$ and $\|\vec{\varphi}_2\|$, found to be (see Appendix)

$$\|\vec{\varphi}_1\| = \sqrt{\frac{2}{\Omega}} \quad \text{and} \quad \|\vec{\varphi}_2\| = \sqrt{\frac{2}{3\Omega}}$$

Let us pay attention to the negative eigenvalue. Physical intuition tells that there must be only one negative eigenmode, corresponding to the direction in the functional space associated with escape of the particle. One can use also oscillation theorems to determine how many eigenvalues less than λ_τ and λ_ϕ left. For one-dimensional Shrodinger equation this is nothing but number of nodes of the eigenfunction that tells its position number in the ordered series of corresponding eigenvalues $\lambda_0 < \lambda_1 < \lambda_2 < \dots$. We have managed with the negative eigenvalue just as it was done in one-dimensional case (see [Col77, CC77, Col85] for details). There an analytical continuation of the Gaussian integral over negative eigenmode has been used. A special feature is the factor $\frac{1}{2}$, arising from a half of the Gaussian peak. The integration over the other half axis turns out to be fake. Thus the contribution of the negative eigenmode integral is

$$\int \frac{dC_-}{\sqrt{2\pi}} e^{-\frac{1}{2}C_-^2 \lambda_-} = \pm \frac{i}{2\sqrt{-\lambda_-}}$$

The sign here depends on how the analytical continuation is done. In future we will omit this sign as it is not important. The precise value of λ_- is not important also as it cancel with λ_- in the formula for the ratio of the determinants (2.9)

Eventually,

$$\int \frac{dC_\phi}{\sqrt{2\pi}} \int \frac{dC_\tau}{\sqrt{2\pi}} \int \frac{dC_-}{\sqrt{2\pi}} e^{-\frac{1}{2}C_-^2 \lambda_-} = \frac{1}{2\sqrt{-\lambda_-}} \frac{1}{2\pi} \frac{\Omega^2}{\sqrt{3\alpha}} \int_0^{2\pi} d\phi \int_{-T}^T d\tau \quad (2.22)$$

We will retain this integrals unsolved for some time. Note, that the integration over the angular variable ϕ appears *naturally* from the integration over C_ϕ along the direction in the functional space corresponding to the ϕ -symmetry zero mode. This is nothing to do with path integral written in polar coordinates, for which an additional care must be taken.

2.8 Contribution of the trivial trajectory

The determinant J_0 of the Jacobi fields along the trivial trajectory $\vec{r}_{cl} = 0$ is estimated by analogy with J . The calculation is rather simple now.

$$\hat{A}_0 = \begin{pmatrix} -\partial_\tau^2 + \Omega^2 + \omega_c^2/4 & \omega_c \partial_\tau \\ -\omega_c \partial_\tau & -\partial_\tau^2 + \Omega^2 + \omega_c^2/4 \end{pmatrix}$$

So that the system $\hat{A}_0 \vec{\varphi}(\tau) = 0$ reads

$$\begin{cases} -\xi + \omega_c \eta + (\Omega^2 + \omega_c^2/4)\xi = 0 \\ -\eta - \omega_c \xi + (\Omega^2 + \omega_c^2/4)\eta = 0 \end{cases}$$

with the same boundary conditions (2.12) and (2.13). The system can be solved by standard methods. We only write the final answer for the determinants of the Jacobi fields in case of the pure parabolic potential

$$J_0 \simeq \frac{e^{4\Omega T}}{4\Omega^2}$$

2.9 Instanton gas

Finally, substituting the determinants and eigenvalues found above to (2 8) and (2 9), we obtain the contribution of one instanton trajectory (more strictly of a group of equivalent instantons with different time and angular positions, as we have integrated over the zero modes already)

$$\frac{Z_1}{Z_0} = e^{-S_{cl}} \left[\frac{J}{J_0 \lambda_\phi \lambda_\tau \lambda_-} \right]^{-1/2} \frac{i}{2\sqrt{-\lambda_-}} \frac{1}{2\pi} \frac{\Omega^2}{\sqrt{3}\alpha} \int_0^{2\pi} d\phi \int_{-T}^T d\tau = e^{-S_{cl}} K \int_0^{2\pi} d\phi \int_{-T}^T d\tau$$

with

$$K = \frac{i2\Omega^4}{\alpha 2\pi}$$

We must also take into account the contribution of the multi-instanton trajectories. Also, we must integrate over their positions both in time and angular space. Thus

$$\frac{Z_n}{Z_0} = e^{-nS_{cl}} K^n \int_0^{2\pi} d\phi_1 \int_{-T}^T d\tau_1 \int_0^{2\pi} d\phi_2 \int_{-T}^{\tau_1} d\tau_2 \dots \int_0^{2\pi} d\phi_n \int_{-T}^{\tau_{n-1}} d\tau_n = e^{-nS_{cl}} K^n \frac{(2\pi 2T)^n}{n!}$$

represents the contribution of a trajectory with n instantons distributed in the time interval $(-T, T)$ and arbitrary directed with respect to the angular coordinate. Finally, we must sum all the contributions to get the survival amplitude

$$G(\vec{0}, T, \vec{0}, -T) = Z_0 + Z_1 + Z_2 + \dots = Z_0 \sum_{n=0}^{\infty} e^{-nS_{cl}} K^n \frac{(2\pi 2T)^n}{n!} = Z_0 \exp(2\pi 2TK e^{-S_{cl}})$$

Thus the probability decay rate is

$$\Gamma = 2ImE = 4\pi K e^{-S_{cl}} = \frac{4\Omega^4}{\alpha} e^{-S_{cl}} \quad (2 23)$$

This simple expression is just that one, that we were looking for. To complete the calculation we must transform back to the real cyclotron frequencies $\omega_c \rightarrow -i\omega_c$, so that the frequency Ω becomes a square root of the sum now $\Omega = \sqrt{\omega^2 + \omega_c^2/4}$

We can rewrite the formula (2 23) in the following way using the expression for the classical action (2 4)

$$\Gamma = 12\Omega S_{cl} e^{-S_{cl}} = 12\Omega (\sqrt{S_{cl}})^2 e^{-S_{cl}}$$

The factor $\sqrt{S_{cl}}$ has appeared twice here, just as much as the number of zero modes
This is a common situation in the instanton technique (e.g. Coleman, "Aspects of
Symmetry" [Col85] p 337 gets 4 factors $\sqrt{S_{cl}}$ in case of four zero modes)

Chapter 3

WKB method

3.1 Hamiltonian

Now we will get the same result using different method. Even the way, in what we deal with the magnetic field is different here. The Hamiltonian corresponding to our initial system (2.1) is

$$\hat{H} = \frac{(p_x - \frac{e}{c}A_x)^2}{2} + \frac{(p_y - \frac{e}{c}A_y)^2}{2} + U(r), \quad U(r) = \frac{\omega^2}{2}r^2 - \alpha r^4$$

Using the same gauge $\vec{A} = (-\frac{yB}{2}, \frac{xB}{2}, 0)$, it can be rewritten as follows

$$\hat{H} = \frac{p_x^2 + p_y^2}{2} + \frac{\omega_c^2}{8}(x^2 + y^2) - \frac{\omega_c}{2}L + U(r) = \hat{H}_0 - \frac{\omega_c}{2}\hat{L}$$

where L is angular momentum operator $L = xp_y - yp_x$ and we have defined

$$\hat{H}_0 = \frac{p_x^2 + p_y^2}{2} + \frac{\omega_c^2}{8}(x^2 + y^2) + U(r)$$

3.2 The use of symmetries

The important point here is that \hat{H}_0 introduced above commutes with the angular momentum $[\hat{H}_0, \hat{L}] = 0$. This is because of the rotational invariance of the system, as the potential (including the magnetic field term) in the Hamiltonian \hat{H}_0 is a pure function of radial distance $r = \sqrt{x^2 + y^2}$.

Consider the matrix $R(-\phi)$, rotating the vectors in the counterclockwise direction

$$R(-\phi) = \begin{pmatrix} \cos \phi & \sin \phi \\ -\sin \phi & \cos \phi \end{pmatrix}$$

Then the angular momentum operator \hat{L} generates rotations of the wave function.

$$e^{-i\hat{L}\phi}\psi(\vec{r}) = \psi(R(-\phi)\vec{r})$$

This can be seen as follows (e.g. [Tha00] p 219). One can find generator of the rotation unitary group by differentiating with respect to ϕ

$$\begin{aligned} i\frac{d}{d\phi}\psi(R(-\phi)\vec{r})|_{\phi=0} &= i\nabla\phi(R(-\phi)\vec{r})\frac{d}{d\phi}R(-\phi)\vec{r}|_{\phi=0} = \\ &= i\nabla\psi(\vec{r}) \begin{pmatrix} y \\ -x \end{pmatrix} = -i\left(x\frac{\partial}{\partial y} - y\frac{\partial}{\partial x}\right)\psi(\vec{r}) = \hat{L}\psi(\vec{r}) \end{aligned}$$

Thus \hat{L} is indeed the generator of the unitary group of rotations

With all this in mind, the amplitude (2.2) becomes

$$G(\vec{0}, T, \vec{0}, -T) = \langle \vec{0} | e^{-i2\hat{H}T} | \vec{0} \rangle = \langle \vec{0} | e^{-i2\hat{H}_0T} e^{i\omega_c\hat{L}T} | \vec{0} \rangle = \langle \vec{0} | e^{-i2\hat{H}_0T} | \vec{0} \rangle$$

as the rotation of the state $|\vec{0}\rangle$ is equal to itself. Thus the problem has reduced to finding the decay rate of the particle in the potential of the same shape with the renormalized frequency $\omega \rightarrow \sqrt{\omega^2 + \omega_c^2/4} \equiv \Omega$ in absence of the magnetic field

$$\hat{H} = \frac{p_x^2 + p_y^2}{2} + U_{eff}(r) \quad \text{with} \quad U_{eff}(r) = \frac{\Omega^2}{2}r^2 - \alpha r^4$$

3.3 WKB expansion

Schrodinger equation in polar coordinates reads

$$\left[-\frac{\hbar^2}{2} \left(\frac{\partial^2}{\partial r^2} + \frac{1}{r} \frac{\partial}{\partial r} + \frac{1}{r^2} \frac{\partial^2}{\partial \phi^2} \right) + U_{eff}(r) \right] \psi = E\psi$$

with $\hat{L} = -i\hbar \frac{\partial}{\partial \phi}$ and $\psi = e^{i\phi} f(r)$

$$\left[-\frac{\hbar^2}{2} \left(\frac{\partial^2}{\partial r^2} + \frac{1}{r} \frac{\partial}{\partial r} - \frac{l^2}{r^2} \right) + U_{eff}(r) \right] f(r) = Ef(r)$$

As we are interested in the tunneling from the lowest state we take $l = 0$. Consider ψ in the form $f(r) = e^{\frac{i}{\hbar} S(r)}$ with $S(r) = S_0 - i\hbar S_1 + \dots$ according to the standard WKB expansion

$$f(r) = e^{\frac{i}{\hbar} S(r)}$$

$$f'(r) = \left(\frac{i}{\hbar} S_0' + S_1' + \dots \right) e^{\frac{i}{\hbar} S(r)}$$

$$f''(r) = \left(-\frac{1}{\hbar^2} S_0'^2 + \frac{2i}{\hbar} S_0' S_1' + \frac{i}{\hbar} S_0'' + \dots \right) e^{\frac{i}{\hbar} S(r)}$$

Substituting to the Schrodinger equation above and equalizing terms near the same power of \hbar we get

$$\frac{1}{2} S_0'^2 + U_{eff}(r) = E$$

$$2S_0' S_1' + S_0'' + \frac{1}{r} S_0' = 0$$

From now we can assume $\hbar = 1$. The first equation gives

$$S_0 = \pm \int \sqrt{2(U_{eff}(r) - E)} \equiv \int p(r), \quad p(r) = \sqrt{2(U_{eff}(r) - E)}$$

Dividing the second one by S_0'

$$2S_1' + (\ln S_0')' + \frac{1}{r} = 0$$

that is also easily integrable. Eventually, we get the underbarrier WKB wave function in polar coordinates

$$\psi(r) = C \frac{1}{\sqrt{rp(r)}} \exp\left(-\int_{r_1}^r p(r) dr\right)$$

where r_1 is the first classical turning point corresponding to the energy E . The constant C can be found comparing the result with the normalized ground state wave function for the two-dimensional parabolic well

$$\psi(r) = \sqrt{\frac{\Omega}{\pi}} e^{-\frac{\Omega r^2}{2}}$$

For the underbarrier WKB wave function near the bottom (but far enough from the turning point, so that WKB works already) the integral under the exponent is approximated by

$$\int_{r_1}^r p(r) dr \approx \int_{r_1}^r \sqrt{\Omega^2 r^2 - 2E} dr = \frac{\Omega r^2}{2} - \frac{E}{2\Omega} - \frac{E}{2\Omega} \ln \frac{2r^2 \Omega^2}{E}$$

for E as a small parameter. Taking $E = \Omega$ as the lowest energy level for two-dimensional parabolic well and equalizing the both wavefunctions, we get

$$C \frac{1}{\sqrt{\Omega r^2}} e^{-\left[\frac{\Omega r^2}{2} - \frac{1}{2} - \frac{1}{2} \ln 2r^2 \Omega\right]} = \sqrt{\frac{\Omega}{\pi}} e^{-\frac{\Omega r^2}{2}}$$

where $p(r)$ was also decomposed up to the lowest order $p(r) \approx \Omega r$. All this leads to

$$C = \sqrt{\frac{\Omega}{2\pi e}}$$

The outgoing wave function ($r > r_2$, with r_2 as a second turning point outside the well)

$$\psi(r) = C \frac{1}{\sqrt{rp(r)}} \exp\left(-\int_{r_1}^{r_2} p(r) dr + i \int_{r_2}^r p(r) dr\right)$$

This is just the wave function, we are specially interested in. Using it, we can estimate density of the probability current

$$\begin{aligned}
 J &= \frac{i}{2} \left(\psi \frac{\partial}{\partial r} \psi^* - \psi^* \frac{\partial}{\partial r} \psi \right) = \frac{i}{2} \frac{C^2}{r p(r)} \exp \left(-2 \int_{r_1}^{r_2} p(r) dr \right) (-i p(r) - i p(r)) \\
 &= \frac{C^2}{r} \exp \left(-2 \int_{r_1}^{r_2} p(r) dr \right) = \frac{\Omega}{2\pi r e} \exp \left(-2 \int_{r_1}^{r_2} p(r) dr \right)
 \end{aligned}$$

We must integrate the current density over the circumference to get the total probability current coming outside the well

$$D = \int_0^{2\pi} 2\pi r J d\phi = \frac{\Omega}{e} e^{-W(E)}$$

As the wave function inside the well is normalized, this expression corresponds to the transition probability through the barrier, i.e. decay rate. We have denoted $W(E) = 2 \int_{r_1}^{r_2} p(r) dr$

3.4 Correspondence with the previous results

To link this result with the one, obtained by the instanton technique, we must represent the decay rate in terms of $W(0)$. This can be done as follows. We separate the integral into three parts

$$W(E)/2 = \int_{r_1}^{r'_1} p(r) dr + \int_{r'_1}^{r'_2} p(r) dr + \int_{r'_2}^{r_2} p(r) dr$$

Where the points r'_1 and r'_2 are chosen between the turning points r_1 and r_2 so, that the first integral is calculated keeping the quadratic term only of the potential, the second one is calculated making expansion in $E/U(r)$ and the last integral is calculated approximating the potential by a linear function near the turning point r_2

$$\int_{r_1}^{r'_1} p(r) dr \approx \int_{r_1}^{r'_1} \sqrt{\Omega^2 r^2 - 2E} dr = \int_0^{r'_1} \sqrt{2U_{eff}(r) - \frac{E}{2\Omega} - \frac{E}{2\Omega} \ln \frac{2r^2 \Omega^2}{E}}$$

$$\int_{r'_1}^{r'_2} p(r)dr \approx \int_{r'_1}^{r'_2} \sqrt{2U_{eff}(r)} - \int_{r'_1}^{r'_2} \frac{E}{\sqrt{2U_{eff}(r)}} dr =$$

$$= \int_{r'_1}^{r'_2} \sqrt{2U_{eff}(r)} + \frac{E}{\Omega} \ln \left| \frac{(\Omega + \sqrt{\Omega^2 - 2\alpha r'_2})r'_1}{(\Omega + \sqrt{\Omega^2 - 2\alpha r'_1})r'_2} \right|$$

Near the second turning point r_2 we approximate potential by a linear function with zero at the the point $r_0 = \Omega/\sqrt{2\alpha}$, such that $U_{eff}(r_0) = 0$

$$U_{eff}(r) \approx -\frac{\Omega^3}{\sqrt{2\alpha}}(r - r_0)$$

so that the third integral becomes

$$\int_{r'_2}^{r_2} p(r)dr \approx \int_{r'_2}^{r_2} \sqrt{2\left(\frac{\Omega^3}{\sqrt{2\alpha}}(r_0 - r) - E\right)} dr = \int_{r'_2}^{r_0} \sqrt{2U_{eff}(r)} dr - \frac{2\alpha E}{\Omega^3} \sqrt{2\left(\frac{\Omega^3}{\sqrt{2\alpha}}(r_0 - r'_2)\right)}$$

Combining this terms altogether and taking the limits $r'_1 \rightarrow 0$ and $r'_2 \rightarrow r_0$ we obtain

$$W(E) \approx W(0) - \frac{E}{\Omega} - \frac{E}{\Omega} \ln \left(\frac{4\Omega^4}{\alpha E} \right)$$

that gives

$$D = \frac{4\Omega^4}{\alpha} e^{-W(0)}$$

where

$$W(0) = 2 \int_0^{r_0} \sqrt{U_{eff}(r)} dr = 2 \int_0^{r_0} \sqrt{\Omega^2 r^2 - 2\alpha r^4} dr = \int_0^{r_0^2} \sqrt{\Omega^2 - 2\alpha r^2} dr^2 = \frac{\Omega^3}{3\alpha} \equiv S_{cl}$$

what coincides with S_{cl} (2.4). Evidently, using the different method we have got the same result (2.23) that was derived by the instanton technique

Chapter 4

Summary

Now we are able to calculate the expulsion magnetic field, at what the vortex leaves superconducting dot. Using the London approximation and the method of images, the potential well inside the disk can be estimated [BB94, BF96]

$$V(r) = \frac{d\Phi_0^2}{16\pi^2\lambda^2} \left[\frac{h^2}{4} + \ln(R/\xi) - h(1 - r^2) + \ln(1 - r^2) \right]$$

where $h = H\pi R^2/\Phi_0$ and r is the distance from the centre in units of the radius R . The minimum exists until the field $h = 1$. However, due to quantum tunneling the vortex leaves the well at higher $h > 1$. We approximate this potential by the inverted double well and use the formula for the decay rate calculated above to estimate the expulsion field. This leads to the next dependence on the radius of the disk shown on the Fig 4.1. For comparison we also present the typical dependence due to thermal activation process for some fixed temperature.

In deriving the formula for the decay rate using the instanton approach we have restricted ourselves to the small values of ω_c . In the WKB result we have not made such an assumption, so that the obtained formula turned out to be more general.

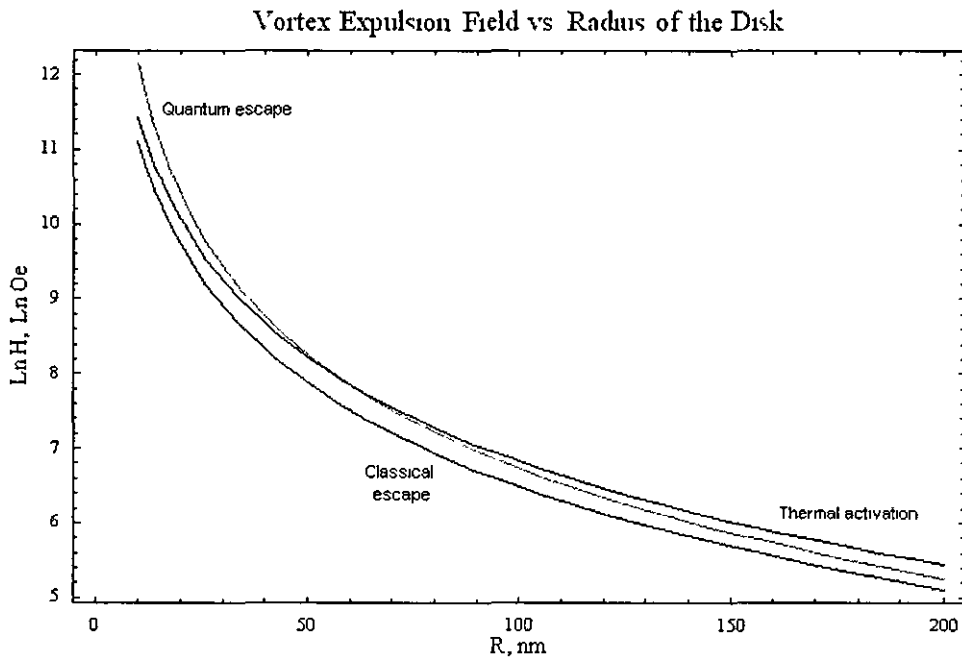


Figure 4.1 Dependence of the expulsion field on the radius of the HTSC disk. Expulsion field is characterized by the value of magnetic field at what an Abrikosov trapped by the surface barrier leaves the superconducting dot. As Abrikosov vortex carries magnetic flux, this process manifests itself as magnetic relaxation of the superconductor. Three mechanisms of magnetic relaxation are shown for comparison: pure classical escape, quantum escape and thermal activation at some fixed temperature.

Therefore, it is worthwhile to look at the instanton trajectories even for $\omega_c/2 \sim \omega$. In this regime the trajectories are spirals, spinning outwards and inwards close to the top of the hill. A question arises: how do the trajectories near the top "feel" the behavior of the potential on large distances and reproduce the right dependence of the decay rate on the 4th power term of the double well? Let us analyze this situation more carefully. During almost all the period of the instanton, the spirals are perpendicular

to the gradient direction whereas the velocities are small at the top, because of zero energy at the top. Thus both the trajectories and the action must depend strongly on high order derivatives of the potential, including the 4th power term.

Let us summarize the results

(1) The instanton technique has been successfully applied to 2D models in magnetic field

(ii) Analytical continuation in ω_c has been introduced to avoid the problem of imaginary action

(iii) Coincidence with standard WKB has been obtained

(iv) Decay rate of a superconducting quantum dot with a trapped Abrikosov vortex has been calculated

The instanton method is a non-perturbative method that plays a crucial role in quantum field theory and quantum mechanics [Col77, CC77, Col85]. The advantages of the instanton technique (IT) are: (i) Stronger than standard Wentzel-Kramers-Brillouin (WKB) method [LL65, KST00]. Generally, it is hard to tell whether WKB result is accurate, whereas the IT is controlled by well-defined expansion parameters. (ii) No connection formulas are needed. Indeed, in our calculations with the standard WKB method we were binding several solutions together – a wave function in a parabolic well with a wave function under the barrier. In the instanton method this procedure is absent. (iii) In some cases it is more accurate than WKB [GP77]. (iv) Instantons, as elementary excitations are topological objects. Configurations with different number of instantons are topologically distinct.

Appendix A: Useful integrals

The following definite integrals can be useful for the calculations arising in this problem

$$\int_{-\infty}^{\infty} \frac{dx}{\cosh^2 x} = 2$$

$$\int_{-\infty}^{\infty} \frac{\sinh^2 x}{\cosh^4 x} dx = \frac{2}{3}$$

$$\int_{-\infty}^{\infty} \frac{dx}{\cosh^4 x} = \frac{4}{3}$$

Appendix B: Faddeev-Popov procedure

There exists another way how the zero eigenvalues can be eliminated. This is so called Faddeev-Popov procedure [FP67, GP77] very useful for systems with constraints in quantum field theory.

As our initial path integral (2.6) is not properly defined because of overcounting of zero eigenmodes, we need to define correct measure of integration in order to disregard the contribution of the equivalent trajectories related by symmetry group transformations (in the field theory this usually corresponds to gauge transformations). Thus there are two constraints on our path integral

$$F_1[\vec{r}(\tau + \eta, \phi_0 + \theta)] \equiv \langle \vec{r}(\tau + \eta, \phi_0 + \theta), \vec{\varphi}_1(\tau, \phi_0) \rangle$$

$$F_2[\vec{r}(\tau + \eta, \phi_0 + \theta)] \equiv \langle \vec{r}(\tau + \eta, \phi_0 + \theta), \vec{\varphi}_2(\tau, \phi_0) \rangle$$

where φ_1 and φ_2 are zero modes associated with the classical trajectories (2.5). Consider the identity

$$\Delta[F_1[\vec{r}(\tau, \phi_0)], F_2[\vec{r}(\tau, \phi_0)]] \int_{-T}^T d\eta \int_0^{2\pi} d\theta \delta(F_1[\vec{r}(\tau + \eta, \phi_0 + \theta)]) \delta(F_2[\vec{r}(\tau + \eta, \phi_0 + \theta)]) \equiv 1 \quad (4.1)$$

where the Faddeev-Popov determinant $\Delta[F_1, F_2]$ is the Jacobian of transformation of integration variables Δ , as well as the action along the trajectories close to the classical ones, is invariant under translations in time and ϕ

$$\Delta[F_1[\vec{r}(\tau + \eta, \phi_0 + \theta)], F_2[\vec{r}(\tau + \eta, \phi_0 + \theta)]] = \Delta[F_1[\vec{r}(\tau, \phi_0)], F_2[\vec{r}(\tau, \phi_0)]]$$

Indeed, this can be easily proved by shifting variables inside the integral (4.1)

Introducing the identity (4.1) to the path integral (2.6)

$$\begin{aligned} \int D\vec{r} e^{-S[\vec{r}]} &= \\ &= \int_{-T}^T d\eta \int_0^{2\pi} d\theta \int D\vec{r} e^{-S[\vec{r}(\tau, \phi_0)]} \Delta[F_1, F_2] \delta(F_1[\vec{r}(\tau + \eta, \phi_0 + \theta)]) \delta(F_2[\vec{r}(\tau + \eta, \phi_0 + \theta)]) = \\ &= \int_{-T}^T d\eta \int_0^{2\pi} d\theta \int D\vec{r} e^{-S[\vec{r}(\tau, \phi_0)]} \Delta[F_1, F_2] \delta(F_1[\vec{r}(\tau, \phi_0)]) \delta(F_2[\vec{r}(\tau, \phi_0)]) \end{aligned}$$

where we have used the invariance both of the Faddeev-Popov determinant and the action as well as the identity $D\vec{r}(\tau + \eta, \phi_0 + \theta) = D\vec{r}(\tau, \phi_0)$. Thus we have transformed our integrations over zero modes to the integration over the groups of translational symmetry

The Faddeev-Popov determinant is found to be

$$\begin{aligned} \Delta[F_1, F_2] &= \det \begin{pmatrix} \frac{\partial F_1}{\partial \theta} & \frac{\partial F_1}{\partial \eta} \\ \frac{\partial F_2}{\partial \theta} & \frac{\partial F_2}{\partial \eta} \end{pmatrix}_{\theta=0, \eta=0} = \\ &= \det \begin{pmatrix} \langle \frac{\partial \vec{r}(\tau, \phi_0)}{\partial \phi_0}, \vec{\varphi}_1(\tau, \phi_0) \rangle & \langle \frac{\partial \vec{r}(\tau, \phi_0)}{\partial \tau}, \vec{\varphi}_1(\tau, \phi_0) \rangle \\ \langle \frac{\partial \vec{r}(\tau, \phi_0)}{\partial \phi_0}, \vec{\varphi}_2(\tau, \phi_0) \rangle & \langle \frac{\partial \vec{r}(\tau, \phi_0)}{\partial \tau}, \vec{\varphi}_2(\tau, \phi_0) \rangle \end{pmatrix} = \frac{\Omega^2}{\sqrt{3}\alpha} \end{aligned}$$

(compare with (2.22)) This is another way to take into account the contribution of zero modes

Part II

**SWITCHING PHENOMENA IN
LARGE JOSEPHSON
JUNCTIONS**

Chapter 5

Annular Josephson Junction of Intermediate Length

In this chapter we consider annular Josephson junctions of "intermediate lengths" In this way we call junctions whose size is bigger than Josephson penetration length λ_J (for example $10\lambda_J$ like in experiments [FWK⁺03]), but they still exhibit small-like switching characteristics, in particular, $T^{2/3}$ dependence of the standard deviation on temperature

5.1 Introduction

Thermal escape in Josephson devices associated with the transition from superconducting to resistive state has been studied for a very long time. Originally, it was Kramers who first estimated the probability of thermal escape from a metastable state [Kra40]. Small Josephson junctions (JJ) are among the most studied of all superconducting devices. There two types of escape, quantum and classical, have been observed. The classical or thermal escape usually arises at high temperatures while the quantum escape manifests itself at low temperatures.

The thermal or quantum escape in small Josephson junctions is equivalent to escape of a quantum particle from a metastable state. In this paper we investigate the thermal escape of an object which has an extended dimension, i.e. very different from such point like objects like particles. Such an extended object – let us call it a string – may arise in a long annular Josephson junction (AJJ). In contrast to a small Josephson junction the phase difference $\phi(x)$ in AJJ depends on the position on the ring x . The phase difference satisfies periodic boundary conditions $\phi(0) = \phi(L)$ where L is the circumference of the AJJ. Thus, the dependence $\phi(x)$ is associated with a string of length L . The string is a one-dimensional object in contrast to a small JJ that is zero-dimensional. Similar behavior appears for dislocations in solids. The issue of the classical and quantum escape of an extended object such as a string or dislocation from a metastable state has been the subject of long-term interest [KP70, PP72], which is still under intensive discussion [VSC⁺01, NLR⁺04]. In these papers it was suggested that if the extended object is very long the escape process begins with the escape of some part of the object, namely with the nucleation of a kink-antikink pair (or a fluxon-antifluxon pair in the case of the Josephson junction). Eventually, this nucleation process gives rise to the escape of the whole object such as a long string. However, if the size of a kink-antikink pair becomes comparable with the length of the string, the escape may arise via a different mechanism without nucleation of the pair.

We study a current-biased annular Josephson junction subjected to in-plane magnetic field. In recent years this system has attracted much of attention. Existing annular junctions are favorite extended objects to study dynamics of Josephson vortices subjected to an induced periodic potential. Their quantum switching of AJJ [FWK⁺03] has been experimentally observed and quantum dynamics of a single fluxon has been investigated in detail [WLL⁺03]. This prompts a possible application of AJJ for quantum computer implementation.

The use of the collective coordinate method in terms of vortex/antivortex positions

is an effective tool to describe very long JJ. However, for moderate length junctions the method gives some discrepancy with experimental data in the magnetic field dependence of the switching current and the standard deviation [FWK⁺03]. The experiments show increase and then saturation with magnetic field while the existing theory fails to predict the correct saturation. The reason is that effective size of a vortex-antivortex pair depends crucially on the applied bias and may even exceed the length of the junction. Thus, the description in terms of vortex-antivortex positions breaks down. In the present work we consider the situation when the escape of a string from a metastable state occurs in the form of a transition of the whole object homogeneously all along the junction. In this view, the vortex-antivortex pair may develop on the later stage of the phase evolution – *after* the escape occurred. Such behavior is expected for moderate length annular junctions at low temperatures.

In our calculations we start from basic statistical field theory principles. We consider a string describing a superconducting phase difference across the junction. In classical statistical mechanics a thermal activation of a string is described as a most optimal or a most probable fluctuation. In the framework of our approach, the saturation behavior found in experiments is naturally explained. Also, the critical current dependence on magnetic field is calculated. It perfectly fits the experimental data.

5.2 Formulation

Our main purpose is to investigate the switching of an annular Josephson junction from superconducting to resistive state. It occurs when a parallel magnetic field and a bias voltage are applied and reach some critical value. We introduce a field $\varphi(x)$ to denote the superconducting phase difference across the junction. In this view, the analogy with classical mechanics becomes clear. The field $\varphi(x)$ describes a string in the perturbed sine-Gordon potential. We analyze thermal fluctuation of this string

and find the most optimal fluctuation associated with thermal activated switching of the junction from superconducting to resistive state. We study the classical thermal activation and therefore we have to consider only stationary configurations of the phase difference $\varphi(x)$ across the junction. They are the only important ones since the other type of fluctuations give a negligible contribution in this limit. The energy of AJJ under parallel external magnetic field h and bias current γ applied may be described with the use of the following expression (we use normalized units)

$$V[\varphi] = \int_{-L/2}^{L/2} dx \left[\frac{\varphi_x^2}{2} + (1 - \cos \varphi) + \gamma \varphi + h \varphi \cos kx \right] \quad (5.1)$$

where $k = 2\pi/L$ and L is the circumference of the annular junction. The classical configurations associated with the extremal points of the energy functional, Eq (1) are given by the perturbed sine-Gordon equation (e.g. [MM96a, MM96b])

$$\varphi_{xx} - \sin \varphi - \gamma - h \cos kx = 0 \quad (5.2)$$

with periodic boundary conditions

$$\begin{cases} \varphi(-L/2) = \varphi(L/2) \\ \varphi_x(-L/2) = \varphi_x(L/2) \end{cases} \quad (5.3)$$

With such boundary conditions the total number of Josephson vortices trapped in the junction is constrained to zero. Close to the critical field configuration we make the following decomposition $\varphi_c(x) \equiv -\pi/2$ at $h = 0$ and introduce a new field variable $\xi(x) = \varphi(x) + \pi/2$. We expect that this decomposition works well in the range $|\xi(x)| \lesssim \pi/2$, since in this region the value $\sin \xi \simeq \xi - \xi^3/6$ differs by less than 10% there¹. For moderate length junctions $L \simeq 10\lambda_J$ this requirement is satisfied when $h \lesssim 1$ as can

¹One should be careful when doing this decomposition. Note, that some terms can be dismissed in this way when calculating the standard deviation. They can become important in case of a short junction ($L \lesssim 6$). In case of $L \simeq 10$ the dismissed terms can be shown to be negligible.

be checked at the end of the calculations. Also, we introduce a new bias parameter $\delta = 1 - \gamma < 1$. With the use of this new variable the energy functional takes the form, which is equivalent to the previous one, up to an arbitrary constant

$$V[\xi] = \int_{-L/2}^{L/2} dx \left[\frac{\xi_x^2}{2} + \frac{\xi^3}{6} - \delta\xi + h\xi \cos kx \right] \quad (5.4)$$

while the equation of motion is

$$\xi_{xx} - \frac{\xi^2}{2} + \delta - h \cos kx = 0 \quad (5.5)$$

with periodic boundary conditions implied. We use the variational method where our variational function or an approximate solution [MM96b] is taken in the form $\xi(x) = \sqrt{2}A \cos kx + B$. Substituting this function into (5.4) we get an expression for the energy as a function of two variables A and B

$$V[\sqrt{2}A \cos kx + B] = \frac{L}{2} \left(A^2(B + k^2) + \frac{1}{3}B^3 - 2B\delta + \sqrt{2}Ah \right)$$

The extremal points of this function are determined by

$$\begin{cases} 2A(B + k^2) + \sqrt{2}h = 0 \\ A^2 + B^2 - 2\delta = 0 \end{cases} \quad (5.6)$$

Using the first equation, the energy of a classical string configurations can be reduced to

$$V_\delta(B) = \frac{L}{2} \left(-\frac{h^2}{2(B + k^2)} + \frac{1}{3}B^3 - 2B\delta \right) \quad (5.7)$$

with a single constraint

$$V'_\delta(B) = \frac{L}{2} \left(\frac{h^2}{2(B + k^2)^2} + B^2 - 2\delta \right) = 0 \quad (5.8)$$

Whence the problem is simplified to a single parametrical description. At zero magnetic field $h = 0$ there are two solutions $B = \pm\sqrt{2\delta}$. One of them corresponds to a stable configuration, while the other one to the unstable one

5.3 Critical $\delta_c(h)$

Switching to a resistive state occurs when these two configurations (the stable and the unstable ones) become close to each other. We find the critical bias parameter $\delta_c(h)$ for such switching when these configurations coincide in the bifurcation point of the equation (5.5). Using Eq. (5.7) we can easily find it

$$V_\delta''(B_c) = 0$$

Combining this equation with the constraint (5.8), we recover the dependence $\delta_c(h)$ in the following implicit form

$$\begin{cases} \delta_c(h) = B_c(B_c + \frac{k^2}{2}) \\ 2B_c(B_c + k^2)^3 = h^2 \end{cases} \quad (5.9)$$

The dependence $\delta_c(h)$ found from these equations describes the experimental data [FWK⁺03] very well. To be consistent with experiments we have taken the value $L = 10.5\lambda_J$.

Having started from original sine-Gordon equation we are able to obtain a more general expression for the critical current involving Bessel functions with the use of the more general approach developed in [MM96b], which is a generalization what we did above. Nevertheless even in this simple two parametric approximation, the agreement with the experiment is surprising (Fig. 5.2).

5.4 Barrier height

According to the thermal activation (Arrhenius) law, the thermal activation rate is defined by the barrier height. Let us find the behavior of the barrier height U close to the critical bias δ_c . Introduce the notation $\Delta \equiv (\delta - \delta_c) > 0$. Let B_0 and B_1 correspond to the stable and unstable string configurations. We use the Taylor

expansion to decompose $V_\delta(B_1) = V_\delta(B_c + b_1)$ and $V_\delta(B_0) = V_\delta(B_c + b_0)$ close to B_c

$$U(\Delta) = V_\delta(B_1) - V_\delta(B_0) \simeq [V'_\delta(B_c)b_1 - V'_\delta(B_c)b_0] + \frac{1}{3!} [V'''_\delta(B_c)b_1^3 - V'''_\delta(B_c)b_0^3] \quad (5\ 10)$$

Note that by the definition of the critical point B_c the second derivative at this point vanishes as $V''_\delta(B_c) = 0$, while the first derivative of the action is equal to

$$V'_\delta(B_c) = V'_{\delta_c}(B_c) - L(\delta - \delta_c) = -L\Delta$$

The two corrections b_1 and b_0 to the critical value B_c are determined by the equation

$$V'_\delta(B_c + b) = 0 \quad (5\ 11)$$

Again, we use the Taylor series applied to the function $V'_\delta(B_c + b)$ to get

$$-L\Delta + \frac{1}{2}V'''_\delta(B_c)b^2 \simeq 0$$

The two solutions to this equation are

$$b_{0,1} \simeq \pm \sqrt{\frac{2L\Delta}{V'''_\delta(B_c)}} = \pm \sqrt{\frac{2\Delta(B_c + k^2)}{4B_c + k^2}}$$

Eventually, after the substitution of this solutions to (5 10) we have,

$$U(\Delta) \simeq \frac{4}{3} \sqrt{\frac{L}{V'''_\delta(B_c)}} \Delta^{3/2} L = \frac{4\sqrt{2}}{3} \sqrt{\frac{B_c + k^2}{4B_c + k^2}} \Delta^{3/2} L \quad (5\ 12)$$

with B_c given by the equation

$$2B_c(B_c + k^2)^3 = h^2$$

At zero magnetic field this expression for the barrier height coincides with the similar expression for a small Josephson junction

5.5 Standard deviation

To evaluate the standard deviation of the switching current distribution $P(I)$ we mostly follow the approach developed by Garg [Gar95]. It is related to the decay rate Γ according to the equation [Kur72, FD74]

$$P(I) = \frac{\Gamma}{I} \exp\left(-\int_0^I \frac{\Gamma}{I} dI\right)$$

where the decay rate Γ is given by a standard formula

$$\Gamma \simeq \frac{\omega_p}{2\pi} \Delta^{1/4} \exp\left(-\frac{U}{k_B T}\right)$$

Because of the weak dependence on the preexponential prefactor, we take it in the form for a small Josephson junction in case of a moderate dissipation regime. Then, following [Gar95], the standard deviation is

$$\sigma \simeq \frac{\pi\sqrt{2}}{3\sqrt{3}} \left[\log\left(\frac{2I_{c0}A}{3I\mathcal{B}^{5/6}}\right) \right]^{-1/3} \mathcal{B}^{-2/3} \quad (5.13)$$

We have taken the decay rate in the form

$$\Gamma = A\Delta^{1/4} \exp(-\mathcal{B}\Delta^{3/2})$$

In our case,

$$A \simeq \frac{\omega_p}{2\pi}$$

and

$$\mathcal{B} \simeq \frac{4\sqrt{2}}{3} \frac{E_0}{k_B T} \sqrt{\frac{B_c + k^2}{4B_c + k^2}} L$$

where E_0 defines a unit of energy (e.g. [KI96] p.12)

$$E_0 = \frac{\Phi_0}{2\pi} j_c W \lambda_J$$

in SI units. For the width $W = 0.5 \mu\text{m}$, the critical current density $j_c = 220 \text{A}/\text{cm}^2$ and the Josephson length $\lambda_J \simeq 30 \mu\text{m}$ we get

$$E_0 \simeq 8 \times 10^2 \text{K}$$

Finally, we obtain the following expression for $\sigma(h, T)$ (normalized to the critical current)

$$\sigma(h, T) \simeq \frac{\pi\sqrt{2}}{3\sqrt{3}} \left[\frac{5}{6} \log(T/T_0) \right]^{-1/3} \left(\frac{3k_B T}{4\sqrt{2}LE_0} \right)^{2/3} \left(\frac{4B_c + k^2}{B_c + k^2} \right)^{1/3} \quad (5.14)$$

where we have introduced

$$k_B T_0 \simeq \frac{4\sqrt{2}}{3} \left(\frac{3\pi I}{\omega_p I_{c0}} \right)^{6/5} E_0 L$$

neglecting the h dependence of the non-exponential terms. We have estimated T_0 about $0.7 \times 10^{-5} K$ for the experiments [FWK⁺03]

One can notice that the presence of the expression $(4B_c + k^2)/(B_c + k^2)$ in the formula (5.14) results in saturation of the standard deviation σ for high magnetic fields. Indeed, $(4B_c + k^2)/(B_c + k^2) \rightarrow 4$ when $|B_c| \rightarrow \infty$ and $|B_c| \rightarrow \infty$ when $h \rightarrow \infty$ (see (5.9)). This agrees with the experimental data (Fig. 5.3) where the saturation of the standard deviation with increasing magnetic field has been observed. Also, the developed model well explains small dips of the standard deviation at small values of magnetic field (Fig. 5.3). On the other hand, the VA dissociation theory fails to predict the correct behaviour of the standard deviation in this region [FWK⁺03]. To make comparison with existing experimental data [FWK⁺03] we have used the following values for the critical current, $I_{c0} \simeq 340 \mu A$ and for the sweep rate, $I \simeq 0.245 A/s$.

5.6 The deviation from $T^{2/3}$ law

The phase switching in the annular Josephson junction may arise both in the form of a string transition and via the vortex-antivortex pair dissociation [FWK⁺03]. When the value L is smaller than some critical value $L_c(T)$, the switching to resistive state occurs in the form of a string as described in the present paper. The consequence of this is the dependence $\sim T^{2/3}$ of the standard deviation observed in experiments [FWK⁺03].

Indeed, this means that this AJJ of a moderate length behaves effectively similar to a small SJJ and rather than a long JJ [Kat00], which would exhibit $\sim T^{4/5}$ dependence. Furthermore, it is important to note that the index of the power law dependence observed in the experiments [FWK⁺03] is even less than 2/3 which is smaller than the index $4/5 \simeq 0.80$ characteristic for LJJ.

Such behavior can be well explained with the use of the Garg's formula (5.13). Indeed, by differentiating the logarithm of (5.14), we find an effective slope of the logarithmic $\sigma(T)$ dependence

$$\frac{\partial \log \sigma}{\partial \log T} = \frac{2}{3} - \frac{1}{3 \log(T/T_0)} \quad (5.15)$$

For the range of temperatures $T \sim 1K$ this gives

$$\frac{\partial \log \sigma}{\partial \log T} \simeq 0.64 \quad (5.16)$$

This value agrees with the experimental data [FWK⁺03] where a noticeable deviation from 2/3 power law has been observed.

5.7 Quantum case

We start from the Euclidean action

$$S_E[\xi] = \int_0^\beta d\tau \int_{-L/2}^{L/2} dx \left[\frac{\xi_\tau^2}{2} + \frac{\xi_x^2}{2} + (1 - \cos \varphi) + \frac{\xi^3}{6} - \delta \xi + h \xi \cos kx \right]$$

The classical solutions (instantons) satisfy the equation of motion

$$\xi_{\tau\tau} + \xi_{xx} - \frac{\xi^2}{2} + \delta - h \cos kx = 0$$

In the view of the same approximation we treat A and B as time dependent variables

$$S_E[\sqrt{2}A \cos kx + B] = \frac{L}{2} \int_0^\beta d\tau \left(A^2 + B^2 + A^2(B + k^2) + \frac{1}{3}B^3 - 2B\delta + \sqrt{2}Ah \right)$$

with equations of motion

$$\begin{cases} 2A = 2A(B + k^2) + \sqrt{2}h \\ 2B = A^2 + B^2 - 2\delta \end{cases} \quad (5.17)$$

$$S_{inst} = S_E[\xi(x, \tau)] - S_E[\xi_0(x)] = L \int_0^\beta d\tau \left(\frac{a^2}{2} + \frac{b^2}{2} + V(a, b) \right)$$

$$V(a, b) = A_0 a b + \frac{b^3}{6} + \frac{B_0 b^2}{2} + \frac{a^2 (B_0 + k^2 + b)}{2}$$

where

$$A_0 = A_c + a_0, \quad B_0 = B_c + b_0$$

$$a_0 = \sqrt{\frac{2\Delta B_c}{4B_c + k^2}}, \quad b_0 = \sqrt{\frac{2\Delta(B_c + k^2)}{4B_c + k^2}}$$

A_c and B_c are the parameters close at the critical point. From the previous calculations,

$$A_c^2 = B_c(B_c + k^2), \quad 2B_c(B_c + k^2)^3 = h^2$$

This is just the problem of a particle tunneling from a two-dimensional well. On the (a,b)-plane the instanton trajectory comes from the origin (0, 0) and then goes close to the saddle point (2a₀, 2b₀). We can reduce it to a one dimensional problem assuming the scaling $a = b a_0/b_0 = b \sqrt{B_c/(B_c + k^2)}$

$$S_{inst} = L \int_0^\beta d\tau \left(\frac{mb^2}{2} + V\left(b \sqrt{\frac{B_c}{B_c + k^2}}, b\right) \right)$$

The effective mass

$$m = 1 + \frac{a_0^2}{b_0^2} = \frac{2B_c + k^2}{B_c + k^2}$$

After that we can use the formula for escape rate of a particle from a metastable state in the semiclassical WKB approximation (see Likharev p 176 and Wallraff p 118 eq 7.2 "Fluxon Dynamics in AJJ", Ref [Leg84])

$$\Gamma = \frac{\omega}{2\pi} \left(864\pi \frac{V_{max}}{\hbar\omega} \right)^{1/2} \exp\left(-\frac{36}{5} \frac{V_{max}}{\hbar\omega}\right)$$

where

$$\omega^2 = \frac{1}{m} \frac{d^2 V(b \sqrt{\frac{B_c}{B_c + k^2}}, b)}{db^2} \Big|_{b=0} = \frac{\sqrt{2\Delta(B_c + k^2)(4B_c + k^2)}}{2B_c + k^2}$$

and

$$V_{max} = U(\Delta) = \frac{4\sqrt{2}}{3} \sqrt{\frac{B_c + k^2}{4B_c + k^2}} \Delta^{3/2} L$$

according to the formula (5.12). Eventually,

$$S_{inst} = \frac{36 V_{max}}{5 \hbar \omega} = \frac{48}{5} \left[\frac{2(B_c + k^2)(2B_c + k^2)^2}{(4B_c + k^2)^3} \right]^{1/4} \Delta^{5/4} L$$

5.8 Vortex-antivortex pairs: dissociation and annihilation

While in a moderate length AJJ the escape of the phase string may not happen in the form of vortex-antivortex dissociation, nevertheless, the vortex-antivortex pair can develop later during subsequent dynamical evolution of the string (*after* the escape). Thermal escape itself happens during a very short time. The profile of the string does not change dramatically. On the other hand, the evolution of the string *after* the escape event is very dramatic and may lead to formation of fluctuating vortex-antivortex pair. This effect will manifest itself in the experimental current-voltage characteristics as a voltage step different from that of a homogeneous phase rotation.

Moreover, phase escape in the form of vortex-antivortex pair can be observed. This may result in vortex-antivortex annihilation or creation of an oscillating breather depending on the dissipation rate. Let the bias magnetic field be close to zero. According to the terminology used by [OS67] and [MM96a] the critical current curve (see Fig. 5.2) corresponds to a "0 to 1 pair mode" characterizing the degree of penetration of a vortex-antivortex pair into the junction. While being at small magnetic field, the system is in the stable 0-1 pair mode. When increasing the field, the 1-2 mode becomes stable.

whereas the 0-1 mode disappears. If we decrease the field, the system will persist in the metastable 1-2 mode configuration, so that (thermal or/and quantum) decay onto the stable 0-1 mode can be observed in the experiments. At *zero bias* the size of soliton is of the order $\sim \lambda_J$ which is less than the circumference of the junction $\sim 10\lambda_J$. Whence, the metastable 1-2 configuration has a form of a fully developed fluxon and antifluxon trapped by a small magnetic field in opposite sides of the junction.

5.9 Annular Josephson junction with impurity

Real Josephson junctions studied experimentally always have inhomogeneities and impurities associated with imperfections during the fabrication process. In this chapter we consider a possible impact of an impurity on switching properties of an annular Josephson junction when trapped fluxons are absent. Presence of an impurity changes the critical current [MS78, KI96]. The energy of a phase configuration is

$$S[\varphi] = \int_{-L/2}^{L/2} dx \left[\frac{\varphi_x^2}{2} + (1 + \epsilon\delta(x - x_0))(1 - \cos \varphi) + \gamma\varphi + h\varphi \cos kx \right]$$

where $k = 2\pi/L$ and L is the circumference of the annular junction. The case $\epsilon > 0$ corresponds to enhanced critical current density in a narrow region of the junction (the authors [KI96] use $\epsilon = -\epsilon$). The classical configurations minimizing the energy are given by

$$\varphi_{xx} - (1 + \epsilon\delta(x - x_0))\sin \varphi - \gamma - h \cos kx = 0 \quad (5.18)$$

with periodic boundary conditions

$$\begin{cases} \varphi(-L/2) = \varphi(L/2) \\ \varphi_x(-L/2) = \varphi_x(L/2) \end{cases}$$

We consider a special case where the impurity is placed symmetrically with respect to

the magnetic field assuming $x_0 = L/2$. Thus, up to an additive constant

$$S[\varphi] = \int_{-L/2}^{L/2} dx \left[\frac{\varphi_x^2}{2} + (1 - \cos \varphi) + \gamma \varphi + h \varphi \cos kx \right] - \epsilon \cos \varphi(L/2)$$

$$\varphi_{xx} - \sin \varphi - \gamma - h \cos kx = 0$$

with boundary conditions

$$\begin{cases} \varphi(-L/2) = \varphi(L/2) \\ \varphi_x(-L/2) = \varphi_x(L/2) + \epsilon \sin \varphi(L/2) \end{cases}$$

The last condition follows from eq (5.18)

$$\int_{L/2-0}^{L/2+0} \varphi_{xx} = \epsilon \sin \varphi(L/2)$$

Again, we make decomposition close to the critical field configuration $\varphi_c(x) \equiv -\pi/2$ at $h = 0$ and introduce new field variable $\xi(\tau) = \varphi(\tau) + \pi/2$ and new bias parameter $\delta = 1 - \gamma < 1$.

$$S[\xi] \simeq \int_{-L/2}^{L/2} \left[\frac{\xi_x^2}{2} + \frac{\xi^3}{6} - \delta \xi + h \xi \cos kx \right] - \epsilon \xi(L/2)$$

where we have approximated $\cos(-\pi/2 + \xi(L/2)) \simeq \xi(L/2)$

$$\xi_{xx} - \frac{\xi^2}{2} + \delta - h \cos kx = 0$$

with

$$\begin{cases} \xi(-L/2) = \xi(L/2) \\ \xi_x(-L/2) \simeq \xi_x(L/2) - \epsilon \end{cases} \quad (5.19)$$

The case of homogeneous AJJ ($\epsilon = 0$) was considered by us before. We briefly review the main considerations. We have used the approximation $\xi(x) = \sqrt{2}A \cos kx + B$ to get the effective energy as a function of A and B

$$S[\sqrt{2}A \cos kx + B] = \frac{L}{2} \left(A^2(B + k^2) + \frac{1}{3}B^3 - 2B\delta + \sqrt{2}Ah \right)$$

The equations of motion

$$\begin{cases} 2A(B + k^2) + \sqrt{2}h = 0 \\ A^2 + B^2 - 2\delta = 0 \end{cases}$$

We have got the following results

$$\begin{cases} \delta_c(h) = B_c(B_c + \frac{k^2}{2}) \\ 2B_c(B_c + k^2)^3 = h^2 \end{cases}$$

$$U(\Delta) \simeq \frac{4\sqrt{2}}{3} \sqrt{\frac{B_c + k^2}{4B_c + k^2}} \Delta^{3/2} L$$

Standard deviation normalized to the critical current

$$\sigma(h, T) \simeq \frac{\pi\sqrt{2}}{3\sqrt{3}} \left[\frac{5}{6} \log(T/T_0) \right]^{-1/3} \left(\frac{3k_B T}{4\sqrt{2} L E_0} \right)^{2/3} \left(\frac{4B_c + k^2}{B_c + k^2} \right)^{1/3}$$

where

$$k_B T_0 \simeq \frac{4\sqrt{2}}{3} \left(\frac{3\pi I}{\omega_p I_{c0}} \right)^{6/5} E_0 L$$

In general case of non-zero ϵ we change the approximation adding a quadratic part in order to satisfy the boundary conditions (5 19)

$$\xi(x) = \sqrt{2}\tilde{A} \cos kx + \tilde{B} + \frac{\epsilon k}{4\pi} x^2$$

The problem can be reduced to the homogeneous case with the action

$$S = \frac{L}{2} \left(A^2(B + k_{eff}^2) + \frac{1}{3}B^3 - 2B\delta_{eff} + \sqrt{2}Ah_{eff} \right),$$

new variables

$$\begin{aligned} A &= \tilde{A} - \frac{\epsilon}{\sqrt{2}k\pi} \\ B &= \tilde{B} + \frac{\epsilon\pi}{12k} \end{aligned}$$

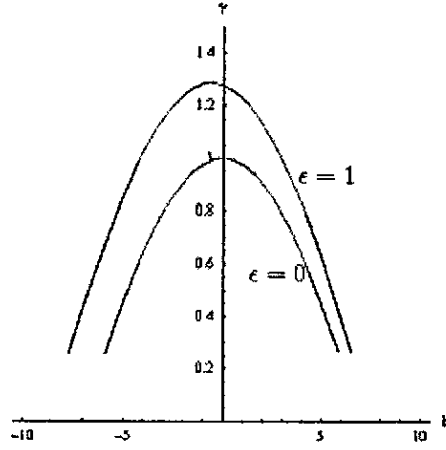


Figure 5.1 Switching current vs magnetic field for $\epsilon = 0$ and $\epsilon = 1$

and effective parameters

$$\begin{aligned}\delta_{eff} &= d + \frac{\epsilon^2}{4k^2\pi^2} + \frac{\epsilon k}{2\pi} - \frac{\epsilon^2\pi^2}{360k^2} \\ h_{eff} &= h - \frac{\epsilon^2}{6k^2} + \frac{13\epsilon^2}{8k^2\pi^2} + \frac{\epsilon k}{\pi} \\ k_{eff}^2 &= k^2 + \frac{\epsilon}{8k\pi}\end{aligned}$$

From that follows

$$\begin{cases} \gamma_c(h) = 1 - B_c(B_c + \frac{k_{eff}^2}{2}) + \frac{\epsilon^2}{4k^2\pi^2} + \frac{\epsilon k}{2\pi} - \frac{\epsilon^2\pi^2}{360k^2} \\ 2B_c(B_c + k_{eff}^2)^3 = h_{eff}^2 \end{cases} \quad (5.20)$$

For positive $\epsilon > 0$ the critical current lobe shifts up to the higher values. This results in a broadening of the normalized $I_c(h)/I_c(0)$ dependence.

5.10 Conclusion

In conclusion, the switching distribution of the annular Josephson junction to a

resistive state has been investigated. We have invoked the statistical field theory formulation of a string escape problem where the superconducting phase difference plays a role of a string. We have used a two parametric approximation and the variational method to describe the string escape from a metastable state. This approach is more powerful than the collective coordinates method in the form of vortex/antivortex positions for investigation of the switching current distributions. Indeed, we have shown that the existing experimental results for AJJ can be well described in terms of the thermal activation of a string crossing the potential barrier. The agreement with experiments has been obtained without any adjusting parameters.

Although the length of the annular junctions considered above is larger than λ_J , their switching characteristics remind more those of a short Josephson junction rather than long junctions (at least at the range of temperatures $T < 1$). In particular, they exhibit $T^{2/3}$ behaviour of the standard deviation similar to point Josephson junctions. In order to observe the genuine long junction behaviour one may need to move toward longer lengths or higher temperatures (see "phase diagram" on Fig 9.7 in the Summary of the thesis).

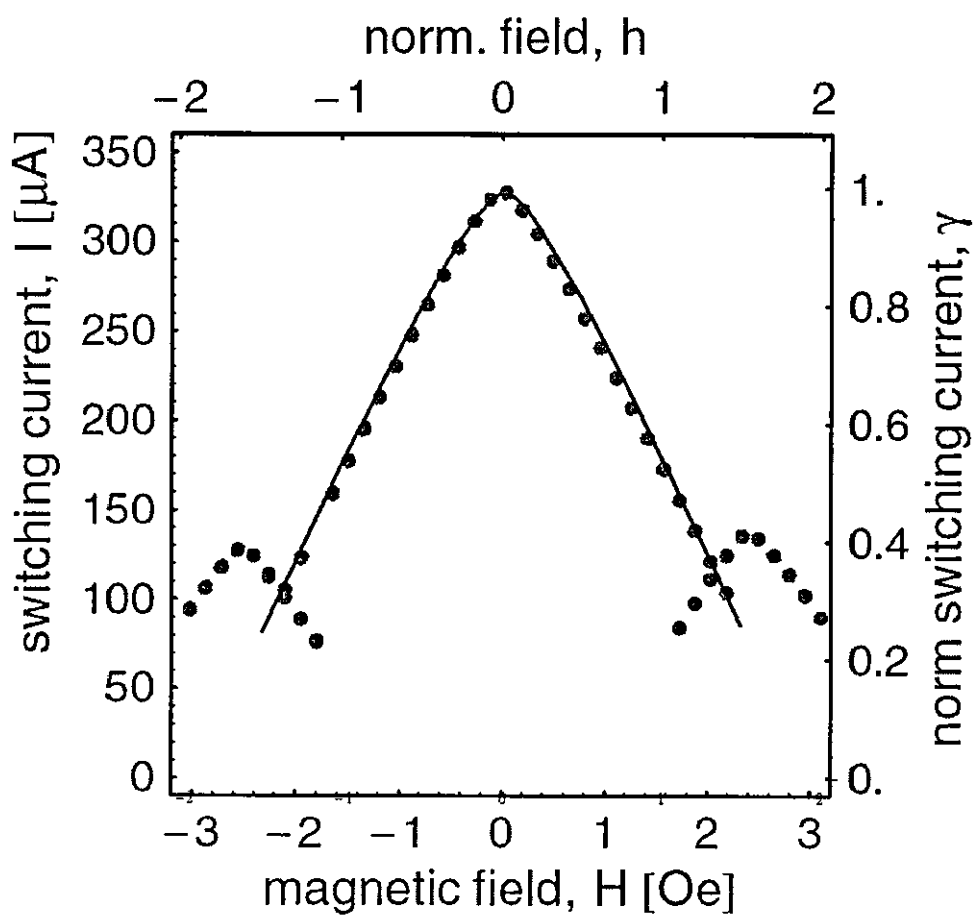


Figure 5.2 Dependence of the switching current on magnetic field for an annular Josephson junction with circumference $L = 10.5 \lambda_J$. The dots are experimental data [FWK⁺03]. The solid line is the theoretical calculation using our string escape model.

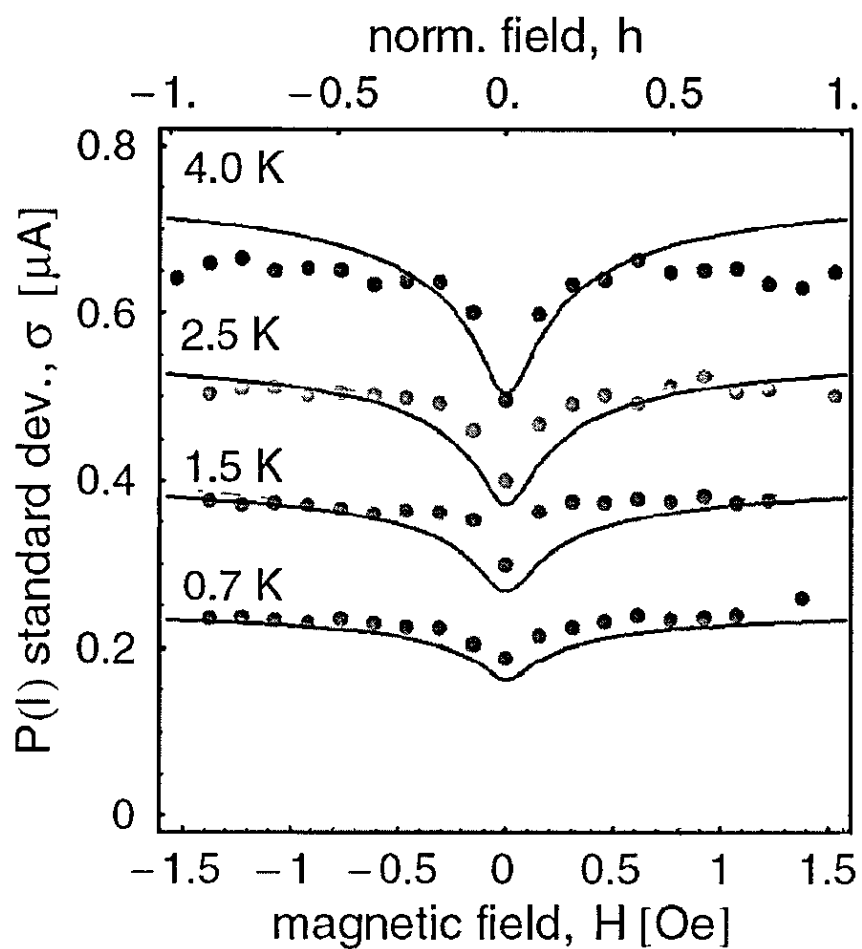


Figure 5.3 Standard deviation of the switching current distribution for an annular Josephson junction with circumference $L = 10.5 \lambda_J$ versus magnetic field. The dots are experimental data [FWK⁺03]. Solid line is the theoretical calculation using our string escape model.

Chapter 6

Long Annular Josephson Junction

In this chapter we consider truly long Josephson junctions, which are both longer than λ_J and exhibit appropriate switching characteristics, in particular, $T^{4/5}$ dependence of the standard deviation on temperature. We find the temperature dependent crossover between intermediate and long junction domains. Also, in this chapter we explain weak dependence of the standard deviations on magnetic field of very long Josephson junctions.

6.1 Long Annular Josephson Junction limit: simple considerations

Consider a very long annular Josephson junction, $L \gg 1$ where L is the circumference. The energy is

$$V[\varphi] = \int_{-L/2}^{L/2} dx \left[\frac{\varphi_x^2}{2} + (1 - \cos \varphi) + \gamma \varphi + h \varphi \cos kx \right] \quad (6.1)$$

with $k = 2\pi/L$. The extremal configurations satisfy

$$\varphi_{xx} - \sin \varphi - \gamma - h \cos kx = 0 \quad (6.2)$$

and

$$\begin{cases} \varphi(-L/2) = \varphi(L/2) \\ \varphi_x(-L/2) = \varphi_x(L/2) \end{cases} \quad (6.3)$$

As the junction is very long, the escape process begins at some part of the junction. Obviously, the most "biased" region for positive h is close to $x = 0$. In this region, the term $h \cos kx$ can be approximated by 1. Thus,

$$\varphi_{xx} - \sin \varphi - \tilde{\gamma} = 0 \quad (6.4)$$

with $\tilde{\gamma} = \gamma + h$. The switching current is $\gamma_c(h) = \tilde{\gamma}_c - h = 1 - h$. For arbitrary magnetic fields

$$\gamma_c(h) = 1 - |h|$$

This should result in a sharp peak at the top of the switching current dependence on magnetic field. This can be seen clearly on the experimental data obtained by A. Price from Prof. Ustinov's experimental group in Erlangen (Germany), Fig. 6.1 and Fig. 6.2.

Thus, the magnetic field only shifts the switching current by h . Obviously, the barrier height $U(\gamma_c(h) - \gamma(h)) = U(\tilde{\gamma}_c - \tilde{\gamma})$ does not depend on h . Therefore, the standard deviation is also independent of h .

$$\sigma(h) = \text{const}$$

This explains the experimental data Fig. 6.1 and Fig. 6.2 where the observed standard deviation is almost independent on magnetic field.

6.2 Long - short junction crossover

The energy after decomposition,

$$V[\xi] = \int_{-L/2}^{L/2} dx \left[\frac{\xi_x^2}{2} + \frac{\xi^3}{6} - \delta\xi + h\xi \cos kx \right] \quad (6.5)$$

while the equation of motion is

$$\xi_{xx} - \frac{\xi^2}{2} + \delta - h \cos kx = 0 \quad (6.6)$$

Close to $x = 0$,

$$\xi_{xx} - \frac{\xi^2}{2} + \Delta = 0 \quad (6.7)$$

$$\Delta = \delta - h$$

This is analogous to a classical equation of motion with ξ and x playing a role of a coordinate and time correspondingly. The classical particle is subjected to the potential $U(\xi) = -\frac{\xi^3}{6} + \xi\Delta$. There are two "stationary" solutions

$$\xi_{0,1}(x) = \pm\sqrt{2\Delta}$$

corresponding to a particle resting at the top or bottom of the potential correspondingly. The particles also may undergo periodic oscillations close to the bottom $\xi \sim -\sqrt{2\Delta}$. The minimal period of this oscillations is given by

$$\omega = U''(-\sqrt{2\Delta}) = (2\Delta)^{1/4}$$

Due to the periodic boundary conditions, this oscillatory solution may appear only if

$$L > \frac{2\pi}{\omega}$$

From what follows the crossover length

$$L_c \simeq \frac{2\pi}{(2\Delta_{sw})^{1/4}}$$

here Δ_{sw} is the average value when the switching occurs. According Garg,

$$\Delta_{sw} \simeq \left(\frac{3k_B T \log X}{4\sqrt{2} L E_0} \right)^{2/3}$$

with $\log X = 5/6 \log(T/T_0)$ in my notation (case of moderate damping). Here we have used the expression for the barrier height

$$U = \frac{4\sqrt{2}}{3} \Delta^{3/2} L$$

normalized to the unit energy E_0 . Thus,

$$L_c^{5/6} \simeq \frac{2\pi}{2^{1/4}} \left(\frac{4\sqrt{2} E_0}{3 k_B T \log X} \right)^{1/6}$$

$$L_c \simeq 8.4 \left(\frac{E_0}{k_B T \log X} \right)^{1/5} \quad (6.8)$$

From

$$\log X \simeq 11$$

$$E_0 = 8600 K$$

$$T \sim 3 K$$

that corresponds to the samples R35W3 ($L \simeq 18$) and R50W3 ($L \simeq 26$) we get

$$L_c \simeq 26$$

that is just about the length of the sample R50W3

6.3 Another derivation

In case of a very long AJJ the escape occurs through the unstable solution

$$\xi_2(x) = \sqrt{2\Delta} (1 - 3 \operatorname{sech}^2(2x/r))$$

with $r = 4/(2\Delta)^{1/4}$ being the width of the solution (e.g. [BL81], Eq. (2.14)). That is different from the homogeneous solution $\xi_1(x) = -\sqrt{2\Delta}$ in case of a small junction. Let us formulate the criteria when the solution $\xi_2(x)$ is valid. We require the width of the solution (size of the VA pair) to be smaller than half length of the junction

$$\frac{4}{(2\Delta)^{1/4}} < L/2 \quad (6.9)$$

Hence, the crossover length is

$$L_c \simeq \frac{8}{(2\Delta_{sw})^{1/4}}$$

Thus, $L < L_c$ switching properties of the junction should be analyzed using "harmonic" approximation of the type $\xi(x) \sim A \cos(kx) + B$, i.e. the junction is effectively "short"

For $L > L_c$ one should use the solution of the SAN type (small-amplitude nucleus according Buettiker [BL81]) that is $\xi_2(x)$ as the escape goes through the VA pair nucleation

$$\Delta_{sw} \simeq \left(\frac{5 k_B T \log X}{48 2^{1/4} E_0} \right)^{4/5}$$

Barrier height in normalized units

$$U = V[\xi_1(x)] - V[\xi_0(x)] = \frac{48}{5} 2^{1/4} \Delta^{5/4}$$

Eventually,

$$L_c \simeq \frac{8}{2^{1/4}} \left(\frac{48 2^{1/4} E_0}{5 k_B T \log X} \right)^{1/5}$$

$$L_c \simeq 11 \left(\frac{E_0}{k_B T \log X} \right)^{1/5} \quad (6.10)$$

For the same $\log X \sim 11$ (we assume that $\log X$ should be about the same value as above) this gives $L_c \sim 33$. From the calculations above one can estimate the width of the crossover region as a difference of the formula (6.8) and (6.10),

$$\Delta L_c \simeq 2.6 \left(\frac{E_0}{k_B T \log X} \right)^{1/5} \sim 7$$

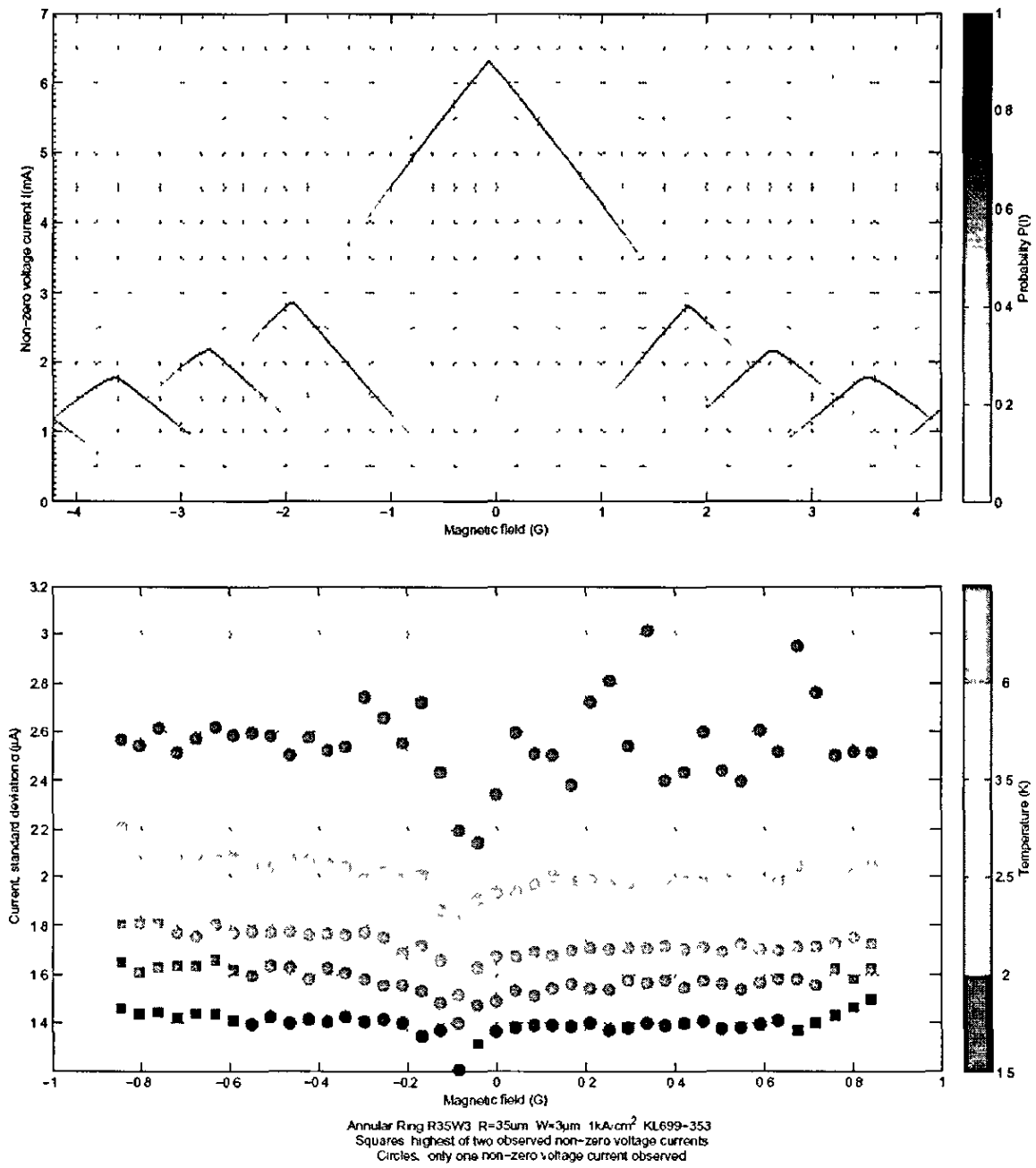


Figure 6.1 *Experimental switching diagram of a long annular Josephson junction with radius $R=35\ \mu\text{m}$ (top) and its standard deviation (bottom). The experimental data is obtained by collaborating experimental group of Prof. Ustinov in Erlangen (Germany). The measurements were carried out by A. Brice.*

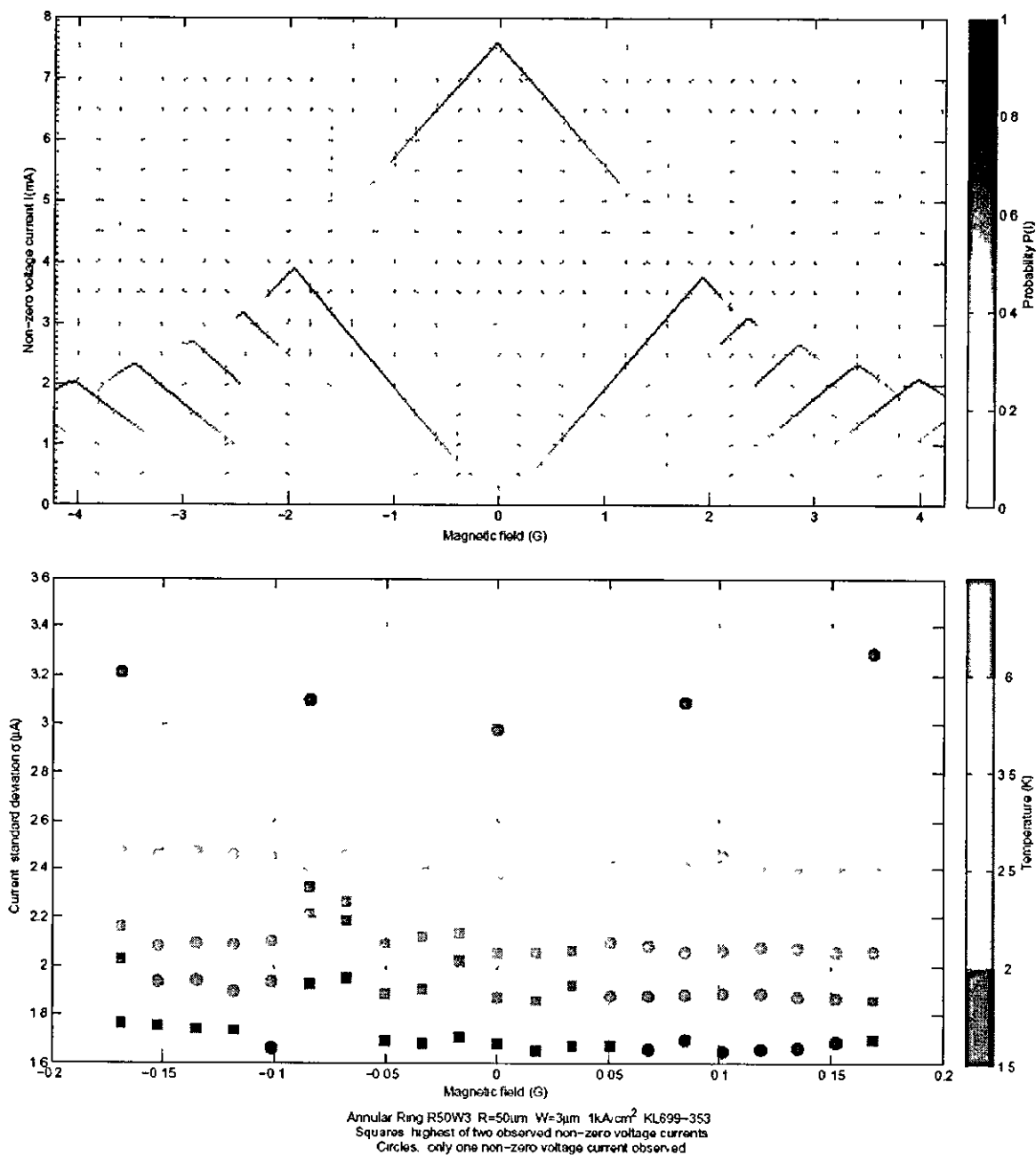


Figure 6.2 *Experimental switching diagram of a long annular Josephson junction with radius $R=50 \mu\text{m}$ (top) and its standard deviation (bottom). The experimental data is obtained by collaborating experimental group of Prof. Ustinov in Erlangen (Germany). The measurements were carried out by A. Price.*

Chapter 7

Fluxon in an Annular Josephson Junction. Microshort Qubit.

We develop a model of a quantum qubit based of an annular Josephson junction (AJJ) with a microshort. The both cases of lytographical and pseudo-microshorts are considered. Due to the microshort, a barrier for a quantum fluxon motion is formed. Applying a magnetic field parallel to the junction plane we show that such microshort forms a double well potential for a fluxon. As a result the fluxon is trapped in one of the potential wells.

7.1 Introduction

The use of superconductors for quantum computation is a prominent idea that inspire scientists over the recent years. It relies on the significant advantages of using macroscopically coherent state such as superconducting state. Indeed, in the superconducting state the elementary charge shot noise is absent, while the reduced number of degrees of freedom due to a formation of superconducting long-range order helps to enhance the coherence properties.

Recently different realizations of superconducting qubits have been proposed. One of them is a formation of a charge qubit in Cooper boxes [NPT99, YPA⁺03, PYA⁺03, CBS⁺04]. The other one is a flux qubit [MOL⁺99]. A superconducting tunnel junction circuit that behaves as a two-level atom: the "quantronium" has been designed. An arbitrary evolution of its quantum state has been programmed with a series of microwave pulses, and a projective measurement of the state has been performed by a pulsed readout subcircuit [VAC⁺02]. Evidence for Entangled States of Two Coupled Flux Qubits has been clearly presented [IGI⁺04]. Reading out the state inductively and microwave spectroscopy of an interferometer-type charge qubit has been performed [BSK⁺04]. The idea of a vortex qubit has been realised in different way, with the use of a circuit consisting of small Josephson junctions [GII05]. In another work of this group [GIvdP⁺05] a direct Josephson coupling between superconducting flux qubits has been also realised. There is a recent development of quantum computing with the use of annular Josephson junction [WKL⁺00, KWU02, FU03, Cla03]. There the fluxon quantum states in a long annular JJ are proposed to use for quantum computation. The idea has got a further development. Quantum tunneling of a single vortex [WLL⁺03] and read out of vortex states were successfully demonstrated for the heart shape annular JJ [KWU02]. Creation of a double well in a long annular Josephson junction has been also discussed recently [SK04]. Here we propose to implement a qubit by means of an annular Josephson junction (AJJ) with an inhomogeneity called microshort. We show that such microshort together with magnetic field parallel to the junction create a two states available for quantum computation. Both the operation and readout regimes for such qubit can be realized with the use of the external magnetic field and external bias current. We also show that in some limit such qubit can be described by a model of the point impurity in an annular JJ, similar to those proposed by [Kat00] and by [SK04].

7.2 Microshort qubit: general considerations

The two quantum states of the microshort qubit (MSQ) arise as a competition of two forces – formation of a potential well due to magnetic field and a repulsion of the fluxon by the impurity located in the centre of this potential well. Different layouts of a microshort qubit are possible – ear-ring layout and wave layout Fig. 7.1. We concentrate our attention on the first one, that is based on an annular Josephson junction.

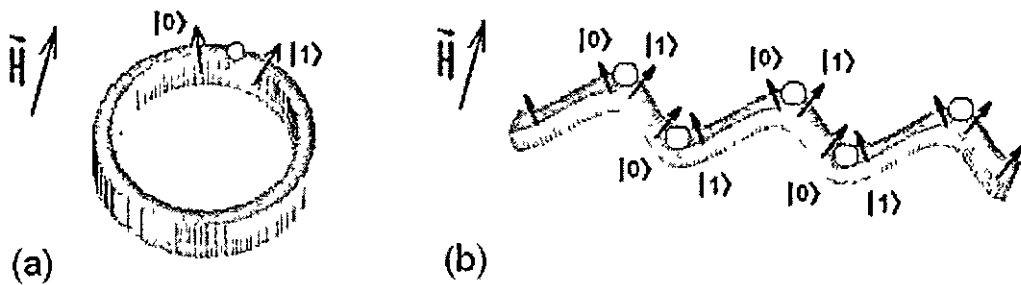


Figure 7.1 Ear-ring and wave layouts

7.3 Annular Josephson junction with different microshort types

Consider the model of a microshort with the energy of phase configuration

$$V[\varphi(x)] = \int_{-L/2}^{L/2} dx \left(1 + \frac{\Delta l \Delta W(x)}{W_0} \right) \left[\frac{\varphi_x^2}{2} + (1 - \cos \varphi) + \gamma \varphi - h \varphi \sin kx \right] \quad (7.1)$$

where $\Delta W(x) = \Delta W$ on the pseudo-microshort having the width $W_0 + \Delta W$ and the length Δl . There is no variation $\Delta W(x) = 0$ elsewhere. The manufacture of such a pseudo-microshort can be produced with the use of a standard lithographic

process. Such realistic manufacture methods makes these microshorts very attractive for experimental investigations [PGK⁺]

Also, let us consider a model of the conventional microshort, where there is a local enhancement of a critical current [MS78, KI96, Kat00] is described as a local point impurity. The energy of the superconducting phase configuration for a long Josephson junction with such a conventional microshort located at the position $\tau = 0$ may be derived with a similar procedure and defined by the eq

$$V[\varphi(\tau)] = \int_{-L/2}^{L/2} d\tau \left[\frac{\varphi_x^2}{2} + \left(1 + \frac{\Delta l \Delta j_c}{J_c} \right) (1 - \cos \varphi) + \gamma \varphi - h \varphi \sin k\tau \right] \quad (7.2)$$

where $k = 2\pi/L$ and L is a normalized circumference of the annular junction, Δl is a normalized length of the impurity. One may notice strong similarities between the models presented by the eq 7.1 and the eq 7.2. The classical configurations minimizing both expressions, the (7.1) and the (7.2) are given by the perturbed sine-Gordon equation

$$\varphi_{xx} - \sin \varphi - \gamma + h \sin kx = 0, \quad x \notin \text{microshort} \quad (7.3)$$

and the periodic boundary conditions

$$\begin{cases} \varphi(-L/2) = \varphi(L/2) - 2\pi \\ \varphi_x(-L/2) = \varphi_x(L/2) \end{cases}$$

in case of a single fluxon trapped in the junction

We consider a trial function in the form of a non-perturbed sine-Gordon soliton and use variational method with respect to a single collective coordinate x_0 (fluxon position). Substituting

$$\varphi(\tau) = 4 \arctan e^{x-x_0} \quad (7.4)$$

to the expressions for energies (9.22) and (9.21), we get an effective energy as a function of x_0

$$V(x_0) = -\gamma 2\pi x_0 - \frac{2\pi h \cos(kx_0)}{k \cosh(k\pi/2)} + \frac{2\epsilon}{\cosh(x_0)^2} \quad (7.5)$$

which is valid for a small microshort strength $\epsilon \ll 1$, with

$$\epsilon = \begin{cases} \Delta l \Delta j_c / j_c, & \text{for a conventional microshort} \\ 2 \Delta l \Delta W / W_0, & \text{for a pseudo-microshort} \end{cases}$$

7.4 Switching current branches

Let us find the critical current when the switching of the junction to a resistive state occurs. One of the branches of the critical current is associated with a fluxon escaping from a well induced by the magnetic field. In case of a long AJJ and small impurity strength $\epsilon \ll 1$, it is reasonable to assume that this critical current is weakly influenced by the impurity. Therefore,

$$\gamma_{c1}(h) \simeq \frac{h}{\cosh(\frac{k\pi}{2})} \quad (7.6)$$

The second branch is due to the impurity. In this case we assume $x_0 \sim 0$ and decompose the action (up to an additive constant)

$$V(x_0) \simeq -2\pi\gamma x_0 - x_0^2 \left(2\epsilon - \frac{h k \pi}{\cosh(\frac{k\pi}{2})} \right) + \frac{2}{3} x_0^4 \left(2\epsilon - \frac{h k^3 \pi}{8 \cosh(\frac{k\pi}{2})} \right) \quad (7.7)$$

That is a biased double well potential. At large L we neglect the last term in brackets

$$V(r_0) \simeq -2\pi\gamma r_0 - r_0^2 \left(2\epsilon - \frac{h k \pi}{\cosh(\frac{k\pi}{2})} \right) + \frac{4\epsilon}{3} r_0^4 \quad (7.8)$$

The fluxon positions and the critical point are defined by the equations

$$V'(x_0) = 0 \quad \text{and} \quad V''(x_0) = 0 \quad (7.9)$$

Then, the second critical current is

$$\gamma_{c2}(h) \simeq \frac{\left(2\epsilon - \frac{h k \pi}{\cosh(\frac{k\pi}{2})} \right)^{3/2}}{3\pi\sqrt{2\epsilon}} \quad (7.10)$$

7.5 Quantum properties

To investigate quantum properties of AJJ with a microshort, we consider the Euclidean action

$$S_E[\varphi(\tau, \tau)] = \int_0^\beta d\tau \int_{-L/2}^{L/2} dx \left[\frac{\varphi_\tau^2}{2} + \frac{\varphi_x^2}{2} + (1 + \epsilon\delta(x))(1 - \cos\varphi) + \gamma\varphi - h\varphi \sin kx \right] \quad (7.11)$$

The vortex coordinate $x_0(\tau)$ is treated as time dependent now

$$\varphi(x, \tau) = 4 \arctan e^{x-x_0(\tau)} \quad (7.12)$$

Hence, the effective action obtained via an integration the eq 7.11 over x has the form

$$S_E[\varphi(x, \tau)] = \int_0^\beta d\tau \left(\frac{mx_0^2}{2} + V(x_0) \right) \quad (7.13)$$

This is a problem of one-dimensional tunneling of a particle with mass

$$m = \int_{-L/2}^{L/2} dx \left(\frac{\partial\varphi}{\partial x_0} \right)^2 \simeq \int_{-\infty}^{\infty} dx \left(\frac{\partial\varphi}{\partial x_0} \right)^2 = 8 \quad (7.14)$$

At zero current the instanton action, determining the coupling between the two wells, is given by

$$S_{inst} = \frac{36 \Delta V_{max}}{5 \omega} \quad (7.15)$$

normalized by $E_0 k_B / (\hbar \omega_p)$. The frequency at the bottom of the wells ω is determined by

$$\omega^2 = \frac{V''(\pm x_{eq})}{m}, \quad (7.16)$$

where $\pm x_{eq}$ are equilibrium positions of a fluxon, satisfying $V'(\pm x_{eq}) = 0$. Eventually, we got very simple expression for the action associated with the fluxon tunneling

$$S_{inst} = \frac{27}{10 \sqrt{2} \epsilon} \left(2\epsilon - \frac{h k \pi}{\cosh(\frac{k\pi}{2})} \right)^{3/2} \quad (7.17)$$

One may see that this action decreases with magnetic field. This means that the barrier height associated with the microshort decreases. It is obvious that for a longer junction the influence of the magnetic field is weaker.

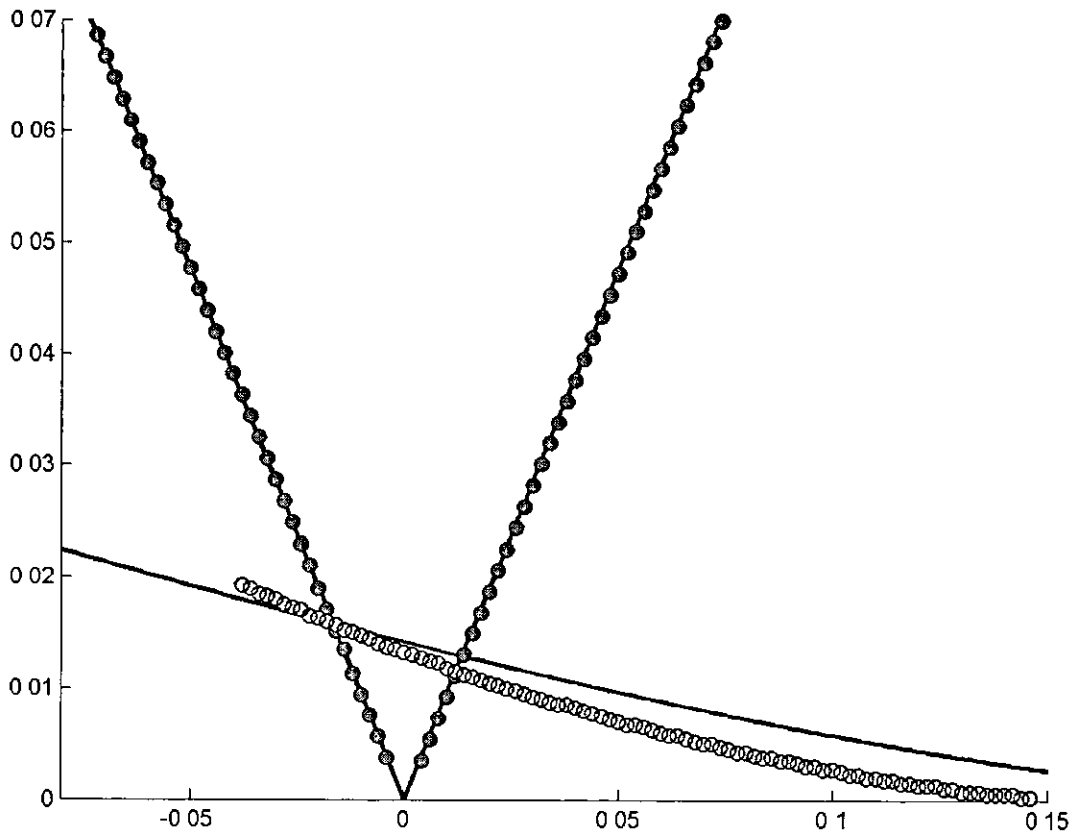


Figure 7.2 Dots are numerical calculation. Solid lines are the theoretical estimations of the critical currents.

Chapter 8

Perturbation Theory of Localized Excitations. Decay of a Breather.

In chapter 5 has been noticed that phase escape of a weakly biased annular Josephson junction under magnetic field may result in a creation of a breather – a bound state of a fluxon and an antfluxon. In this chapter we consider the dynamics of such a breather in the presence of small dissipation. We develop perturbation theory especially designed to describe excitations localized in a confined area. We have carried out numerical simulations with dissipative sine-Gordon equation and have made comparison with the McLaughlin-Scott theory. Significant distinction between the McLaughlin-Scott calculation for a breather decay and our numerical result indicates that the history dependence of the breather evolution can not be neglected even for small damping parameter.

8.1 Introduction

The sine-Gordon equation is one of the most famous in physics. It was known yet in 19th century, but its importance grew up when its localized solitary waves [Raj82] or

solitons were discovered. First it was borrowed by particle physicists, but now appears in various areas of physics. It describes chains of mechanical pendula, dislocations in crystals and is extremely important in theory of superconducting Josephson junctions.

In ideal case when the Josephson junction is infinitely long and narrow, Josephson solitons can be described analytically by well known exact solutions of the sine-Gordon equation. However, there is always dissipation associated with quasiparticle current through the Josephson junction and inhomogeneities associated with its width and thickness. Moreover, real physical systems are always subjected to the influence of external forces. All these factors may have a significant impact on soliton behaviour.

Although, the strictly one dimensional sine-Gordon equation is integrable [AS80, Raj82], the perturbations to this equation associated with the external forces and inhomogeneities spoil its integrability and the equation can not be solved exactly. Nevertheless, if their influence is small, the solution can be found perturbatively. The perturbation theory for solitons was described in detail by [KM77]. Later, in application to the dynamics of vortices in Josephson contacts, perturbation analysis of the sine-Gordon equation was developed by McLaughlin and Scott [MS78].

In many applications there appears a need in localized oscillatory solutions of the sine-Gordon equation. For instance, a Josephson vortex pinned by an inhomogeneity or a bound state of a vortex with an antivortex known as breather. Breather may appear as a result of collision of a fluxon with an antifluxon or even in the process of measurements of switching current characteristics [GK06]. The role of breathers is ambiguous. Depending on our expectations, they can be parasitic excitations or, vice versa, a good substance for generation of THz waves.

There have been many theoretical and numerical studies dedicated to continuous sine-Gordon breathers [IC79, Ino79, KRS82, Kar82, LOS84, BFL⁺83, LS86, GJKS91, GK93, OS81, CPS⁺78, DHN75, MT79, Ram01]. In particular, the decay of a breather into a fluxon and antifluxon induced by an external current has been studied by many

authors [IC79, Ino79, KRS82, Kar82, LOS84] Moreover, it was shown [BFL⁺83, LS86, GJKS91, GK93] that a breather can be stabilized by an ac drive even in the presence of energy losses Also, the influence of the boundaries on breather dynamics [OS81, CPS⁺78] has been investigated and quantization of its energy spectrum [DHN75, MT79] has been predicted

Nevertheless, despite numerous theoretical studies, the dynamics of a breather under dissipation has not been fully understood McLaughlin-Scott theory gets overcomplicated when applied to nontrivial solutions such as breathers, whereas its simplifications fail to predict the correct dynamics We have performed numerical simulations of breather dynamics and found that there is a significant discrepancy with the McLaughlin-Scott calculation In particular, it manifests itself in the dependence of the breather energy on time, Fig 8 1 The thin line is the dependence following from the McLaughlin-Scott calculation (formula (5 5) in Ref [MS78]) and the solid line represents our numerical simulations This discrepancy stimulated us to look into this problem once again and develop a perturbation theory that is designed especially for localized solutions of the sine-Gordon equation We have found that at the construction of such theory it is very important to take into account the history dependence of the breather evolution Also, we have carried out direct numerical simulations with the dissipative sine-Gordon equation The numerical results appear in perfect agreement with our theory

8.2 Perturbation theory for localized solutions

Consider the (1+1)-dimensional sine-Gordon equation

$$\varphi - \varphi_{xx} + \sin \varphi = 0 \tag{8 1}$$

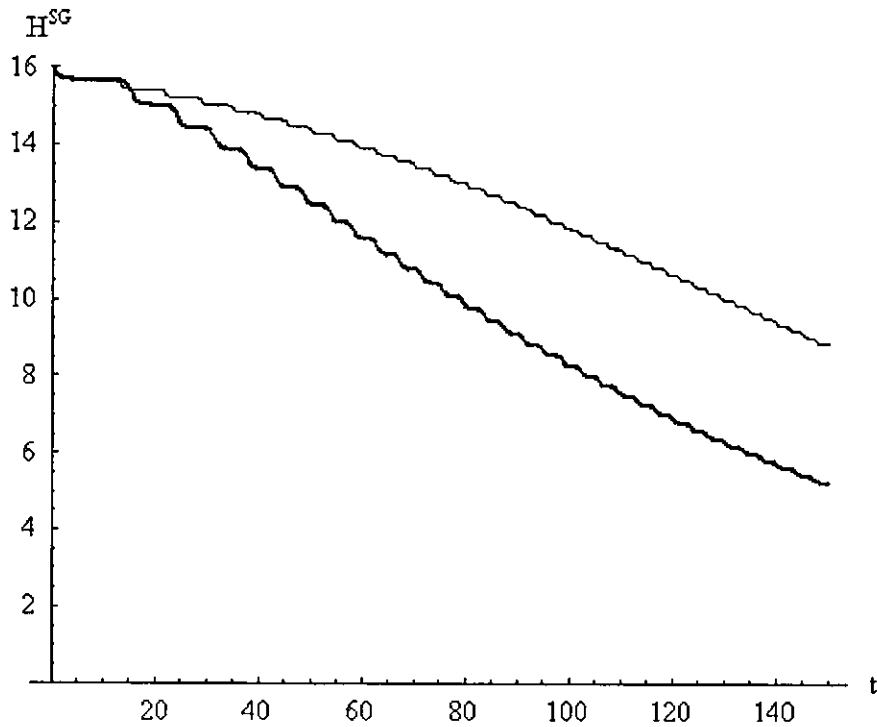


Figure 8.1 Dissipative dynamics of a sine-Gordon breather. Dependence of the energy H^{SG} of a breather on time t calculated according to the McLaughlin-Scott formula (5.5) from Ref. [MS78] is presented by the thin solid line. Dependence of the energy H^{SG} of a breather on time t calculated by direct numerical simulations of sine-Gordon equation with damping is shown by the thick solid line. The damping constant is $\alpha = 0.01$.

The equation possesses solutions in the form of solitons (antisolitons)

$$\varphi(x, t) = 4 \arctan \exp \left(\pm \frac{x - ut}{\sqrt{1 - u^2}} \right) \quad (8.2)$$

The peculiar feature of solitons is that they keep their shapes while moving and even restore their shapes after collision. The attractive forces between a soliton and anti-

soliton allow their bound state – a sine-Gordon breather [Raj82, MS78] (sometimes called doublet or bion),

$$\varphi(x, t) = 4 \arctan \left(\frac{\sin \frac{ut}{\sqrt{1+u^2}}}{u \cosh \frac{x}{\sqrt{1+u^2}}} \right) \quad (8.3)$$

which oscillates periodically in time with frequency $\omega = u/\sqrt{1+u^2}$

The reason why the McLaughlin-Scott formula for breather decay (the formula (5.5) in Ref [MS78]) fails to predict correctly the dissipative dynamics of a breather is the following. Breather is an oscillatory solution that is characterized by some "phase" that depends on the history of the evolution. In their general formulation McLaughlin and Scott treat this difficulty by introducing the history dependent term $\int_{t_0}^t u(t') dt'$ and allowing additional time-dependent modulation of the free parameters (such as initial positions of fluxons or phases of breathers) in the non-perturbed solution [KM77, MS78]. The modulation of the free parameters is governed by additional differential equations. Obviously, this leads to additional complications because of the coupled differential equations for the modulated parameters. Moreover, with such a modulation the original solution no longer satisfies the non-perturbed sine-Gordon equation exactly so that additional perturbation terms appear [MS78]. Here we describe a method that does not involve the modulation of free parameters, but correctly deals with the time-dependent dynamics due to an appropriately chosen ansatz of the non-perturbed sine-Gordon solution.

Consider a solution of the sine-Gordon equation (8.1) in the form $\varphi(g(u)x, g(u)ut, u)$ with $g(u) = 1/\sqrt{1 \pm u^2}$. Such a parametrization is natural for the sine-Gordon equation and obviously comprises the special cases of a soliton (8.2) and a breather (8.3). The sine-Gordon Hamiltonian is a functional of the field variable φ ,

$$H^{SG}[\varphi] = \int_{-\infty}^{\infty} dx \left[\frac{\varphi^2}{2} + \frac{\varphi_x^2}{2} + 1 - \cos \varphi \right] \quad (8.4)$$

Substitution of $\varphi = \varphi(g(u)x, g(u)ut, u)$ gives the effective energy as a function of a

single parameter u ,

$$H_{eff}^{SG}(u) = H^{SG}[\varphi(g(u)x, g(u)ut, u)]$$

The second argument of $\varphi(g(u)x, g(u)ut, u)$ which we call here a phase $T(t) = g(u)ut$ can be written in different ways, such as $T(t) = g(u) \int_0^t u dt'$ or $T(t) = \int_0^t g(u) u dt'$. Obviously, in the case of u independent of time these cases are equivalent and the choice does not make any difference. However, this definition of the phase is very important when taking into account the influence of perturbations, as will be shown below.

In the presence of perturbations we assume that the dominant effect is to modulate the parameter $u = u(t)$. In other words, with appropriate choice of $u(t)$ we may satisfy the perturbed sine-Gordon equation

$$\varphi - \varphi_{xx} + \sin \varphi = \epsilon f$$

by the function $\varphi = \varphi(g(u(t))x, T(t), u(t))$. Here, we take the perturbation ϵf in a general form

$$\epsilon f = - \sum_i \mu_i \delta(x - x_i) \sin \varphi - \gamma - \alpha \varphi$$

In contrast to the case of constant u , the choice of the non-perturbative solution is not unique anymore. Indeed, depending on the choice of the phase $T(t)$, we come out with different functions of t . We will show, that with the appropriate choice of the phase $T(t)$ we may correctly describe the time evolution of localized sine-Gordon solutions in presence of perturbations. We describe the dynamics by a single modulated parameter $u = u(t)$ without introducing additional modulation of the free parameters. This gives considerable simplification and improvement because the other free parameters such as initial location of solitons or initial phases of breathers remain fixed and do not result in auxiliary differential equations like those introduced in the Ref [MS78]

Consider the ansatz

$$\varphi(g(u(t)) x, T(t), u(t)) \quad \text{with} \quad T(t) = \int_0^t g(u(t')) u(t') dt' \quad (8.5)$$

where function φ is an exact solution of non-perturbative sine-Gordon equation (8.1). In further consideration we omit highlighting the explicit dependence of the functions $u = u(t)$ and $T = T(t)$ for typographical convenience. Obviously, the drawback of the time modulation of u affects the time derivative of φ ,

$$\varphi = \frac{d}{dt} \varphi(g(u) x, T, u) = \varphi_1 g_u u x + \varphi_2 g u + \varphi_3 u$$

Where φ_1 , φ_2 and φ_3 are derivatives of φ with respect to first, second and third argument correspondingly. As we consider localized solutions confined in some area $|x| < C$, the term $\varphi_1 g'(u) u x$ is of the order $O(\epsilon)$. The third term also can be neglected as it does not contain explicit linear terms in x and t . Therefore, denoting $\varphi_T \equiv \varphi_2$,

$$\varphi = \varphi_T g u + O(\epsilon) \quad (8.6)$$

that remains valid even in the limit of large times, $t \rightarrow \infty$. Obviously, another choice of $T(t)$ would spoil this equation with terms explicitly dependent on time t , e.g. for $T(t) = g(u(t)) \int_0^t u(t') dt'$ we would have

$$\varphi(g(u) x, T, u) = \varphi_1 g_u u x + \varphi_2 g u + \varphi_2 g_u u \int_0^t u(t') dt' + \varphi_3 u$$

that contain a non-zero term $\int_0^t u(t') dt'$ proportional to t . Thus, in this case the dynamics would not be correctly described on large time scales, $t \rightarrow \infty$. Mclaughlin and Scott overcome this problem introducing additional modulation of free parameters.

Substituting (8.6) to (8.4) we obtain the effective energy as a function of $u(t)$,

$$H^{SG}[\varphi(g(u(t)) x, T(t), u(t))] \simeq H_{eff}^{SG}(u(t)) \quad (8.7)$$

that is valid for any values of t . It is important to note that this expression coincides exactly with the effective energy of non-perturbed solution (8.4) and depends on time indirectly only via $u(t)$.

In the presence of external forces, we may write the full Hamiltonian,

$$H = H^{SG} + H^P$$

and take into account the dissipative perturbations affecting the energy dissipation rate [MS78]

$$\frac{dH}{dt} = - \int_{-\infty}^{\infty} \alpha \varphi^2 dx$$

The Hamiltonian H^P serves to describe non-dissipative perturbations induced by external potential forces. This could be microshorts, microresistors or applied driving current

$$H^P = \int_{-\infty}^{\infty} \left(\sum_i \mu_i \delta(x - x_i) (1 - \cos \varphi) + \gamma \varphi \right) dx$$

Thus,

$$\frac{dH^{SG}}{dt} = - \int_{-\infty}^{\infty} \left(\sum_i \mu_i \delta(x - x_i) \varphi \sin \varphi + \gamma \varphi + \alpha \varphi^2 \right) dx$$

Substituting (8.7), we obtain the equation for parameter u ,

$$u \frac{dH_{eff}^{SG}}{du} = - \int_{-\infty}^{\infty} \left(\sum_i \mu_i \delta(x - x_i) \varphi \sin \varphi + \gamma \varphi + \alpha \varphi^2 \right) dx \quad (8.8)$$

where $\varphi = \varphi(g(u), x, T)$ and $\varphi \simeq \varphi_T g(u) u$ should be substituted. This equation is coupled to the equation for T ,

$$T = g(u) u \quad (8.9)$$

In some cases it can be convenient to rewrite this system of differential equations for independent variable T ,

$$\begin{cases} \frac{du}{dT} = - \left(\frac{dH_{eff}^{SG}}{du} g(u) u \right)^{-1} \int_{-\infty}^{\infty} \left(\sum_i \mu_i \delta(x - x_i) \varphi \sin \varphi + \gamma \varphi + \alpha \varphi^2 \right) dx \\ \frac{dt}{dT} = (g(u) u)^{-1} \end{cases} \quad (8.10)$$

The dynamics is described by $u(T(t))$, where $T(t)$ is an inverse function of $t(T)$.

8.3 Pinning by a microresistor

Let us consider a single solution

$$\varphi(g(u)x, T) = 4 \arctan \exp(g(u)x - T), \quad g(u) = 1/\sqrt{1-u^2}$$

subjected to the attractive potential of a microresistor

$$\epsilon f = -\mu \delta(x) \sin \varphi, \quad \mu < 0$$

The energy of a soliton is equal to

$$H_{eff}^{SG}(u) \simeq \frac{8}{\sqrt{1-u^2}}$$

From (8.8) and (8.9) we obtain the next system of coupled differential equations,

$$\begin{cases} u = \frac{1}{2}\mu(1-u^2) \operatorname{sech}^2(T(t)) \tanh(T(t)) \\ T = \frac{u}{\sqrt{1-u^2}} \end{cases} \quad (8.11)$$

We have found that after some simplifications, the McLaughlin-Scott's formula (4.3) from Ref [MS78] can be reduced to the exactly the same system of differential equations. Although, both approaches lead to exactly the same result, McLaughlin-Scott's formulation is, obviously, more cumbersome.

8.4 Decay of a breather

Consider a breather solution

$$\varphi(g(u)x, T, u) = 4 \arctan \left(\frac{\sin T}{u \cosh(g(u)x)} \right)$$

with $g(u) = 1/\sqrt{1+u^2}$. As a perturbation we consider the dissipative term

$$\epsilon f = -\alpha \varphi$$

The effective energy is

$$H_{eff}^{SG}(u(t)) \simeq \frac{16}{\sqrt{1+u(t)^2}}$$

From (8 10) we obtain the next system of coupled differential equations

$$\begin{cases} \frac{du}{dT} = \alpha \frac{(1+u^2)^{3/2} \cos^2 T}{\sin^2 T + u^2} \left[1 + \frac{u^2 \operatorname{arctanh}\left(\frac{\sin T}{\sqrt{\sin^2 T + u^2}}\right)}{\sin T \sqrt{\sin^2 T + u^2}} \right] \\ \frac{dt}{dT} = \frac{\sqrt{1+u^2}}{u} \end{cases} \quad (8 12)$$

where $u = u(T(t))$. This is a new result that may not be obtained from the McLaughlin-Scott theory by straightforward manipulation. The system can be solved numerically. The dissipative dynamics of a breather is well reflected by time dependence of its energy, Fig 8 2. The results are in perfect agreement with our numerical simulations using the complete sine-Gordon equation with dissipative term.

8.5 Conclusion

In summary, we have found that our perturbation theory describes well the dynamics of localized excitations subjected to influence of external forces such as various inhomogeneities and damping associated with quasiparticle current. In particular, we have described a fluxon trapped in a potential well which could be related to a microresistor in the Josephson junction. Here the equations derived with the use of our method coincides identically with equations derived by McLaughlin-Scott [MS78]. However the derivation of these equations obtained by our method is significantly simpler. Second we have described the decay of the breather under dissipation. In this case, the equations are different from the McLaughlin-Scott's [MS78]. According to our calculation the breather is decaying significantly faster. In order to resolve this difference we have performed numerical simulations with dissipative sine-Gordon equation. The results of these numerical simulations are in close agreement with our theoretical results. The

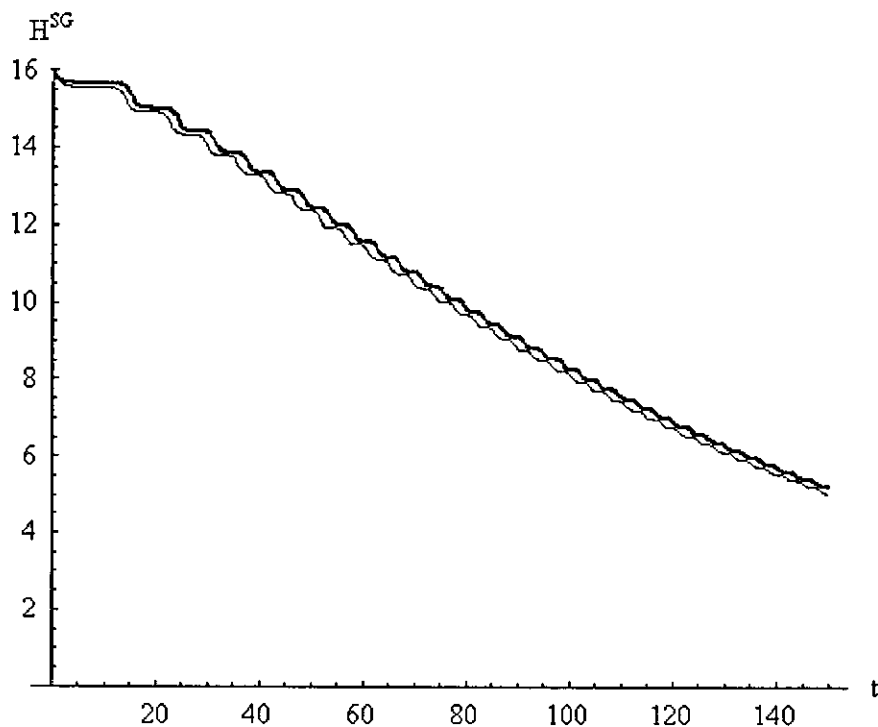


Figure 8.2 Dissipative dynamics of a sine-Gordon breather. Dependence of the energy H^{SG} of a breather on time t calculated using perturbation theory for localized sine-Gordon solutions (thin line). Dependence of the energy H^{SG} of a breather on time t calculated by direct numerical simulations of sine-Gordon equation with damping is shown by the thick solid line. The damping constant is $\alpha = 0.01$.

comparison of our perturbation theory with the McLaughlin-Scott's calculation [MS78] indicates that the history dependence of the breather evolution has a strong influence on its dynamics even at low damping.

To conclude, we have developed the perturbation theory which perfectly describes the localized in space solutions of sine-Gordon equation. The theory may allow generalization to higher dimensions. This can be of use to study localized pulsating solutions.

of sine-Gordon in two spatial dimensions [PZ98]

Chapter 9

Two-dimensional Josephson Junctions

In the previous chapters we have discussed a thermal escape of a superconducting phase difference in a long annular Josephson junction. It has been stated that the escape process is analogous to the escape of a classical string from a potential well. Here we consider the case of a two dimensional geometry where a similar role is played by a membrane. Starting with a two dimensional formulation and appropriate boundary conditions we reduce the description to an effective single variable equation.

9.1 2D Josephson junctions

Stationary 2D sine-Gordon equation in normalized Cartesian coordinates has the form

$$\nabla^2\varphi - \sin\varphi = 0 \tag{9.1}$$

The boundary conditions follow from the continuity of the tangential component of magnetic field H_{\parallel} parallel to the junction's boundary and the relation [BP82] (pp. 79,

112)

$$\nabla\varphi = \frac{2\pi\mu_0 d}{\Phi_0} \mathbf{H} \times \mathbf{e}_z \quad (9.2)$$

(MKS units) where d is a magnetic thickness of the junction ($d \simeq 2\lambda_L$), \mathbf{e}_z is a normal to the plane of the junction, \mathbf{H} is a superposition of external magnetic field \mathbf{H}^{ext} and magnetic field generated by currents. We can normalize this expression to the Josephson penetration depth, that in MKS system is given by

$$\lambda_J = \sqrt{\frac{\hbar}{2e\mu_0 d j_c}} = \sqrt{\frac{\Phi_0}{2\pi\mu_0 d j_c}} \quad (9.3)$$

Assume the magnetic field is laying in the plane of the Josephson junction (XY plane) and the normal vector \mathbf{n} is defined on the junction boundary pointing outside. Thus the boundary conditions expressed in normalized coordinates are

$$\mathbf{n} \cdot \nabla\varphi = \kappa \mathbf{n} \cdot (\mathbf{H} \times \mathbf{e}_z), \quad \text{with} \quad \kappa = \frac{1}{\lambda_J j_c} \quad (9.4)$$

where the right hand side can be written explicitly,

$$\mathbf{n} \cdot \nabla\varphi = \kappa (n_x H_y - n_y H_x) \quad (9.5)$$

Magnetic field induced by the bias current at the point r in normalized coordinate system,

$$\mathbf{H}(\mathbf{r}) = \frac{\lambda_J}{4\pi} \int \frac{\mathbf{J}(\mathbf{r}') \times (\mathbf{r} - \mathbf{r}')}{|\mathbf{r} - \mathbf{r}'|^3} d^3\mathbf{r}' \quad (9.6)$$

As we assume homogeneity of the current, $\mathbf{J}(\mathbf{r}') = -j\mathbf{e}_z$, we may take it out from the integral. Using $\mathbf{r} = \rho + z\mathbf{e}_z$ we integrate over z (in the limit of an infinite film width),

$$\mathbf{H}(\rho) = -\frac{j\lambda_J}{4\pi} \int \frac{\mathbf{e}_z \times (\rho - \rho')}{|\rho - \rho'|^2} d^2\rho' \quad (9.7)$$

Or explicitly

$$H_x(x, y) = -\frac{j\lambda_J}{2\pi} \int \int \frac{(y' - y) dx' dy'}{(x' - x)^2 + (y' - y)^2} \quad (9.8)$$

and

$$H_y(x, y) = \frac{j\lambda_J}{2\pi} \int \int \frac{(x' - x) dx' dy'}{(x' - x)^2 + (y' - y)^2} \quad (9.9)$$

9.2 Square geometries

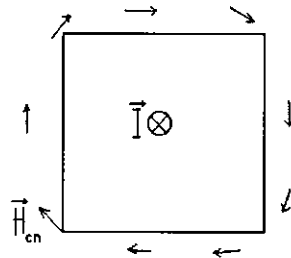


Figure 9 1

In case of square geometry, the value of magnetic field on the corner

$$H_{cn} = \frac{j \lambda_J L k_{cn}}{2\pi}$$

and on the border close to the corner

$$H|_{\text{close to the corner}} = \frac{H_{cn}}{\sqrt{2}} = \frac{j \lambda_J L k_{cn}}{2\sqrt{2} \pi}$$

where k_{cn} is a geometrical factor for the corner of the square,

$$k_{cn} \simeq 1.60$$

When calculating the geometrical factor using the formulas above we have neglected the magnetic properties of the material and have assumed $\mu=1$

Let us consider a large junction of square geometry, $L \gg 1$. Introduce the coordinates (ξ, η) with a center at the left bottom corner

$$\xi = \frac{x+y}{\sqrt{2}} \quad \eta = \frac{x-y}{\sqrt{2}}$$

$$\varphi_{\xi\xi} + \varphi_{\eta\eta} - \sin \varphi = 0$$

The boundary conditions become

$$\frac{\partial \varphi}{\partial \xi} \Big|_{(0,0)} = \frac{\gamma L k_{cn}}{2\pi}$$

$$\frac{\varphi_\xi - \varphi_\eta}{\sqrt{2}} \Big|_{(\xi,\xi)} = \frac{\gamma L k_{cn}}{2\sqrt{2}\pi}$$

where we have introduced $\gamma = J/J_c$. From the last condition,

$$\varphi_\eta \Big|_{\eta=\xi} = \varphi_\xi \Big|_{\eta=\xi} - \frac{\gamma L k_{cn}}{2\pi}$$

Assuming $\varphi_\xi \Big|_{\eta=\xi} \simeq \varphi_\xi \Big|_{\eta=0}$ as the vortex penetrates in ξ direction,

$$\varphi_\eta \Big|_{\eta=\xi} \simeq \varphi_\xi \Big|_{\eta=0} - \frac{\gamma L k_{cn}}{2\pi}$$

On the other hand, from the symmetry we also may conclude that

$$\varphi_\eta \Big|_{\eta=0} = 0$$

Hence, with the use of the boundary conditions on the corner

$$\varphi_{\eta\eta}(\xi) \simeq \frac{\varphi_\eta \Big|_{\eta=\xi}}{\xi} = \frac{\varphi_\xi(\xi) \Big|_{\eta=0} - \varphi_\xi(0) \Big|_{\eta=0}}{\xi} \simeq \varphi_{\xi\xi}(\xi)$$

That is valid close to the corner of the square. On the other hand, the equality $\varphi_{\eta\eta} \simeq \varphi_{\xi\xi}$ is also satisfied in the center of the square due to the symmetry. Eventually we get an approximate one dimensional equation

$$2\varphi_{\xi\xi} - \sin \varphi \simeq 0$$

The solution to this equation is a sine-Gordon soliton stretched along the ξ axis,

$$\varphi(\xi) = 4 \arctan e^{(\xi-\xi_0)/\sqrt{2}}$$

The maximal slope guaranteed by this solution is

$$\varphi'(\xi_0) = \sqrt{2}$$

From what the critical current follows

$$\sqrt{2} = \frac{\gamma_c L k_{cn}}{2\pi}$$

$$\gamma_c = \frac{2\sqrt{2}\pi}{L k_{cn}} \simeq \frac{5.6}{L}$$

The critical current in physical units,

$$I_c \simeq 5.6 j_c L \lambda_J^2$$

that in case of a large square depends linearly on the size of the junction compared to the case of a small junction

In conclusion, the switching to resistive state of large square Josephson junctions occurs due to Josephson fluxons penetrating from the corners of the geometry. They can be approximately described as stretched sine-Gordon solitons

9.3 Derivation of the microshort models

In order to derive an effective 1D model from the discussed above 2D model we have to start with the conventional 2D Sine Gordon equation written in normalized polar coordinates

$$\frac{\partial^2 \varphi}{\partial r^2} + \frac{1}{r} \frac{\partial \varphi}{\partial r} + \frac{1}{r^2} \frac{\partial^2 \varphi}{\partial \theta^2} - \sin \varphi = 0 \quad (9.10)$$

Let us assume, that the bias current I is flowing uniformly, parallel to the junction axis. The magnetic field generated by a thin cylinder is equal to $I/2\pi r \lambda_J$ (r - a distance from the symmetry axis) outside and 0 inside. Thus, the boundary conditions can be written as

$$\frac{\partial \varphi}{\partial r} \Big|_{r=R_i} = \kappa H^{ext} \sin \theta \quad (9.11)$$

$$\frac{\partial \varphi}{\partial r} \Big|_{r=R_e} = \kappa H^{ext} \sin \theta - \frac{\kappa I}{2\pi R_e \lambda_J} \quad (9.12)$$

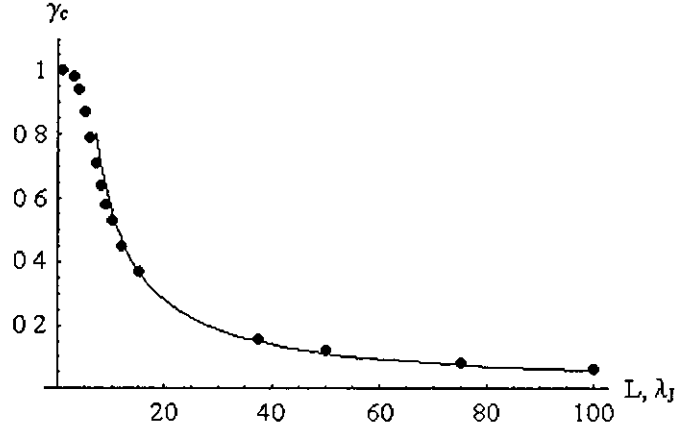


Figure 9.2 Dependence of the normalized critical current γ_c on the linear size of the square junction under constant material parameters λ_J and j_c . The dots correspond to numerical calculation with a 2D geometry. The solid line is the theoretical dependence for large squares ($L \gg 1$). The last 4 points are calculated for the lengths $L=37.5$, 50, 75 and 100, that corresponds to the experimental samples $15 \times 15 \mu m^2$, $20 \times 20 \mu m^2$, $30 \times 30 \mu m^2$, $40 \times 40 \mu m^2$ and $\lambda_J = 0.4 \mu m$.

For $\Delta R < 1$ (i.e. the width is less than λ_J) we assume that $\partial\varphi/\partial r$ is linear function of r

$$\frac{\partial\varphi}{\partial r} = \kappa H^{ext} \sin\theta - \frac{\kappa I}{2\pi R_e \lambda_J} \frac{(r - R_i)}{\Delta R} \quad (9.13)$$

$$\frac{\partial^2\varphi}{\partial r^2} = -\frac{\kappa I}{2\pi R_e \Delta R \lambda_J} \quad (9.14)$$

Substituting into the eq. (9.10) and using $\Delta R \ll R_i, R_e$

$$\frac{1}{R^2} \varphi_{\theta\theta} - \sin\varphi - \gamma + h \sin\theta = 0 \quad (9.15)$$

with $R \simeq R_i \simeq R_e$, and we have introduced the notations

$$\gamma = \frac{\kappa I}{2\pi R \Delta R \lambda_J} = \frac{I}{I_c}, \quad \text{where } I_c = 2\pi R \Delta R \lambda_J^2 j_c \quad (9.16)$$

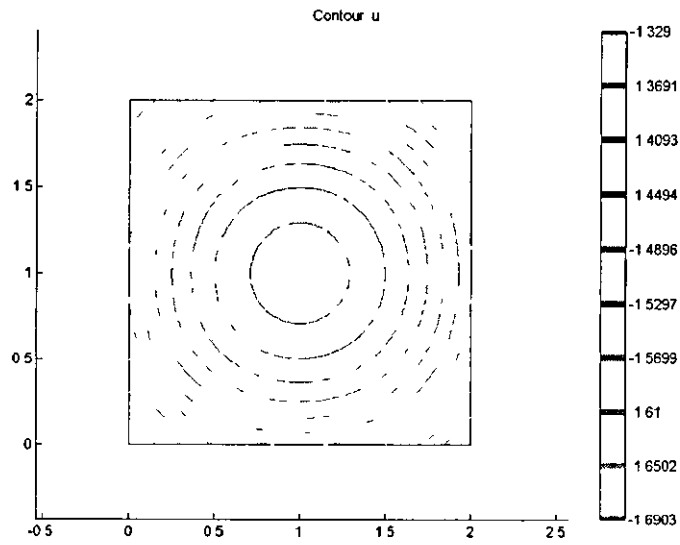


Figure 9 3 Numerical calculation for a 2D square geometry with a side $L=2$

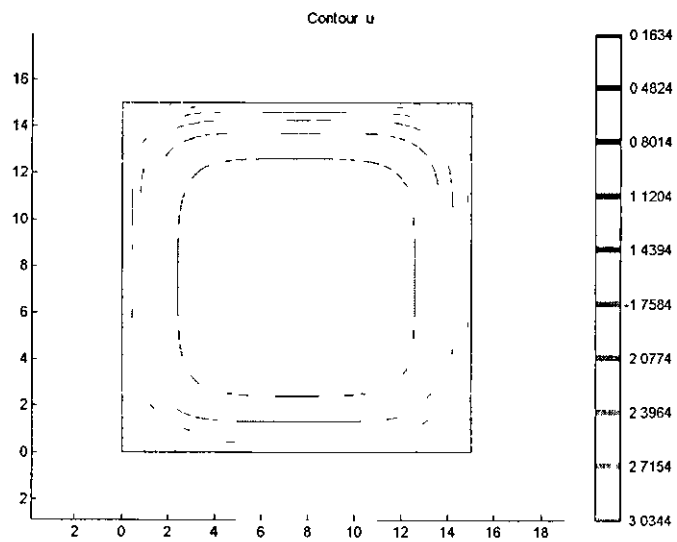


Figure 9 4 Numerical calculation for a 2D square geometry with a side $L=15$

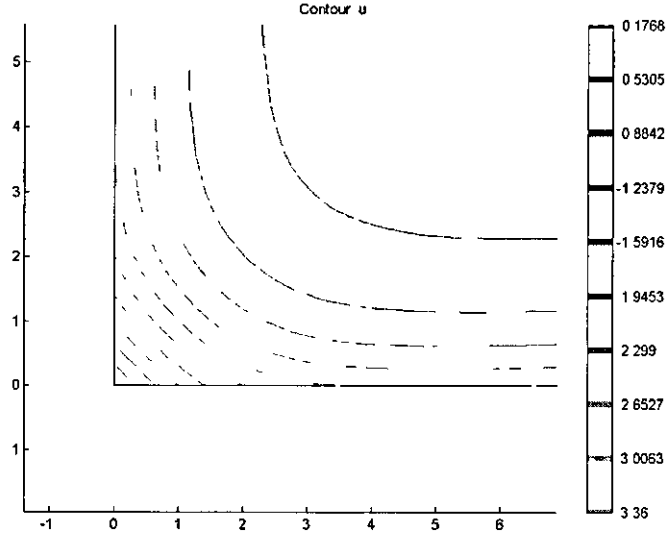


Figure 9.5 Numerical calculation for a 2D square geometry with a side $L=50$

The normalized magnetic field is defined as

$$h = \frac{\kappa H^{ext}}{R} \quad (9.17)$$

From this expression we see that the field h is normalized to field unit

$$R/\kappa = \frac{\Phi_0 R}{2\pi\mu_0 d \lambda_J} \quad (9.18)$$

With the substitution $\theta = 2\pi r/L = kr$ we recover the conventional model for AJJ as

$$\varphi_{xx} - \sin \varphi - \gamma + h \sin kx = 0 \quad (9.19)$$

This equation can be obtained directly from the following energy functional

$$V[\varphi(x)] = \int_{-L/2}^{L/2} \left[\frac{\varphi_x^2}{2} + 1 - \cos \varphi + \gamma \varphi - h \varphi \sin kx \right] r dx \quad (9.20)$$

If there is a variation in a local width ΔW or in the thickness Δd of the AJJ in a comparison with the width W_0 or the thickness d of the AJJ the similar procedure

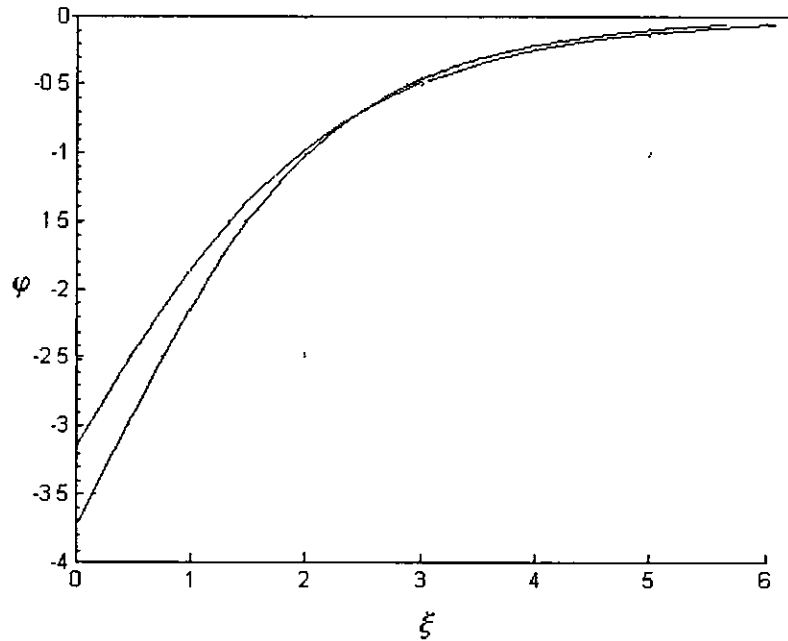


Figure 9.6 Superconducting phase difference $\varphi(\xi)$ across the corner of the square with $L=50$. External current is close to the critical. The lowest curve (blue) – numerical calculation, the top curve (black) – theory

can be applied. In the case when such variations are small we may use the perturbation theory. The perturbation expansion may result to the model

$$V[\varphi(x)] = \int_{-L/2}^{L/2} dx \left(1 + \frac{\Delta l \Delta W(x)}{W_0} \right) \left[\frac{\varphi_x^2}{2} + (1 - \cos \varphi) + \gamma \varphi - h \varphi \sin kx \right] \quad (9.21)$$

where $\Delta W(r) = \Delta W$ on the pseudo-microshort having the width $W_0 + \Delta W$ and the length Δl . There is no variation $\Delta W(x) = 0$ elsewhere. The manufacture of such a pseudo-microshort can be produced with the use of a standard lithographic process. Such realistic manufacture methods makes these micro-shorts very attractive for all possible experimental investigations.

In previous studies it was mentioned the models of the conventional microshort,

where there is a local enhancement of a critical current [MS78, KI96, Kat00] may be described as a local point impurity. The energy of the superconducting phase configuration for a long Josephson junction with such a conventional microshort located at the position $x = 0$ may be derived with a similar procedure and defined by the eq

$$V[\varphi(x)] = \int_{-L/2}^{L/2} dx \left[\frac{\varphi_x^2}{2} + \left(1 + \frac{\Delta l \Delta J_c}{J_c} \right) (1 - \cos \varphi) + \gamma \varphi - \hbar \varphi \sin kx \right] \quad (9.22)$$

where $k = 2\pi/L$ and L is a normalized circumference of the annular junction, Δl is a normalized length of the impurity. One may notice strong similarities between the models presented by the eq 9.21 and the eq 9.22. Within the quasi one-dimensional approximations, the both equations eq 9.21 and the eq 9.22 result in two identical models described in the chapter 7.

$$V(\varphi_0) = -\gamma 2\pi \varphi_0 - \frac{2\pi \hbar \cos(kx_0)}{k \cosh(k\pi/2)} + \frac{2\epsilon}{\cosh(x_0)^2} \quad (9.23)$$

with

$$\epsilon = \begin{cases} \Delta l \Delta J_c / J_c, & \text{for a conventional microshort} \\ 2 \Delta l \Delta W / W_0, & \text{for a pseudo-microshort} \end{cases}$$

Summary and Conclusions

In the first part I have studied the process of quantum tunneling of an Abrikosov vortex responsible for switching of a superconducting dot to a non-magnetic state. Similar process may arise in Josephson contact when tunneling of a single Josephson vortex trapped in an annular Josephson junctions leads to switching to resistive state. This situation may appear when the read out of the proposed microshort qubit is realized. Bias of the annular Josephson junction by an external current decreases the potential barrier that confines the fluxon and forces its escape via quantum tunneling.

I have summarized the switching phenomena of an AJJ on a single "phase diagram" Fig 9.7. One may immediately see its perfect symmetry. This symmetry has a fundamental nature concerned with the analogy between *quantum mechanics of n-dimensional systems* and *classical statistical mechanics in (n+1)-dimensions*. The explanation of this unique resemblance between n-dimensional quantum and (n+1)-dimensional classical worlds is still a mystery. According to A. M. Polyakov the reasons may be concerned with the fundamental properties of the space-time continuum [Pol87].

Let us consider a set of annular Josephson junctions with varying lengths. Suppose we have *small* annular Josephson that effectively behave like a 0-dimensional object and *long* annular junctions that are analogues of 1-dimensional objects. According the statement above, there should be correspondence between *quantum short* annular junctions and *classical long* annular junctions. Mathematically, the instanton trajectories of

quantum short AJJ correspond to stationary trajectories of the vortex-antivortex type of the *classical long* annular junctions. Because the main contribution to the imaginary action is by the periodic-in-time trajectories (see part I of the thesis), the quantum 0-dimensional Josephson junction can be seen as an "annulus in time". As for *quantum long* annular junctions, they are represented by toruses in space-time continuum

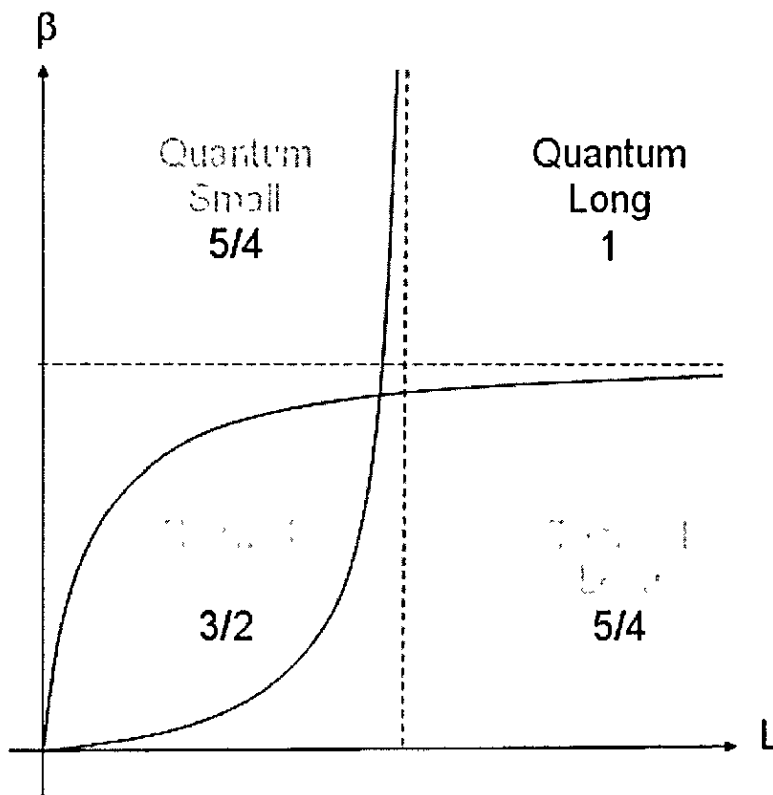


Figure 9.7 "Phase diagram" of an annular Josephson junction. Indices are the critical exponents of the Euclidean (instanton) action close to the switching point. "Thermal" stands for thermal escape according to the classical statistical field theory, "Quantum" - for the phase escape via quantum tunneling.

Let us summarize the results obtained in this study

1. Demagnetization rate of a superconducting quantum dot is found to be given by the formula (2 23).

2 The quantum tunneling rate has been calculated by means of the instanton technique and standard WKB. Both method give the identical result

3 A model of switching of an annular Josephson junction has been proposed The recent experimental data has been explained (Fig 5 2, Fig 5 3)

4 A formula for the crossover length between short and long annular Josephson junctions has been found (Eq (6 8), (6 10))

5. The model of a microshort qubit has been proposed

6 Perturbation theory describing localized excitations has been developed

7 Switching of two-dimensional Josephson junctions has been analyzed In particular, switching current of a large Josephson junction of square geometry has been calculated

Bibliography

- [AS80] M J Ablowitz and H Segur *Solitons and Inverse Spectral Transform* Philadelphia, SIAM, 1980
- [AtS05] *Atomic strategy*, (4) 28, August 2005 [http //www nuclear ru/eng](http://www.nuclear.ru/eng)
- [BB94] A I Buzdin and J P Brison *Phys. Lett A*, 196 267, 1994
- [BC96] M Benkraouda and John R Clem *Phys Rev B*, 53 5716, 1996
- [BCL+06] A Barone, R Cristiano, M Lisitskii, C Nappi, D P De Lara, and G Rottoli *Physica C*, 435 118, 2006
- [BF96] A I Buzdin and D Feinberg. *Physica C*, 256 303, 1996
- [BFL+83] A R Bishop, K Fesser, P S Lomdahl, W C Kerr, M B Williams, and S E Trullinger *Phys Rev Lett* , 50 1095, 1983
- [BI93] Ernst Helmut Brandt and Mikhail Indenbom *Phys Rev B*, 48 12893, 1993
- [BL64] C P Bean and J D Livingstone *Phys Rev Lett* , 12 14, 1964
- [BL81] M Buettiker and R Landauer *Phys Rev. A*, 23 1397, 1981
- [BP82] A Barone and G Paterno *Physics and Applications of the Josephson Effect* John Wiley and Sons, New York, 1982

- [BSK⁺04] D Born, V I Shnyrkov, W Krech, Th Wagner, E Il'ichev, M Grajcar, U Hubner, and H-G Meyer *Phys Rev B*, 70 180501, 2004
- [But68] E Butkov *Mathematical Physics* Addison Wesley, Reading, 1968
- [CBS⁺04] I Chiorescu, P Bertet, K Semba, Y Nakamura, C J P M Harmans, and J E Mooij *Nature*, 431 159, 2004
- [CC77] C G Callam and S Coleman *Phys Rev D*, 16 1762, 1977
- [CDJ⁺99] H Castro, B Dutoit, A Jacquier, M Baharami, and L Rinderer *Phys Rev B*, 59 596, 1999
- [CEF⁺99] R Cristiano, E Esposito, L Frunzio, M P Lisitskii, C Nappi, G Amendola, A Barone, L Parlato, D V Balashov, and V N Gubankov *Appl Phys Lett*, 74 3389, 1999
- [CK03] E M Chudnovsky and A B Kuklov *Phys Rev Lett*, 91 067004, 2003
- [Cla03] J Clarke *Nature*, 425 133, 2003
- [Col77] S Coleman *Phys Rev D*, 15 2929, 1977
- [Col85] S Coleman *Aspects Of Symmetry* Cambridge University Press, Cambridge, 1985
- [CPS⁺78] G Costabile, R D Parmentier, B Savo, D W Mc Laughlin, and A C Scott *Appl Phys Lett*, 32 587, 1978
- [DHN75] R F Dashen, B Hasslacher, and A Neveu *Phys Rev D*, 11 3424, 1975
- [EG64] S F Edwards and Y V Gylaeu *Proc Roy Soc A*, 279 229, 1964
- [FD74] T A Fulton and L N Dunkelberger *Phys Rev B*, 9 4760, 1974

- [Fed77] M V Fedoryuk *Metod perevala [in Russian] (The saddle-point method)*
Nauka, Moscow, 1977
- [FGLL93] M V Feigel'man, V B Geshkenbein, A I Larkin, and S Levit *JETP Lett*, 57 711, 1993
- [FLP⁺01] L Frunzio, L Li, D E Prober, I V Vernik, M P Lisitski, C Nappi, and R Cristiano *Appl Phys Lett*, 79 2103, 2001
- [FP67] L D Faddeev and V N Popov *Phys Lett B*, 25 29, 1967
- [FU03] M V Fistul and A V Ustinov *Phys Rev B*, 68 132509, 2003
- [FWK⁺03] M V Fistul, A Wallraff, Y Koval, A Lukashenko, B A Malomed, and A V Ustinov *Phys Rev Lett*, 91 257004, 2003
- [Gar95] A Gaig *Phys Rev B*, 51 15592, 1995
- [GII05] M Grajcar, A Izmalkov, and E Il'ichev *Phys Rev B*, 71 144501, 2005
- [GIvdP⁺05] M Grajcar, A Izmalkov, S H W van der Ploeg, S Linzen, E Il'ichev, Th Wagner, U Hubner, H-G Meyer, Alec Maassen van den Brink, S Uchaikin, and A M Zagoskin *Phys Rev B*, 72 020503, 2005
- [GJKS91] N Gronbech-Jensen, Yu S Kivshar, and M R Samuelson *Phys Rev B*, 43 5698, 1991
- [GK93] R Grauer and Yu S Kivshar *Phys Rev E*, 48 4791, 1993
- [GK06] D Gulevich and F Kusmartsev *Physica C*, 435 87, 2006
- [GP77] E Gildener and A Patrasciou *Phys Rev D*, 16 423, 1977

- [HYT⁺94] J M Harris, Y F Yan, O K C Tsui, Y Matsuda, and N P Ong *Phys Rev Lett* , 73 1711, 1994.
- [IC79] M Inoue and S G Chung *J. Phys Soc Jpn* , 46 1594, 1979
- [IGI⁺04] A. Izmalkov, M Grajcar, E. Il'ichev, Th Wagner, H-G Meyer, A Yu Smirnov, M H S Amin, Alec Maassen van den Brink, and A M Zagoskin. *Phys Rev Lett* , 93 037003, 2004
- [Ino79] M Inoue *J Phys Soc Jpn.*, 47 1723, 1979
- [Kar82] V I Karpman *Phys Lett A*, 88 207, 1982
- [Kat00] T Kato *J Phys Soc Jpn.*, 69 2735, 2000
- [KI96] T Kato and M Imada *J Phys Soc Jpn* , 65 2963, 1996
- [Kle00] H M Kleinert *Path Integrals in Quantum Mechanics, Statistics, Polymer Physics, and Financial Markets* Gordon and Breach Science Publishers, New York, [http //www physik fu-berlin de/ kleinert](http://www.physik.fu-berlin.de/kleinert), 2000
- [KM77] J P Keener and D W McLaughlin *Phys Rev A*, 16 777, 1977
- [KP70] A P Kazantsev and V L Pokrovskii *JETP*, 31 362, 1970
- [Kra40] H A Kramers *Physica*, 7 284, 1940
- [KRS82] V I Karpman, N A Ryabova, and V V Solov'ev *Phys Lett* , 92 255, 1982
- [KS02] Gwang-Hee Kim and Mincheol Shin *Phys Rev B*, 66 064515, 2002
- [KST00] V G Kiselev, Ya M Shnir, and A Ya Tregubovich *Introduction to Quantum Field Theory* Gordon and Breach Science Publishers, Amsterdam, 2000

- [Kur72] J Kurkijarvi *Phys Rev B*, 6 832, 1972
- [KWU02] A Kemp, A Wallraff, and A V Ustinov *Physica C*, 368 324, 2002
- [LAB+00] M P Lisitskii, G Ammendola, D V Balashov, A Barone, R Cristiano, E Esposito, L Frunzio, V N. Gubankov, C Nappi, S Pagano, L Parlato, G Peluso, and G Pepe *Nucl Instr Meth. Phys Res* , 444 476, 2000
- [Lan67] J S Langer *Ann Phys (N.Y)*, 41 108, 1967
- [LL65] L D Landau and E M Lifshitz *Quantum Mechanics*, volume 3 Addison-Wesley, Reading, Mass , 1965
- [LOS84] P S Lomdahl, O H Olsen, and M R Samuelsen *Phys Rev A*, 29 350, 1984
- [LS77] S Levit and U Smilansky *Proc Amer Math Soc* , 65 299, 1977
- [LS86] P S Lomdahl and M R Samuelsen *Phys Rev A*, 34 664, 1986
- [MM96a] N Martucciello and R Monaco *Phys Rev B*, 53 3471, 1996
- [MM96b] N Martucciello and R Monaco *Phys Rev B*, 54 9050, 1996
- [MOL+99] J E Mooij, T P Orlando, L Levitov, Lin Tian, C H van der Wal, and Seth Lloyd *Science*, 285 1036, 1999
- [MS78] D W McLaughlin and A C Scott *Phys Rev A*, 18 1652, 1978
- [MT79] K Maki and H Takayama *Phys Rev B*, 20 5002, 1979
- [NC97] C Nappi and R Cristiano *Appl Phys Lett* , 70 1320, 1997
- [NCL+02] C Nappi, R Cristiano, M P Lisitskii, R Monaco, and A Barone *Physica C*, 367 241, 2002

- [New06] *Loughborough University news release News@lboro*, (40), February 2006
<http://www.lboro.ac.uk/service/publicity/pages/pubs-newsatlboro-archive.html>.
- [NLR⁺04] C Nappi, M P Lisitskiy, G Rotoli, R Cristiano, and A Barone *Phys Rev Lett*, 93 187001, 2004.
- [NPT99] Y Nakamura, Y A. Pashkin, and J S Tsai *Nature*, 398 786, 1999
- [OS67] C S Owen and D J Scalapino *Phys Rev*, 164 538, 1967
- [OS81] O H Olsen and M R Samuelsen *J Appl Phys*, 52 2913, 1981
- [Pap75] G J Papadopoulos *Phys Rev D*, 11 2870, 1975
- [PGK⁺] A Price, D R Gulevich, A Kemp, F V Kusmartsev, and A Ustinov
 Bistable vortex states in microshort qubit in preparation
- [PI69] D Peak and A Inomata *J Math Phys*, 10 1422, 1969
- [Pol87] A M Polyakov *Gauge Fields and Strings* Harwood Academic Pub, 1987
- [PP72] B V Petukhov and V L Pokrovskii *JETP Lett*, 15 44, 1972
- [PSO⁺95] Beth Parks, S Spielman, J Orenstein, D T Nemeth, Frank Ludwig, John Clarke, Paul Merchant, and D J Lew *Phys Rev Lett*, 74 3265, 1995
- [PYA⁺03] Yu A Pashkin, T Yamamoto, O Astafiev, Y Nakamura, D V Averin and J S Tsai *Nature*, 421 823, 2003
- [PZ98] B Piette and W J Zakrzewski *Nonlinearity*, 11 1103, 1998

- [Raj82] R Rajaraman *Solitons and Instantons an Introduction to Solitons and Instantons in Quantum Field Theory* Amsterdam, Oxford, North-Holland, 1982
- [Ram01] J I Ramos *Appl Math Comp.*, 124 45, 2001.
- [Sch81] L S Schulman *Techniques and Applications of Path Integration* John Wiley and Sons, 1981
- [SDP00] T Sharpee, M I Dykman, and P M Platzman *Phys Rev Lett*, 84 2227, 2000
- [SDP02] T. Sharpee, M I Dykman, and P M Platzman *Phys Rev A*, 65 032122, 2002
- [SET06] *SET for Britain news release*, 2006 [http //www setforeurope org](http://www.setforeurope.org)
- [SIK⁺94a] Th Schuster, M. V. Indenbom, H. Kuhn, E H Brandt, and M Konczykowski *Phys Rev Lett*, 73 1424, 1994
- [SIK⁺94b] Th Schuster, M V Indenbom, H Kuhn, E H Brandt, and M Konczykowski *Phys Rev Lett*, 73 1424, 1994
- [SK04] P D Shaju and V C Kuriakose *Phys Lett A*, 332 326, 2004
- [Suh65] H Suhl *Phys Rev Lett*, 14 226, 1965
- [Tha00] B Thaller *Visual Quantum Mechanics* Springer-Verlag, New York, 2000
- [TS72] F F Teinovski and L N Shekhata *Sov Phys JETP*, 35 1202, 1972
- [VAC⁺02] D Vion, A Aassime, A Cottet, P Joyez, H Pothier, C Urbina, D Esteve, and M H Devoret *Science*, 296 886, 2002

- [vDGK96] A J J van Dalen, R. Griessen, and M. R. Koblishka. *Physica C*, 257 271, 1996
- [vDGL⁺96] A J J van Dalen, R. Griessen, S Libbrecht, Y Bruynseraede, and E Osquiguil *Phys Rev B*, 54 1366, 1996
- [vDGM⁺96] A J J van Dalen, R Griessen, J C Martinez, P Fivat, J-M Triscone, and O Fischer *Phys Rev B*, 53 896, 1996
- [VSC⁺01] Tejs Vegge, James P Sethna, Siew-Ann Cheong, K. W Jacobsen, Christopher R Myers, and Daniel C Ralph *Phys Rev Lett* , 86 1546, 2001
- [WKL⁺00] A Wallraff, Yu Koval, M Levitchev, M V Fistul, and A V Ustinov *J Low Temp Phys* , 118 543, 2000
- [WLL⁺03] A Wallraff, J Lisenfeld, A Lukashenko, A Kemp, M Fistul, Y Koval, and A V Ustinov *Nature*, 425 155, 2003
- [YMS96] Y Yeshurun, A P Malozemoff and A Shaulov *Rev Mod Phys* , 68 911, 1996
- [YPA⁺03] T Yamamoto Yu A Pashkin, O Astafiev, Y Nakamura and J S Tsai *Nature*, 425 941, 2003
- [ZLG⁺94] E Zeldov, A I Larkin, V B Geshkenbein, M Konczykowski, D Majer, B Khaykovich, V M Vinokur, and H Shtrikman *Phys Rev Lett* , 73 1428, 1994

